2020

Revealing chemical evidence from fingerprints through matrix-assisted laser desorption/ionization - mass spectrometry imaging

Paige Lauren Hinners
Iowa State University

Revealing chemical evidence from fingerprints through matrix-assisted laser desorption/ionization - mass spectrometry imaging

by

Paige Hinners

A dissertation submitted to the graduate faculty

in partial fulfillment of the requirements for the degree of

DOCTOR OF PHILOSOPHY

Major: Analytical Chemistry

Program of Study Committee:
Young Jin Lee, Major Professor
Robbyn Anand
Jared Anderson
Joe Burnett
Alicia Carriquiry

The student author, whose presentation of the scholarship herein was approved by the program of study committee, is solely responsible for the content of this dissertation. The Graduate College will ensure this dissertation is globally accessible and will not permit alterations after a degree is conferred.

Iowa State University

Ames, Iowa

2020

TABLE OF CONTENTS

Page

LIST OF FIGURES

Page

Chapter 1

Chapter 2

Chapter 3

Chapter 4

Chapter 5

LIST OF TABLES

Page

Chapter 4

Chapter 5

ACKNOWLEDGMENTS

I would like to begin by thanking Dr. Young Jin Lee, my research advisor, for challenging and trusting me to develop independent projects during my graduate career at Iowa State University. I thank and acknowledge my committee members, Dr. Robbyn Anand, Dr. Jared Anderson, Dr. Alicia Carriquiry, Dr. R. Sam Houk (preliminary defense), and Dr. Joe Burnett for their guidance, support, and questions throughout this research. A sincere thank you to the Chemistry department staff for always being willing to assist myself and other graduate students with our plethora of questions.

I am grateful for the Lee group members including: Dr. Rebecca Hansen, Dr. Maria Emilia Dueñas, Kelly O'Neill, Evan Larson, Trevor Forsman, Emily King, and Andrew Paulson for their insightful discussions and suggestions throughout our time together. An additional thank you to previous Lee group members who were always available for troubleshooting questions. A special thank you to Madison Thomas and Haley Dunn for allowing me to mentor you in your undergraduate research projects.

I am appreciative of the National Institute of Justice (NIJ) for funding the research as well as my travel to professional conferences. I also want to offer my appreciation to all who were willing to participate in my research.

To Lacey and Logan, thank you for listening to me discuss my research and graduate school struggles and always assuring confidence. A huge thank you to George for allowing me to grow as a scientist while you grew as a young man. Finally, I am beyond grateful to all my family and friends for standing by and supporting me throughout my graduate career, I could not have done it without your support.

ABSTRACT

This dissertation presents my efforts to advance the application of matrix-assisted laser desorption/ionization - mass spectrometry imaging (MALDI-MSI) to the chemical analysis of latent fingerprints. The first chapter contains a general introduction to MALDI-MSI, with a focus on the application to fingerprint analysis. The final chapter summarizes the presented work and future directions for the research.

The second chapter presents the feasibility of using carbon fingerprint development powder (CFP) as an existing MALDI matrix. This study compared the ionization efficiency of CFP and other commonly used MALDI matrices. The data revealed that CFP is comparable or better than the currently utilized MALDI matrices for latent fingerprint analysis. MALDI-MSI was performed on fingerprints dusted with CFP and lifted with forensic lifting tape, demonstrating that more realistic samples can also be analyzed using MALDI-MSI. Most importantly, it was shown that MALDI-MSI does not destroy the fingerprint during analysis and the fingerprint can be preserved as forensic evidence.

The third chapter investigated the use of titanium oxide development powder (TiO_2) as a MALDI matrix and elaborates on the impact of adding additional matrices to the signal-to-noise (S/N) ratio of fingerprint compounds. It was demonstrated that TiO_2 worked efficiently as an existing MALDI matrix and did not require the use of a high-resolution mass spectrometer. Additional matrices on top of the TiO_2 showed limited success and caused a decrease in intensity for some compounds. However, additional matrix did allow the analysis of TiO_2 developed fingerprints in negative mode. Importantly this work emphasized the need for knowledge of traditional matrix applicability in fingerprint analysis.

In the fourth chapter, the potential for using MALDI-MSI to develop lifestyle profiles of unknown individuals is presented. Prior work studying exogenous fingerprint compounds focused on illicit substances. In this work, compounds related to consumer products, foods, and beverages could be detected in fingerprint residue using MALDI-MSI. These specific compounds could be used for brand or subtype determination of a particular source, such as subtype of citrus fruit. Each set of compounds detected tells a portion of an individual's lifestyle.

In the fifth chapter, the mechanism of degradation of unsaturated triacylglycerols (TGs) in fingerprints aged under ambient environment conditions was investigated. MALDI-MSI was used to explore TG profiles of fresh and aged latent fingerprints. With time, the unsaturated TGs underwent ambient ozonolysis resulting in a decrease in the abundance of unsaturated TGs that was relatively reproducible in an individual. In addition, two sets of peaks emerged with time, and were determined to be degradation peaks of unsaturated TGs due to ambient ozonolysis. The decrease of unsaturated TGs can be monitored to establish the time since deposition, or age, of latent fingerprints.

CHAPTER 1. GENERAL INTRODUCTION

General Description of Mass Spectrometry

Mass spectrometry (MS) is an analytical technique that measures the mass-to-charge ratio (*m/z*) of ions in the gas phase.[1] A key feature of MS is that the compound being measured must be ionized for detection. An electromagnetic field is generally utilized to separate compounds by *m/z*. Typically ions are plotted in a mass spectrum which contains the abundance on the y-axis and the *m/z* on the x-axis. Depending on the ionization method and polarity being used, ions can appear as a molecular ion, protonated, deprotonated, or as another adduct such as sodiated or potassiated. There are numerous methods to ionize a sample for MS analysis. Electrospray ionization, electron ionization, chemical ionization, fast atom bombardment, inductively coupled plasma, desorption electrospray ionization, laser desorption ionization, and matrix-assisted laser desorption/ionization (MALDI) are some examples of ionization techniques that are commonly coupled to MS.[1] Just as there are numerous ways to introduce the sample, many different mass analyzers exist. The quadrupole, ion trap, time-of-flight, Fourier transform ion cyclotron resonance, Orbitrap, and various combinations are commonly used modern mass analyzers.[1] The work discussed in this dissertation focuses on a specialized form of MS known as MS imaging (MSI).

Mass Spectrometry Imaging

MSI is a powerful analytical tool that provides a spatially resolved chemical profile of the sample. MSI has been used to image metabolites and biomolecules[2–4] and in the recent years has been applied to the analysis of latent fingerprints.[5–8] MALDI is a widely used ionization technique for MSI. MALDI is salt tolerant, label free, and requires minimal sample preparation. Generally, MALDI is a soft technique that causes minimal to no fragmentation, and typically

results in singly charged ions. Each of these traits make it one of the most used MSI techniques for surface analysis of various samples types. As the name would imply, MALDI-MSI requires the application of a matrix to the sample surface to absorb laser energy and assist with desorption/ionization of the sample compounds.[1] A laser is rastered across the sample surface acquiring a mass spectrum at each pixel. Software is utilized to compile the mass spectrum acquired at each position into a pseudo heatmap image showing the intensity of particular compounds (*m/z* values) at each pixel on the sample surface.

Forensic researchers have been drawn to MALDI-MSI for latent fingerprint analysis because it provides ridge detail and a chemical profile in a single analysis while avoiding destruction of the evidence through extraction. The Francese group spearheaded MALDI-MSI of latent fingerprints and developed a protocol for dusting fingerprints with a MALDI matrix followed by spraying with a solvent for recrystallization to make the technique more applicable to the forensic community.[9,10] MSI analysis of latent fingerprints was utilized to potentially predict an individual's age,[5] gender,[11,12] or ethnicity[5] from the abundance of endogenous, or naturally excreted, compounds within the fingerprint. Exogenous compounds, those not naturally excreted from the human body, such as drugs or explosives are also shown to be present in latent fingerprints analyzed by MALDI-MSI.[13,14]

While some previous work partially explored the compatibility of realistic forensic samples with MALDI-MSI, little has been accomplished to utilized developed fingerprints "as received".[15] Most literature reported that fingerprint development techniques were inferior matrices compared to common MALDI matrices or were improved upon with an additional matrix.[16–18] A portion of the work presented here elaborates on the use of forensic development powders as MALDI matrices to streamline the process and increase the likelihood of MALDI-

MSI being adopted by forensic personnel. The remainder of the work focuses on increasing the evidentiary value of latent fingerprints through individual profiling and establishing the fingerprint age.

General MSI Workflow

While the sample preparation for MALDI-MSI varies depending on the sample type, the general workflow for the analysis of latent fingerprints is shown in **Figure 1**. The fingerprint was first collected from the participant on a precleaned glass slide. Depending on the study conducted (i.e. studying the compatibility of a particular development technique with MALDI-MSI), a forensic development technique such as powder dusting[19] or cyanoacrylate fuming[19] could be performed following the fingerprint collection. Next, a MALDI matrix and/or additives were applied to the surface of the fingerprint by sublimation-vapor deposition, spraying, or sputter coating. In this work, organic matrices were sprayed or sublimated, and metal matrices were sputtered. Additives, such as sodium acetate to promote the formation of sodiated adducts were sprayed using a TM Sprayer from HTX Technologies. It is worth noting that the first three steps could be combined in various forms. For example, if the forensic development is used as the matrix itself subsequent matrix or additive application would not be necessary. The fingerprint could also be lifted off the glass slide and analyzed on the back of forensic lifting tape for a more realistic sample. Following matrix application, the MSI experiment was set up and the laser was rastered across the surface while mass spectra were collected. The work presented here utilized a 100-micron raster step with an approximate laser spot size of 15-20 microns to image a section of the fingerprint, therefore preserving the forensic evidence by under-sampling. Next, the mass spectra were investigated for endogenous compound trends and exogenous compounds that

could be utilized to profile an individual. Once a compound was identified it was compiled into a pseudo heatmap image to display the intensity and local presence of the specific *m/z* value.

This work utilized a MALDI-linear ion trap-Orbitrap instrument, modified to incorporate a 355 nm Nd:YAG laser (**Figure 2**). The Orbitrap has high resolving power (30,000 at *m/z* 400) and accurate mass (+/- 5 ppm) providing the collection of high mass resolution mass spectra, while the linear ion trap is used to conduct tandem mass spectrometry (MS/MS). The combination of mass analyzers allowed the use of accurate mass for chemical formula determination and MS/MS for structural confirmation.

Dissertation Organization

This dissertation is organized into six chapters. The chapter above is a general introduction to MS and specifically MALDI-MSI as it applies to forensics. Chapters two through five specifically discuss research work that was published, submitted, and/or prepared for peer reviewed journals. In chapter two the use of a carbon forensic development powder as a matrix for MALDI is addressed. The third chapter analyzes titanium oxide forensic development powder as a MALDI matrix, with a specific focus on the impact of adding traditional MALDI matrices subsequent to development. Chapter four focuses on the development of an individual's lifestyle profile from the identification of exogenous compounds in their fingerprint. Chapter five examines the ambient ozonolysis of unsaturated triacylglycerols in fingerprints, and how it can be applied to determine the time since deposition of a questioned fingerprint. The final chapter summarizes the work mentioned in previous chapters and discusses the outlook of that work for forensic application.

References

(1) Gross, J. H. *Mass Spectrometry*, 2nd ed.; Springer Berlin Heidelberg: Berlin, Heidelberg, 2011. https://doi.org/10.1007/978-3-642-10711-5.

(2) Nemes, P.; Woods, A. S.; Vertes, A. Simultaneous Imaging of Small Metabolites and Lipids in Rat Brain Tissues at Atmospheric Pressure by Laser Ablation Electrospray Ionization Mass Spectrometry. *Anal. Chem.* **2010**, *82* (3), 982–988. https://doi.org/10.1021/ac902245p.

(3) Feenstra, A. D.; O'Neill, K. C.; Yagnik, G. B.; Lee, Y. J. Organic–Inorganic Binary Mixture Matrix for Comprehensive Laser-Desorption Ionization Mass Spectrometric Analysis and Imaging of Medium-Size Molecules Including Phospholipids, Glycerolipids, and Oligosaccharides. *RSC Adv.* **2016**, *6* (101), 99260–99268. https://doi.org/10.1039/C6RA20469D.

(4) Duenas, M.; Larson, E.; Lee, Y. J. Towards Mass Spectrometry Imaging in the Metabolomics Scale : Increasing Metabolic Coverage Through Multiple On-Tissue Chemical Modifications. **2019**, *10* (860). https://doi.org/10.3389/fpls.2019.00860.

(5) Zhou, Z.; Zare, R. N. Personal Information from Latent Fingerprints Using Desorption Electrospray Ionization Mass Spectrometry and Machine Learning. *Anal. Chem.* **2017**, *89* (2), 1369-1372. https://doi.org/10.1021/acs.analchem.6b04498.

(6) Bailey, M. J.; Bright, N. J.; Croxton, R. S.; Francese, S.; Ferguson, L. S.; Hinder, S.; Jickells, S.; Jones, B. J.; Jones, B. N.; Kazarian, S. G.; et al. Chemical Characterization of Latent Fingerprints by Matrix-Assisted Laser Desorption Ionization, Time-of-Flight Secondary Ion Mass Spectrometry, Mega Electron Volt Secondary Mass Spectrometry, Gas Chromatography/Mass Spectrometry, X-Ray Photoelectron Spec. *Anal. Chem.* **2012**, *84* (20), 8514–8523. https://doi.org/10.1021/ac302441y.

(7) Lauzon, N.; Dufresne, M.; Chauhan, V.; Chaurand, P. Development of Laser Desorption Imaging Mass Spectrometry Methods to Investigate the Molecular Composition of Latent Fingermarks. *J. Am. Soc. Mass Spectrom.* **2015**, *26* (6), 878–886. https://doi.org/10.1007/s13361-015-1123-0.

(8) Yagnik, G. B.; Korte, A. R.; Lee, Y. J. Multiplex Mass Spectrometry Imaging for Latent Fingerprints. *J. Mass Spectrom.* **2013**, *48* (1), 100–104. https://doi.org/10.1002/jms.3134.

(9) Ferguson, L.; Bradshaw, R.; Wolstenholme, R.; Clench, M.; Francese, S. Two-Step Matrix Application for the Enhancement and Imaging of Latent Fingermarks. *Anal. Chem.* **2011**, *83* (14), 5585–5591. https://doi.org/10.1021/ac200619f.

(10) Francese, S.; Bradshaw, R.; Ferguson, L. S.; Wolstenholme, R.; Clench, M. R.; Bleay, S. Beyond the Ridge Pattern: Multi-Informative Analysis of Latent Fingermarks by MALDI Mass Spectrometry. *Analyst* **2013**, *138* (15), 4215–4228. https://doi.org/10.1039/c3an36896c.

(11) Ferguson, L. S.; Wulfert, F.; Wolstenholme, R.; Fonville, J. M.; Clench, M. R.; Carolan, V. A.; Francese, S. Direct Detection of Peptides and Small Proteins in Fingermarks and Determination of Sex by MALDI Mass Spectrometry Profiling. *Analyst* **2012**, *137* (20), 4686–4692. https://doi.org/10.1039/c2an36074h.

(12) Emerson, B.; Gidden, J.; Lay, J. O.; Durham, B. Laser Desorption/Ionization Time-of-Flight Mass Spectrometry of Triacylglycerols and Other Components in Fingermark Samples. *J. Forensic Sci.* **2011**, *56* (2), 381–389. https://doi.org/10.1111/j.1556-4029.2010.01655.x.

(13) Bailey, M. J.; Bradshaw, R.; Francese, S.; Salter, T. L.; Costa, C.; Ismail, M.; P Webb, R.; Bosman, I.; Wolff, K.; de Puit, M. Rapid Detection of Cocaine, Benzoylecgonine and Methylecgonine in Fingerprints Using Surface Mass Spectrometry. *Analyst* **2015**, *140* (18), 6254–6259. https://doi.org/10.1039/c5an00112a.

(14) Kaplan-Sandquist, K.; LeBeau, M. A.; Miller, M. L. Chemical Analysis of Pharmaceuticals and Explosives in Fingermarks Using Matrix-Assisted Laser Desorption Ionization/Time-of-Flight Mass Spectrometry. *Forensic Sci. Int.* **2014**, *235*, 68–77. https://doi.org/10.1016/j.forsciint.2013.11.016.

(15) Bradshaw, R.; Denison, N.; Francese, S. Implementation of MALDI MS Profiling and Imaging Methods for the Analysis of Real Crime Scene Fingermarks. *Analyst* **2017**, *142* (9), 1581–1590. https://doi.org/10.1039/c7an00218a.

(16) Bradshaw, R.; Bleay, S.; Wolstenholme, R.; Clench, M. R.; Francese, S. Towards the Integration of Matrix Assisted Laser Desorption Ionisation Mass Spectrometry Imaging into the Current Fingermark Examination Workflow. *Forensic Sci. Int.* **2013**, *232*, 111–124. https://doi.org/10.1016/j.forsciint.2013.07.013.

(17) Kaplan-Sandquist, K. A.; LeBeau, M. A.; Miller, M. L. Evaluation of Four Fingerprint Development Methods for Touch Chemistry Using Matrix-Assisted Laser Desorption Ionization/Time-of-Flight Mass Spectrometry. *J. Forensic Sci.* **2015**, *60* (3), 611–618. https://doi.org/10.1111/1556-4029.12718.

(18) Lauzon, N.; Dufresne, M.; Beaudoin, A.; Chaurand, P. Forensic Analysis of Latent Fingermarks by Silver-Assisted LDI Imaging MS on Nonconductive Surfaces. *J. Mass Spectrom.* **2017**, *52* (6), 397–404. https://doi.org/10.1002/jms.3938.

(19) International Association for Identifcation. *The Fingerprint Sourcebook*; McRoberts, A., Ed.; U.S. Department of Justice, Office of Justice Programs, National Institute of Justice, 2011.

Figures

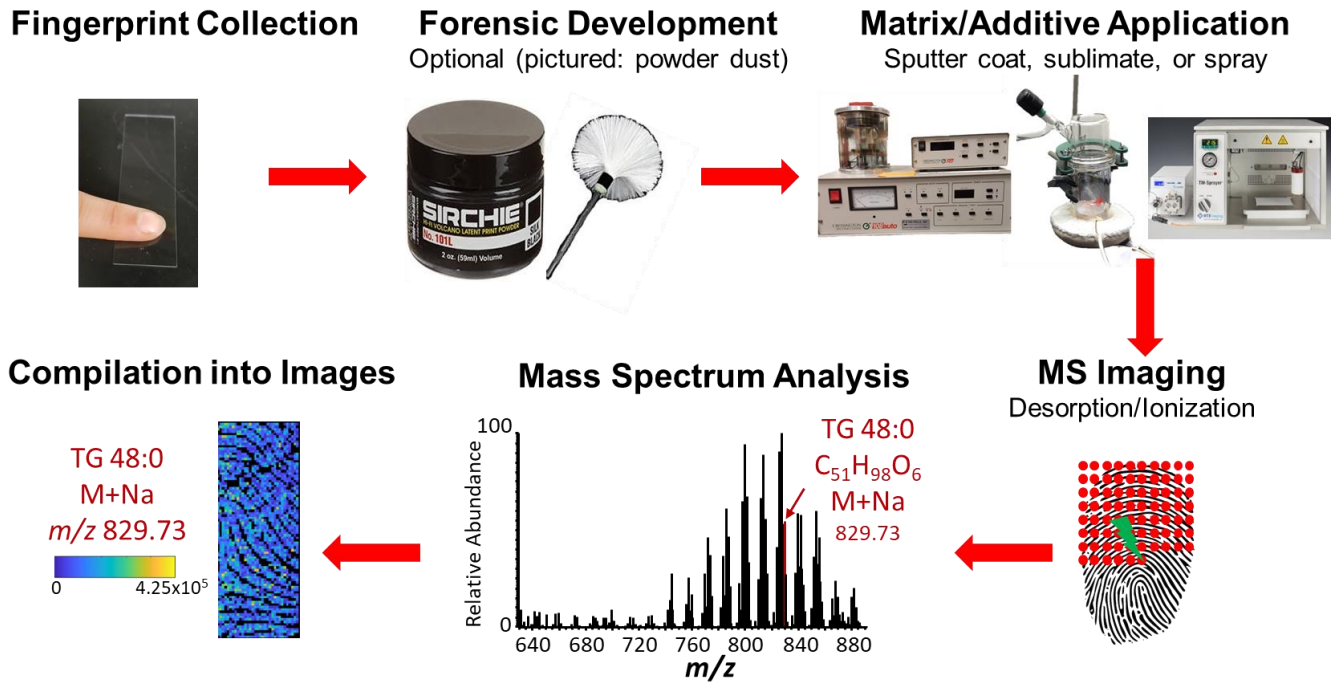

Figure 1. MALDI-MSI workflow for latent fingerprint analysis.

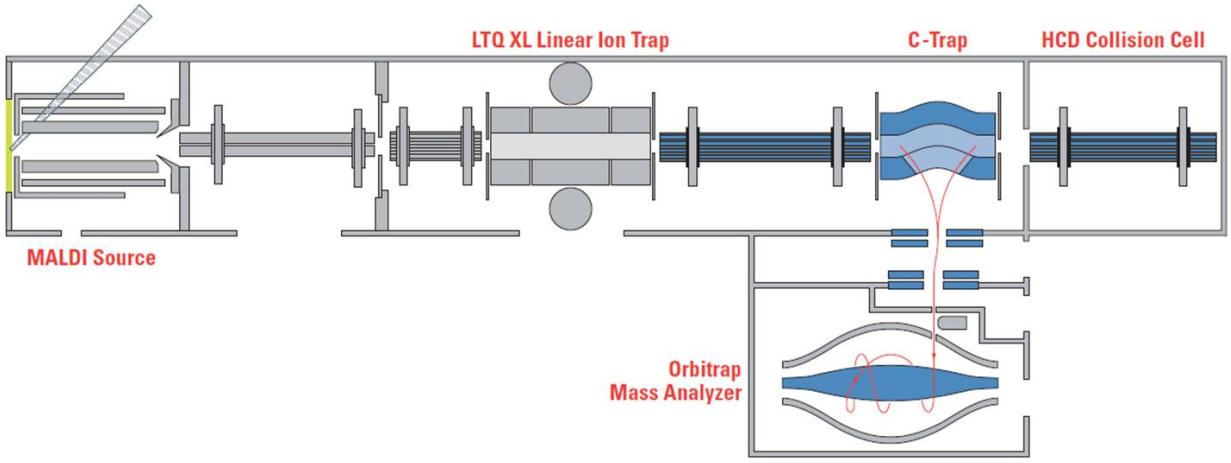

Figure 2. MALDI-linear ion trap-Orbitrap mass spectrometer utilized in this work.

CHAPTER 2. CARBON-BASED FINGERPRINT POWDER AS A ONE-STEP DEVELOPMENT AND MATRIX APPLICATION FOR HIGH-RESOLUTION MASS SPECTROMETRY IMAGING OF LATENT FINGERPRINTS

Paige Hinners and Young Jin Lee[1]

1. Department of Chemistry, Iowa State University, Ames, Iowa, 50011, USA

Modified from a manuscript published in *Journal of Forensic Sciences*

J Forensic Sci., 2019, 64, 1048-1056
Reproduced with permission of John Wiley and Sons

Abstract

Carbon-based materials are often used as matrices for matrix-assisted laser desorption/ionization mass spectrometry (MALDI-MS) and its imaging (MALDI-MSI). However, researchers have refrained from using carbon-based fingerprint powder (CFP) as a matrix due to high background and contamination. In this work the compatibility of CFP is re-evaluated with MALDI-MSI using a high-resolution mass spectrometer (HRMS) and compared to traditional organic matrices. Relevant fingerprint compounds were easily distinguished from carbon cluster peaks when using HRMS. For fair comparison, half of a fingerprint was dusted with CFP while the other half was dusted with traditional organic matrices. All compounds studied had comparable, or higher, signal-to-noise (S/N) ratios when CFP was used as the matrix. Additionally, chemical image qualities closely followed the trend of S/N ratios. CFP proved to be an effective one-step development and matrix application technique for MALDI-MSI of latent fingerprints, when carbon cluster peaks are well separated by a HRMS.

Introduction

The evidentiary value of fingerprints as a means of identification has long been recognized in the field of forensics. Latent prints, those not visible to the naked eye, are made visible using a variety of forensic development techniques. While a range of development

techniques exist, dusting non-porous surfaces with a carbon-based fingerprint powder (CFP) is one of the most widely accepted and utilized by forensic personnel around the world. Following development and collection, fingerprints are examined by fingerprint experts and compared against those in existing databases for identification based on the unique minutiae present. When no match exists in the database, investigators need additional techniques to provide useful forensic evidence. Recent forensic research has focused on the chemical analysis of fingerprints (1–4) in an effort to increase the evidentiary value and build a suspect profile based on the compounds detected, specifically when no match exists in the database. Both endogenous (i.e. triacylglycerols (TGs), fatty acids (FAs), amino acids, and peptides) and exogenous compounds (drugs, explosives, bug sprays, sunscreens, food related, etc.) detected in latent fingerprints have been utilized to develop suspect profiles and differentiate individuals (1–13).

Mass spectrometry imaging (MSI) has been a focus of fingerprint chemical analysis as it provides a spatial representation of all compounds detected. Fingerprint chemical compounds can be clearly distinguished from surface contaminations present before fingerprints are deposited because of their unique ridge patterns. In contrast, gas chromatography-mass spectrometry (GC-MS) analyzes the total extract of fingerprint and surface chemicals and cannot distinguish the two. Matrix-assisted laser desorption/ionization (MALDI) is the most common MSI method applied for the analysis of fingerprint compounds (3,4,13–15). MALDI-MSI requires a matrix to be deposited on the surface, so that laser energy can be absorbed to heat up the local surface and desorb/ionize surface molecules. As a common organic matrix, alpha-cyano-4-hydroxycinnamic acid (CHCA) has been studied thoroughly for the analysis of endogenous and exogenous compounds in fingerprints (4,10,13,16–18). CHCA has been applied to non-developed fingerprints and fingerprints developed with a variety of techniques, where in

some cases the additional matrix was shown to improve the ridge detail of poor development techniques such as vacuum metal deposition (19). The quality of the MS images, of both laboratory made prints and crime scene prints, was mostly affected by the forensic development technique rather than the use of a particular matrix (19,20). A two-step method, dusting of CHCA and solvent spray, showed promise as a development and matrix application for the analysis of fingerprints using MALDI-MSI (16,17). Although researchers have optimized the use of CHCA in the lab as a MALDI matrix, there is still a large gap between the research lab and field forensics. For example, CHCA is not yet widely accepted or cost effective as a development powder, nor would it work on all surfaces.

Various forms of carbon materials, such as carbon nanotubes, graphene, carbon pencil, graphite, and nanodiamond have proven to be effective MALDI matrices (21–25). Adopting an existing development technique, specifically CFP, as a matrix will increase the likelihood of MALDI-MSI being adopted by the forensic community and decrease sample preparation time, therefore streamlining the entire process. Previous studies have claimed that the high background and instrument contamination make CFP incompatible with MALDI-MSI (9,26). Under MALDI-MS conditions, carbon matrices produce a series of carbon clusters in the low mass range, but high-resolution mass spectrometer (HRMS) instruments are capable of separating closely related peaks overcoming the issue of carbon cluster background. It has also been reported that CFP does not work as an efficient matrix, and required additional CHCA for compound detection (27). However, Rowell et al. developed a hydrophobic silica powder containing carbon black that showed promise as a MALDI matrix (11). In this work, the compatibility of CFP as a one-step development and matrix application for MALDI-MSI with a

HRMS is evaluated, previously raised concerns of its use are addressed, and a direct comparison to CHCA and other organic matrices is performed.

Materials and Methods

Sample Preparation

A standard mixture of glycerol tripalmitate (TG 48:0) and palmitic acid (FA 16:0) was prepared at 100 μM in chloroform. A standard mixture for exogeneous compounds composed of pseudoephedrine, procaine, resveratrol, and hesperetin were prepared at 100 μM in methanol. All standards were purchased from Sigma-Aldrich (St. Louis, MO). Each standard mixture was spotted (2 μL) onto microarray plates (Hudson Surface Technology, Fort Lee, NJ) and allowed to air dry. Solutions of CHCA (Sigma-Aldrich) and CFP (Hi-Fi Volcano Latent Print Powder No. 101L; Sirchie, Youngsville, NC) were prepared in methanol, at 5 mg/mL and 2 μL of each matrix was spotted on top of the standards.

Fingerprint collection and analysis was approved by the Iowa State University Internal Review Board. To optically compare the visualization of CFP and CHCA, fingerprints were deposited on a glass slide and placed on a lab benchtop (dark background) and a white paper (light background) and dusted with both CFP and CHCA. For fingerprint compound comparison studies, a glass slide was cut in half. Fingerprint samples were prepared by touching the finger against the forehead followed by pressing lightly onto the precut glass slide. One half of each print was dusted with CHCA while the other half was dusted with CFP. A single brush (The Breeze; Safariland, Jacksonville, FL) was dedicated to each matrix and used through the entirety of the study. Fingerprint dusting studies were also performed with 2,5-dihydroxybenzoic acid (DHB) and 1,5-diaminonaphthalene (DAN), both purchased from Sigma-Aldrich. Mock fingerprints contaminated with exogenous compounds were prepared by applying the consumer

products (procaine, pain relief spray, bug spray, and sunscreen) as directed or handling the powder form of each substance prior to the fingerprint deposition. The same dusting procedure was applied to the exogenous prints as noted for the endogenous studies. CHCA, DHB, and DAN were manually ground prior to the dusting studies to increase their dusting efficiency and adherence to the fingerprints. The size of the particles was not measured.

For lifting experiments, the fingerprints were dusted with CFP and then lifted using fingerprint lifting tape (Scotch Fingerprint Lifting Tape 8004; 3M, St. Paul, MN). Lifted prints were attached onto a glass slide with the print side up using double sided tape. After the initial dusting and lifting, the lifted print was cut. A solvent spray step using a TM Sprayer (HTX Technologies, Chapel Hill, NC) was performed on one region of the cut lifted fingerprint. A solution consisting of 70:30 (v:v) acetonitrile (Sigma-Aldrich):0.1% aqueous trifluoroacetic acid (TFA; Fischer Scientific, Hampton, NH) was sprayed at a flow rate of 0.03 mL per minute for a total of eight passes.

Mass Spectrometry Imaging

Fingerprint samples were analyzed using a MALDI-linear ion trap-Orbitrap mass spectrometer (MALDI-LTQ-Orbitrap Discovery; Thermo Finnigan, San Jose, CA). The mass spectrometer is calibrated monthly or as needed, with which mass accuracy of 5ppm is routinely obtained. Mass spectra can be internally calibrated using matrix peaks when necessary to achieve 3ppm mass accuracy. The instrument was modified to incorporate an external frequency tripled 355 nm Nd:YAG laser (UVFQ; Elforlight, Ltd., Daventry, UK). HRMS images were collected using the Orbitrap mass analyzer (mass resolution setting of 30,000 at *m/z* 400). Data was acquired using a 100 μm raster step over the *m/z* range 100-1000 for positive mode, and 50-1000 for negative mode with a laser spot size of approximately 15 μm. A *m/z* mass range of 500-1000

was utilized for the targeted analysis of TGs. ImageQuest and Xcaliber software (Thermo Finnigan) were used for all data analysis.

Signal-to-Noise Ratio Comparison

The signal intensity and noise of each peak were extracted and averaged from each matrix region of the dusted fingerprints. While noise is automatically removed during Fourier transformation and centroid process, it is stored for each peak in the dataset and can be extracted. A signal-to-noise (S/N) ratio was then compiled for each peak of interest. When multiple adducts were present for a particular compound, the summed intensities was used for signal and a root mean square value was used for noise considering propagation of uncertainty**;** i.e., $\Sigma I_i/(\Sigma N_i^2)^{1/2}$ where I_i and N_i represent intensity of noise of adduct i (i=H^+, Na^+, and K^+). To display several S/N ratios on the same bar graphs, S/N ratios of some compounds were multiplied by a factor. The standard deviation of the S/N ratios was calculated and displayed as error bars in each subsequent graph. The positive error bar may have been truncated, but the magnitude of the variation in S/N ratio is still displayed by the negative portion of the error bar. No normalization for day-to-day or donor-to-donor variation was used.

Results and Discussion

General Compatibility of CFP with HRMS MALDI-MSI

The overall mass spectra, in both polarities, are dominated by carbon clusters, as displayed in **Figure 1**. CFP produces more odd number carbon clusters in positive mode (**Figure 1A**) and even number carbon clusters, some as the hydrogen adduct, in negative mode (**Figure 1B**). This pattern of carbon clusters are very similar to that of colloidal graphite reported by Yagnik et al. (see supplementary information of the reference), suggesting CFP might be mostly made of graphite particles (25). It is worth noting that CHCA also suffers from matrix

contamination of the low mass range, although to a lesser extent (28). Large molecules, such as TGs and diacylglycerols (DGs), are well separated from low mass carbon clusters, and clearly visible in the positive mode mass spectrum (**Figure 1A**). Small molecules in the mass range of carbon clusters are not readily discernible at a glance but can clearly be distinguished from carbon cluster peaks when zoomed in on the narrow mass range as shown in both of the inset mass spectra.

The experimental mass resolution of the HRMS in this study was 39,500 at *m/z* 279 and can readily distinguish minute mass differences. Specifically, in positive mode (**Figure 1A**), there are six peaks around *m/z* 279 but they can all be distinguished, including FA 16:0 ($[M+Na]^+$ at *m/z* 279.228). While the data was acquired in centroid mode, as often done in imaging data acquisition to minimize the file size, the profile mass spectra also showed clear separation (not shown). It is important to note that previous research using a MALDI time-of-flight (TOF) mass spectrometer utilized linear mode with a mass resolution of only around 5,000, with which the separation and assignment may be almost impossible for the small molecules in the carbon cluster mass range (9,26). This suggests that the incompatibility may be due to the limited mass resolution, not MALDI-MS in general. Additionally, MALDI-TOF data can be acquired with a higher mass resolution in reflectron mode but it is expected to suffer from significant background peaks due to metastable decomposition (i.e., post-source decay) of carbon clusters. In contrast, there is no metastable decomposition in the Orbitrap mass analyzer (or Fourier transform ion cyclotron resonance (FTICR) MS, not used in this study) as they will be thermally cooled down before the MS measurement. Thanks to this clear separation in the mass spectra, the extracted endogenous compound images in **Figure 1** also show the quality ridge detail when CFP is dusted as a matrix for MSI, suggesting the presence of carbon clusters does

not hinder our ability to compile relevant compound images. In addition to the *m/z* images of relevant fingerprint compounds, CFP related ions can also be used to compile fingerprint images. As shown in **Figure 2**, FA 16:1 and the $C_{12}H$ ion show essentially the same ridge pattern. Considering the fact that the CFP adheres to the ridges and provides high ion signals for CFP related peaks, the high-quality images of CFP peaks can be used for the database search when the optical image does not provide sufficient image quality. While the CFP and fingerprint related compounds are detected on the fingerprint ridges, the dusting nature of the matrix application did not disturb the location of the compounds by pushing them into the valleys.

Another common claim of the limitation of CFP is that it easily contaminates the MALDI ion source. Following months of studies, accumulation of CFP in the MALDI source was noted when performing general instrument cleaning, but not any more than the typical buildup of organic matrices. More importantly, in spite of the buildup of CFP in the source, no contamination of carbon cluster peaks in other MALDI mass spectra were observed. This is in contrast to other commonly used organic matrices which often contaminate other spectra even when they are not being used as a matrix for that analysis. To demonstrate the lack of cross-spectra contamination, the averaged spectra from two regions of the same fingerprint are shown in **Figure 3**. The top portion of the fingerprint was dusted with CFP and analyzed first, while the bottom portion was dusted with CHCA and analyzed after the CFP portion. The spectrum from the CHCA region contains no carbon clusters, while the CFP and CHCA region contain a contamination DHB peak from other work being done on the instrument. Black dust is expected to be less of an issue on lifted prints as the powder will be more stationary on tape compared to the glass slide.

Comparison of CFP with Organic Matrices

Of the organic matrices studied for the analysis of fingerprints, CHCA has been the most widely applied and studied, particularly with a dusting application (13,16,18). Therefore, to evaluate the feasibility of using CFP as a matrix a direct comparison to CHCA was performed. The comparison of CFP with CHCA began with standards, including endogenous compounds (TG 48:0 and FA 16:0) and potential exogenous compounds (procaine, pseudoephedrine, hesperetin, and resveratrol). Analyzing standards is the most accurate way to measure desorption/ionization efficiency using different matrices because fingerprints themselves are extremely variable, as will be shown later. In traditional MALDI analysis, peaks of interest are often normalized to a matrix peak or total ion count (TIC) to account for run-to-run variation. Normalization allows for the comparison of compounds across different instrument acquisitions. Due to overall intensity differences when comparing two matrices, normalization to the matrix peak or TIC should not be done in this case. A comparison of S/N ratios is the most appropriate method to compare the efficiency of the two different matrices. In each independent experiment, CHCA and CFP were used in parallel, but day-to-day variation of S/N was not corrected. Optimum experimental conditions can vary for different matrices, especially laser energy; however, both CHCA and CFP performed optimally with the laser energy of 90-91% used in this study.

As shown in **Figure 4**, in both positive and negative mode, the standards showed higher S/N ratios when CFP was used as the matrix, with the exception of procaine, a tertiary amine, in positive mode. The x0.1 and x10 refer to a change in the S/N ratio in order to visualize all compounds on the same graph. For example, in positive mode the procaine S/N ratio was multiplied by 0.1 to scale the S/N ratio similar to other studied compounds. The exogenous

compounds studied include pharmaceuticals, pseudoephedrine and procaine, and food related substances, hesperetin and resveratrol. The endogenous standards studied include a FA and TG. Total carbon chain length (xx) and the number of double bonds (yy) in FAs and TGs are represented by xx:yy format. The range of compounds studied were all detected with CFP, demonstrating the promise of CFP as a MALDI matrix for fingerprint related compounds.

Following standard analysis, CFP and CHCA were compared as dusting powders. Latent fingerprints require development for visualization prior to collection and further analysis of the fingerprints. CFP works well for visualization (**Figure 5**) of latent fingerprints, particularly on light backgrounds. Under ambient light, the bright yellow of CHCA offers a development advantage on dark surfaces but not on bright surfaces. No alternate light sources were employed for visualization. Furthermore, CHCA is much more expensive than the CFP, limiting its adoption by the forensic community. Grinding is necessary to improve the dusting efficiency of CHCA as also reported by others (17), because CHCA powder, as received from the supplier, poorly adhered to the fingerprints without grinding. In contrast, it was not necessary to grind CFP to improve adherence to the fingerprint residues.

The matrix potential of CFP versus CHCA after dusting of the two matrices on fingerprints was then evaluated. CFP proved to be an efficient matrix for endogenous compounds in both polarities based on S/N ratios and selected compound images, as shown in **Figure 6A**. Particularly, CFP worked well for the analysis of medium molecular weight compounds in positive mode such as TGs (MW 720-920). The S/N ratios of FAs in positive mode were comparable using both matrices, but CFP is much better in negative mode for all FAs (**Figure 6A**) as well as all the exogeneous compounds that were tested (**Figure 6B**). This is not surprising because in general CHCA is a good matrix for positive mode and carbon matrices are known to

work well in negative mode. In positive mode exogenous compound analysis, tertiary amines and quaternary ammonium compounds (i.e., procaine, cetrimonium ion, and dimethyldioctadecylammonium ion) had higher S/N ratios when using CHCA (**Figure 6B**). Quaternary ammonium compounds are common in cosmetic and hygiene products and are not useful in developing an individual profile from fingerprint chemical analysis.

Exogenous compounds offer the potential for lifestyle determination, as shown in previous work (3). Bug spray and sunscreen, as well as sunburn pain relief spray, would be indicative of an outdoor lifestyle and were therefore used in this study. Although drugs and explosives have previously been studied by other authors, procaine was included to mimic the presence of drugs in fingerprints as it is related to cocaine. The hexose compounds and quaternary ammonium compounds are commonly detected and reported in fingerprints and were not purposefully added. Confident identification of the detected compounds is necessary to strengthen the forensic evidence and confirm the compounds identity. However, MS/MS was not performed in this work as we have already reported the MS/MS in previous work.

The dusting and matrix efficiency of CFP was also compared to other commonly used organic matrices. Endogenous compounds that were not well detected with CHCA were specifically targeted. CHCA did not work well for the detection of TGs in positive mode, nor for FAs in negative mode. DAN and DHB are commonly used organic matrices for small molecule analysis, especially for FAs in negative mode and TGs in positive mode, respectively. DAN and DHB were dusted on fingerprints and analyzed by MALDI-MS in negative and positive mode, respectively, with CFP in parallel. As with CHCA, both DHB and DAN were also ground prior to dusting. CFP showed higher S/N ratios for all FAs than DAN (**Figure 7A**) and for TGs than DHB (**Figure 7B**). Most importantly the ridge quality of the CFP dusted prints was drastically

better than those dusted with DAN or DHB. DHB is a commonly employed organic matrix for the analysis of lipids such as TGs in MALDI-MSI of fingerprints (14,29); however, almost no ridge detail was evident in the DHB images, likely because of its poor adherence to fingerprints.

CFP Dusting and Lifting Studies

Finally, a more realistic experiment where the fingerprints were dusted with CFP, lifted with forensic lifting tape, and analyzed by MALDI-MSI was performed. Multiple types of tapes were tested for lifting but did not conclusively determine which one is particularly better; therefore, the same tape was used for all experiments. In the initial lifting studies, a decrease in the S/N ratio compared to direct on slide analysis was noted. It is not surprising as the lifted fingerprint is second generation to the primary fingerprint on the surface. To compensate for the decreased signal, an additional solvent spray step was investigated that had been suggested to improve desorption/ionization efficiency by the Francese group (16). **Figure 8** shows the S/N ratio of lifted fingerprints without (CFP Dry) and with additional solvent spray (CFP Wet). The S/N ratio of all the compounds detected were lower in lifted fingerprints, both dry and wet, than the previous on-slide dusting studies (**Figure 6**). The signal decrease is relatively mild for FAs, only about a factor of five (**Figure 8A**) but is significant for some other compounds. Signals for sunscreen compounds (avobenzone, octocrylene, oxybenzone) are decreased by more than 200 times, and lidocaine is decreased by approximately 45 times in the dry lifts (**Figure 8B**). Most notably, TG signals are virtually not present without solvent spray. The solvent spray step dramatically increased the S/N ratio for some compounds, greater than a factor of 10, compared to dry lifts and improved the ridge clarity in the compound images. The dry versus wet chemical images are from two regions of the same fingerprint that were cut apart prior to applying the additional solvent. The solvent spray following lifting of the CFP dusted prints did increase the

likelihood of detecting TGs, but the S/N ratio was still around 60 times lower than before tape-lifting. As most compounds could be detected in the dry lifts, signal enhancement with solvent could be optional but is recommended to improve S/N and image clarity for many compounds.

Factors of Consideration for Forensic Personnel

Cross contamination of compounds from one fingerprint to another due to the use of a single brush would be of concern to forensic practitioners. Although disposable brushes are already marketed to prevent contamination from one crime scene to another, downstream chemical analysis from multiple fingerprints at a crime scene could potentially require the use of one brush per fingerprint if cross contamination of chemical compounds were an issue. In this work, a single brush was used for each matrix for the entire study but there was no noticeable contamination. **Figure 9** shows the mass spectra (*m/z* range 200 to 250) and MS images in two subsequent fingerprint imaging experiments. The procaine print was prepared, dusted, and analyzed first, followed by the sunscreen fingerprint. No procaine was present in the spectrum of the sunscreen fingerprint or in the MS image. Utilizing a single brush throughout the entire study did not lead to compound cross contamination between fingerprints, therefore chemical cross contamination from the dusting brush would not be an issue for forensic practitioners.

Fundamentally mass spectrometry is a destructive technique, making the application to real forensic evidence more difficult, especially when extracted with solvent for GC or liquid chromatography (LC)-MS analysis. However, MALDI-MSI is typically performed on only a region of the fingerprint, leaving the remainder undisturbed. Furthermore, the fingerprint is under-sampled in this work using a laser spot size of 15 μm fired every 100 μm with a very gentle laser energy; thus, leaving a majority of the fingerprint unaffected. **Figure 10** shows the optical images before and after MALDI-MSI while the scanned image at the center shows where

MALDI-MSI was performed. Even after acquiring MALDI-MSI for a portion of the fingerprint, there was no apparent difference in optical images, suggesting it can be preserved as forensic evidence. Further work is necessary to fully integrate MALDI-MSI into the forensic workflow, but fingerprints subjected to MALDI-MSI with CFP can still be preserved and submitted for conventional fingerprint identification.

A major consideration for adopting MALDI-MSI into the fingerprint workflow is transportation of the samples. Fingerprints are typically sealed onto a backing card or sealed within an acetate lifter. The Francese group utilized a specialized transportation procedure to transfer lifted fingerprints from the crime scene to the lab (20). Future studies into the best transportation and preservation method are necessary. A particular focus should be on the analysis of fingerprints sealed in an acetate lifter or onto a backing card for transportation and storage.

MALDI-MSI of fingerprints would increase the overall analysis time but it is relatively minimal. A laser spot size of 15 μm was used, but sampling was done with a 100 μm step size for only a region of the fingerprint. The data acquisition time in this work was two hours or less, and there was no sample preparation time, except when additional solvent spray is performed taking roughly ten minutes per fingerprint. The total data acquisition time would be comparable to GC- or LC-MS analysis considering extraction and sample preparation time. Currently, data analysis is the most time-consuming step, especially identification of unknown compounds detected from a non-targeted analysis. With the development of relevant fingerprint compound databases, the analysis time could be minimized in the future. The additional training and analysis time associated with MALDI-MSI of fingerprints would need to be weighed against the severity of the crime. A low-profile property crime may not demand such an in-depth analysis,

while a more high-profile case would justify the additional analysis time and information from MALDI-MSI of latent fingerprints.

Conclusions

Previously published work has already proven the usefulness and potential of individual profiling based on chemical analysis of latent fingerprints. Particular promise has been shown with MALDI-MSI. Importantly, this work serves to simplify and streamline MALDI-MSI of latent fingerprints, for individual profiling through chemical analysis, by using a common forensic development technique as the matrix.

In this work, CFP is shown to be compatible with MALDI-MSI, specifically using a HRMS by clearly distinguishing carbon clusters from fingerprint compounds of interest. An Orbitrap mass analyzer was used in the current study, but other HRMS such as an FTICR mass analyzer or quadrupole TOF mass analyzer would also work well for the current purpose. CFP is an efficient matrix for standards as well as fingerprint compounds in both positive and negative mode. In the direct comparison to other organic matrices, CFP proved comparable, if not better, across many compounds, again in both polarities. The flexibility of using CFP in both positive and negative mode gives it an advantage over CHCA which is generally more useful only in positive mode. Most importantly CFP is adequate for fingerprint visualization as a development powder as well as serving as an efficient MALDI matrix, streamlining the overall process and improving the compatibility of MALDI-MSI with the current forensic practices.

It is worthwhile to note that this streamlined method is applicable for fingerprints developed with CFP. If a different development technique is utilized at the crime scene downstream MALDI matrix application would be necessary. Future work will focus on

untargeted compound identification as well as non-deal samples, such as aged or poorly developed, to further determine the usefulness of MALDI-MSI for forensic chemical profiling.

References

1. Croxton RS, Baron MG, Butler D, Kent T, Sears VG. Development of a GC-MS method for the simultaneous analysis of latent fingerprint components. J Forensic Sci 2006;51(6):1329–33.

2. De Puit M, Ismail M, Xu X. LCMS analysis of fingerprints, the amino acid profile of 20 donors. J Forensic Sci 2014;59(2):364–70.

3. Hinners P, O'Neill KC, Lee YJ. Revealing individual lifestyles through mass spectrometry imaging of chemical compounds in fingerprints. Sci Rep 2018;8:5149.

4. Bailey MJ, Bright NJ, Croxton RS, Francese S, Ferguson LS, Hinder S, et al. Chemical characterization of latent fingerprints by matrix-assisted laser desorption ionization, time-of-flight secondary ion mass spectrometry, mega electron volt secondary mass spectrometry, gas chromatography/mass spectrometry, X-ray photoelectron spectroscopy, and attenuated total reflection fourier transform infrared spectroscopic imaging: an intercomparison. Anal Chem 2012;84(20):8514–23.

5. Zhou Z, Zare RN. Personal information from latent fingerprints using desorption electrospray ionization mass spectrometry and machine learning. Anal Chem 2017;89(2):1369-72.

6. Ferguson LS, Wulfert F, Wolstenholme R, Fonville JM, Clench MR, Carolan VA, et al. Direct detection of peptides and small proteins in fingermarks and determination of sex by MALDI mass spectrometry profiling. Analyst 2012;137(20):4686–92.

7. Cadd SJ, Mota L, Werkman D, Islam M, Zuidberg M, de Puit M, et al. Extraction of fatty compounds from fingerprints for GCMS analysis. Anal Methods 2015;7(3):1123–32.

8. Bailey MJ, Bradshaw R, Francese S, Salter TL, Costa C, Ismail M, et al. Rapid detection of cocaine, benzoylecgonine and methylecgonine in fingerprints using surface mass spectrometry. Analyst 2015;140(18):6254–9.

9. Kaplan-Sandquist K, LeBeau MA, Miller ML. Chemical analysis of pharmaceuticals and explosives in fingermarks using matrix-assisted laser desorption ionization/time-of-flight mass spectrometry. Forensic Sci Int 2014;235:68–77.

10. Groeneveld G, de Puit M, Bleay S, Bradshaw R, Francese S. Detection and mapping of illicit drugs and their metabolites in fingermarks by MALDI MS and compatibility with forensic techniques. Sci Rep 2015;5:11716.

11. Rowell F, Hudson K, Seviour J. Detection of drugs and their metabolites in dusted latent fingermarks by mass spectrometry. Analyst 2009;134(4):701–7.

12. Guinan T, Della Vedova C, Kobus H, Voelcker NH. Mass spectrometry imaging of fingerprint sweat on nanostructured silicon. Chem Commun 2015;51:6088–91.

13. Francese S, Bradshaw R, Ferguson LS, Wolstenholme R, Clench MR, Bleay S. Beyond the ridge pattern: multi-informative analysis of latent fingermarks by MALDI mass spectrometry. Analyst 2013;138(15):4215–28.

14. O'Neill KC, Hinners P, Lee YJ. Chemical imaging of cyanoacrylate-fumed fingerprints by matrix-assisted laser desorption/ionization mass spectrometry imaging. J Forensic Sci 2018;63(6):1854-57.

15. Yagnik GB, Korte AR, Lee YJ. Multiplex mass spectrometry imaging for latent fingerprints. J Mass Spectrom 2013;48:100–4.

16. Ferguson L, Bradshaw R, Wolstenholme R, Clench M, Francese S. Two-step matrix application for the enhancement and imaging of latent fingermarks. Anal Chem 2011;83(14):5585–91.

17. Ferguson LS, Creasey S, Wolstenholme R, Clench MR, Francese S. Efficiency of the dry-wet method for the MALDI-MSI analysis of latent fingermarks. J Mass Spectrom 2013;48(6):677–84.

18. Wolstenholme R, Bradshaw R, Clench MR, Francese S. Study of latent fingermarks by matrix-assisted laser desorption/ionisation mass spectrometry imaging of endogenous lipids. Rapid Commun Mass Spectrom 2009;23(19):3031–9.

19. Bradshaw R, Bleay S, Wolstenholme R, Clench MR, Francese S. Towards the integration of matrix assisted laser desorption ionisation mass spectrometry imaging into the current fingermark examination workflow. Forensic Sci Int 2013;232:111–24.

20. Bradshaw R, Denison N, Francese S. Implementation of MALDI MS profiling and imaging methods for the analysis of real crime scene fingermarks. Analyst 2017;142(9):1581–90.

21. Pan C, Xu S, Hu L, Su X, Ou J, Zou H, et al. Using oxidized carbon nanotubes as matrix for analysis of small molecules by MALDI-TOF MS. J Am Soc Mass Spectrom 2005;16(6):883–92.

22. Dong X, Cheng J, Li J, Wang Y. Graphene as a novel matrix for the analysis of small molecules by MALDI-TOF MS. Anal Chem 2010;82(14):6208–14.

23. Xu S, Li Y, Zou H, Qiu J, Guo Z, Guo B. Carbon nanotubes as assisted matrix for laser desorption/ionization time-of-flight mass spectrometry. Anal Chem 2003;75(22):6191–5.

24. Chen Y-C, Wu J-Y. Analysis of small organics on planar silica surfaces using surface-assisted laser desorption/ionization mass spectrometry. Rapid Commun Mass Spectrom 2001;15(20):1899–903.

25. Yagnik GB, Hansen RL, Korte AR, Reichert MD, Vela J, Lee YJ. Large scale nanoparticle screening for small molecule analysis in laser desorption ionization mass spectrometry. Anal Chem 2016;88(18):8926–30.

26. Kaplan-Sandquist KA, LeBeau MA, Miller ML. Evaluation of four fingerprint development methods for touch chemistry using matrix-assisted laser desorption ionization/time-of-flight mass spectrometry. J Forensic Sci 2015;60(3):611–8.

27. Bradshaw R, Denison N, Francese S. Development of operational protocols for the analysis of primary and secondary fingermark lifts by MALDI-MS imaging. Anal Methods 2016;8(37):6795–804.

28. Calvano CD, Monopoli A, Cataldi TRI, Palmisano F. MALDI matrices for low molecular weight compounds: an endless story? Anal Bioanal Chem 2018;410(17):4015–38.

29. O'Neill KC, Lee YJ. Effect of aging and surface interactions on the diffusion of endogenous compounds in latent fingerprints studied by mass spectrometry imaging. J Forensic Sci 2018;63(3):708–13.

Figures

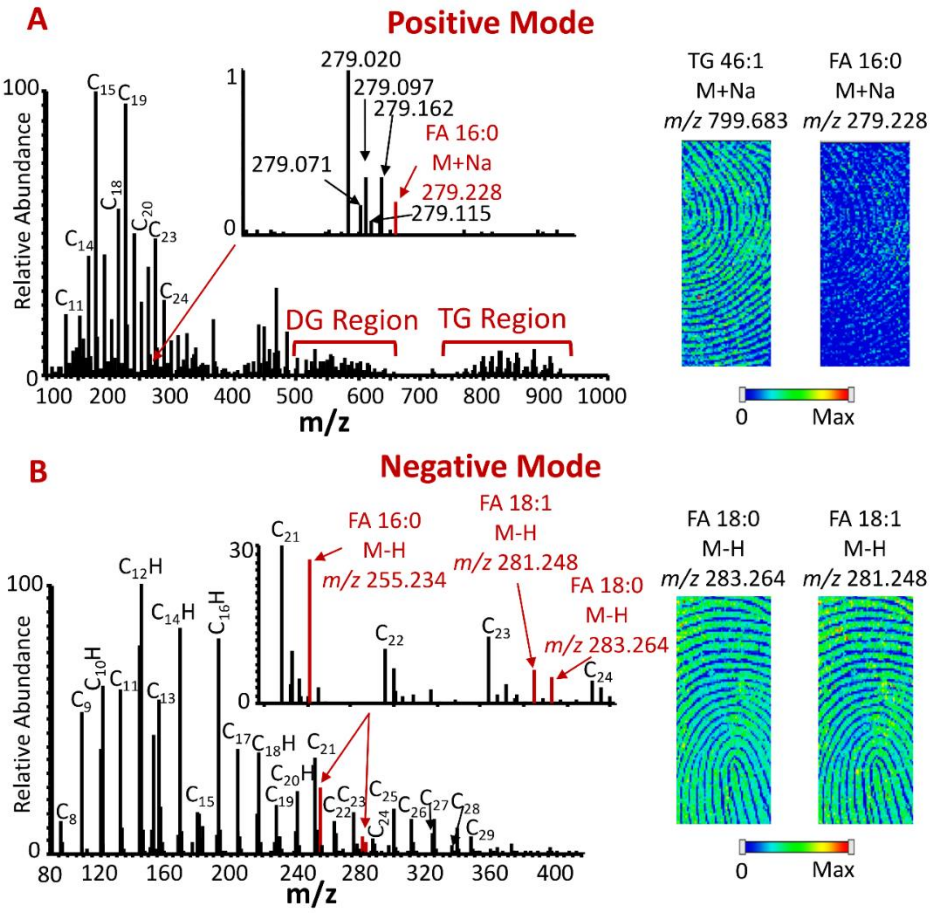

Figure 1. High-resolution mass spectra of CFP dusted fingerprints in positive **(A)** and negative **(B)** polarities. The inset mass spectra display the zoomed-in regions of interest containing fingerprint compounds, demonstrating clear separation from other peaks. High quality compound images are produced when using CFP as a development powder and matrix.

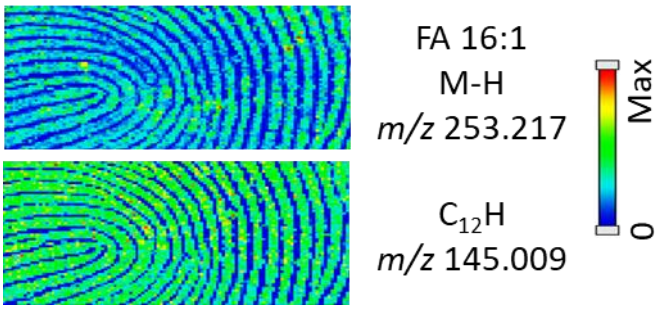

Figure 2. MALDI MS images of a FA and carbon cluster showing the distribution on the fingerprint ridge.

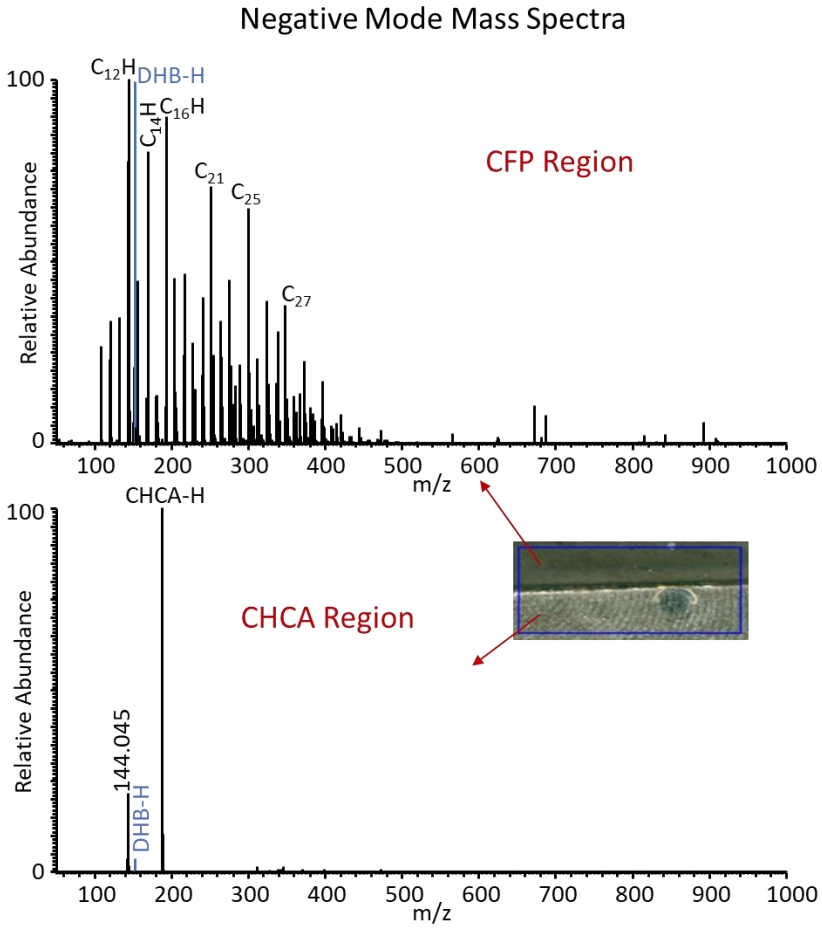

Figure 3. The negative mode mass spectra of the CFP and CHCA region of the same fingerprint. The CHCA region was acquired after the CFP region and contains no carbon cluster contamination.

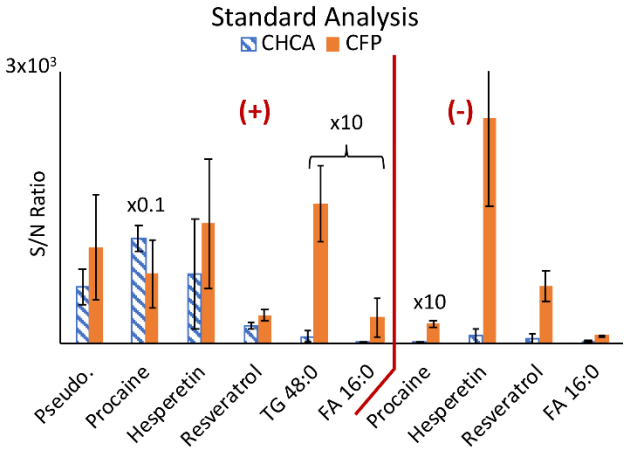

Figure 4. Standard analysis comparing the efficiency of CHCA and CFP as matrices in positive and negative mode. S/N ratios are multiplied by a factor in order to display each compound on the same graph. Multiplication factors are noted in the figure. Pseudo: Pseudoephedrine.

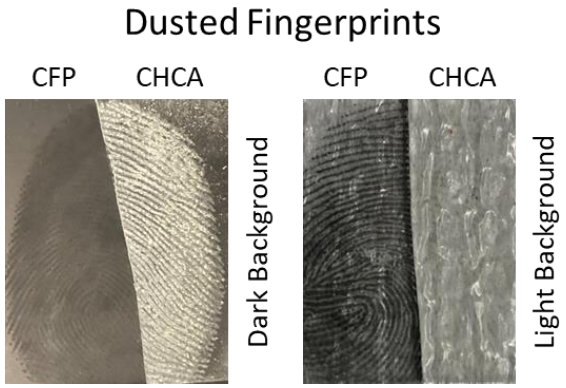

Figure 5. Optical images of CFP and CHCA dusted fingerprints on both dark and light backgrounds.

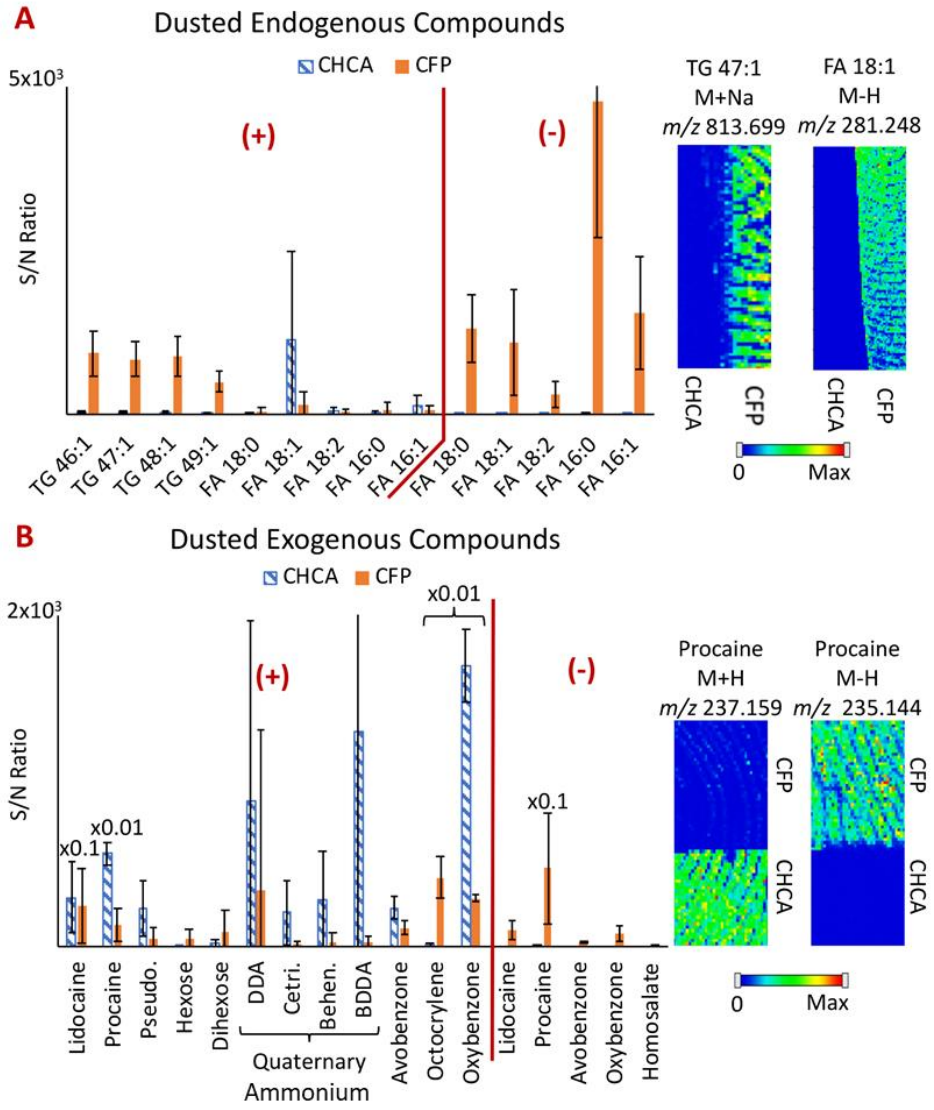

Figure 6. Endogenous **(A)** and exogenous **(B)** compound analysis comparing the MALDI-MS efficiency of CHCA and CFP after fingerprint dusting. Selected MS images are also compared between the two matrices. Total carbon chain length (xx) and the number of double bonds (yy) in FAs and TGs are represented by xx:yy format. S/N ratio multiplication factors are shown in the graph and were used to display all compounds on the same graph. Pseudo: Pseudoephedrine, DDA: Dimethyldioctadecylammonium, Cetri.: Cetrimonium, Behen.: Behentrimonium, BDDA: Benzyldimethyldodecylammonium.

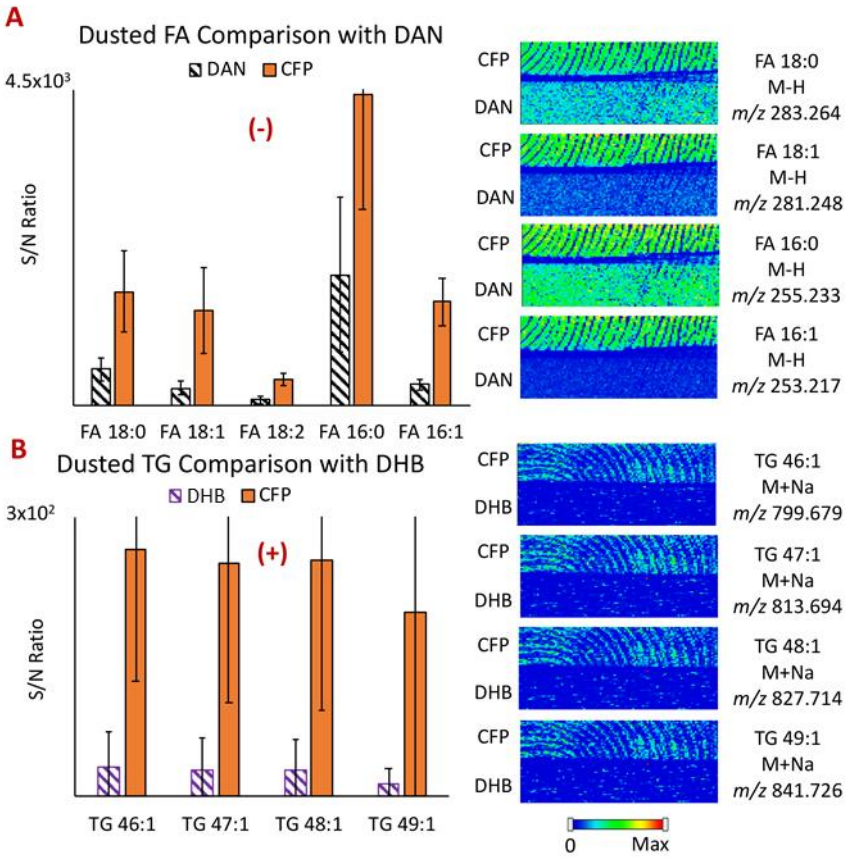

Figure 7. Endogenous compound analysis comparing the MALDI-MS efficiency of CFP with **(A)** DAN in negative mode and **(B)** DHB in positive mode. MS images are also compared between CFP and the organic matrices.

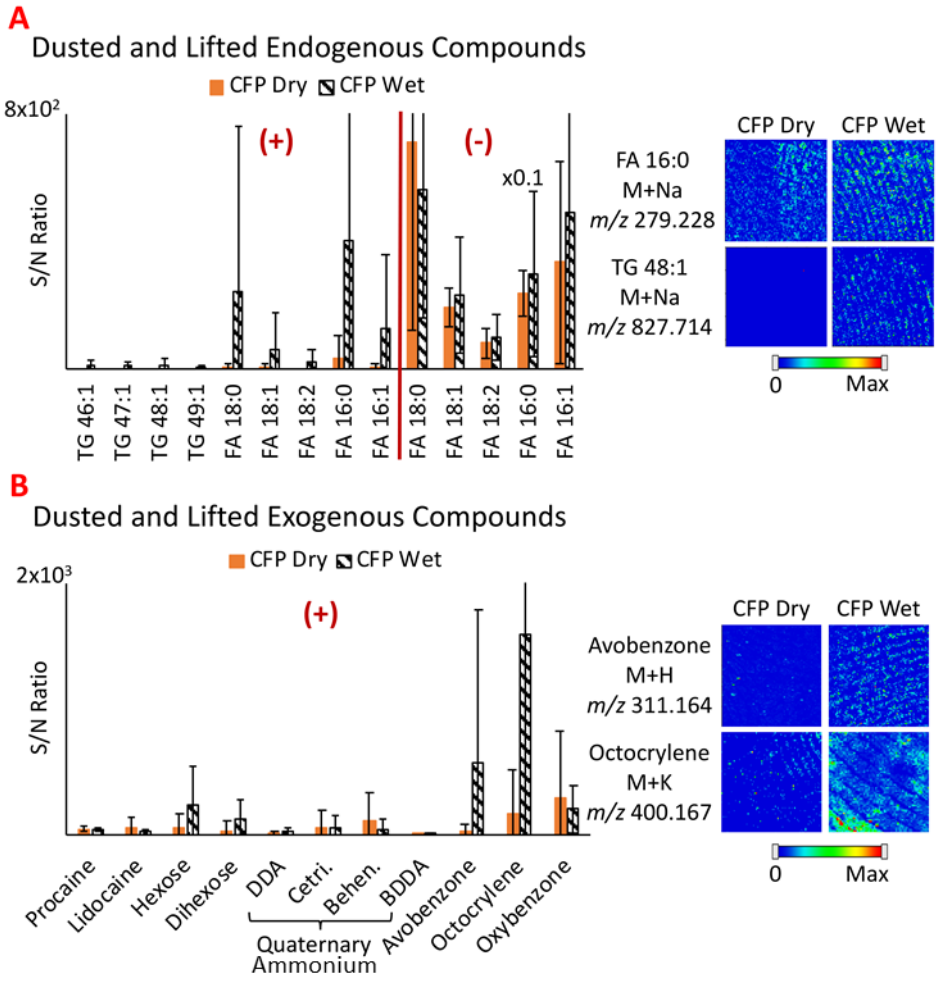

Figure 8. Endogenous **(A)** and exogenous **(B)** compound analysis following dusting with CFP and lifting with forensic tape. 'CFP Dry' denotes direct MALDI-MS analysis of lifted fingerprints. 'CFP Wet' denotes the solvent spray (70:30 acetonitrile:0.1% aqueous TFA in volume) on the lifted fingerprints. The fingerprints analyzed, and images displayed are regions of the same fingerprint cut apart following lifting. S/N ratios were multiplied by a factor (displayed on the graph) to show each compound on the same graph. DDA: Dimethyldioctadecylammonium, Cetri.: Cetrimonium, Behen.: Behentrimonium, BDDA: Benzyldimethyldodecylammonium.

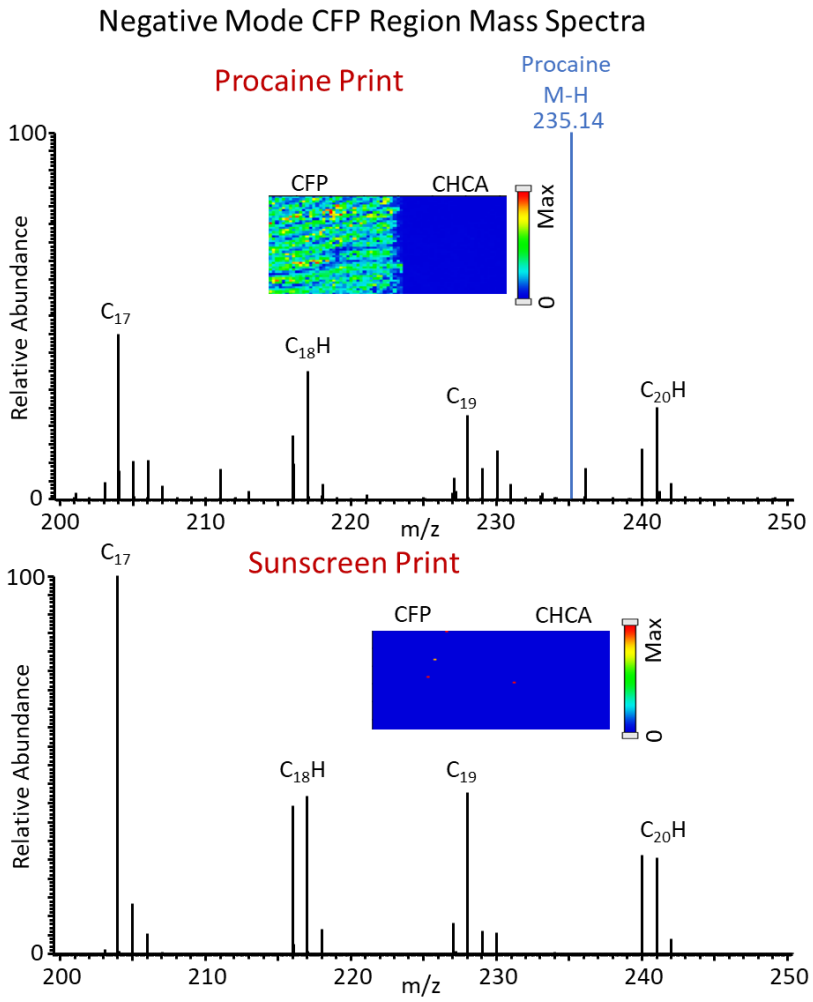

Figure 9. Negative mode mass spectra of two mock exogenous fingerprints. The procaine print was dusted first, followed by the sunscreen print. No peaks related to procaine are detected in the sunscreen spectrum or MS image, suggesting no cross-over contamination by the brush.

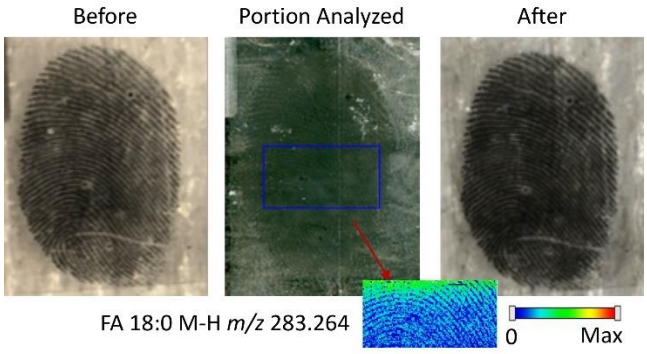

Figure 10. The optical images of a fingerprint before and after MALDI-MSI analysis. The portion of the fingerprint analyzed is still visible following analysis.

CHAPTER 3. MASS SPECTROMETRY IMAGING OF FINGERPRINTS USING TITANIUM OXIDE DEVELOPMENT POWDER AS AN EXISTING MATRIX

Paige Hinners, Haley Dunn, and Young Jin Lee[1]

1. Department of Chemistry, Iowa State University, Ames, Iowa, 50011, USA

Manuscript prepared for submission to *Rapid Communications in Mass Spectrometry*

Abstract

Rationale: Recent research has focused on increasing the evidentiary value of fingerprints through chemical analysis. Researchers optimized the use of organic and metal matrices for matrix-assisted laser desorption/ionization - mass spectrometry imaging (MALDI-MSI) of fingerprints. The use of development powders as matrices has not been fully investigated. Carbon forensic powder (CFP) was shown to be an efficient one-step matrix; however, a high-resolution mass spectrometer was required in low mass range due to carbon clusters. Titanium oxide (TiO_2) is another commonly used development powder, especially for dark surfaces. Here, the use of forensic TiO_2 powder as a single-step development and matrix technique for chemical imaging of fingerprints.

Methods: Split fingerprints were dusted with CFP and TiO_2 forensic powders and analyzed using a MALDI-LTQ-Orbitrap Discovery. The signal-to-noise (S/N) ratio and MS image quality of endogenous and exogenous compounds were directly compared between the matrices. MALDI matrices (alpha-cyano-4-hydroxycinnamic acid (CHCA), 2,5-dihydroxybenzoic acid (DHB), silver, and gold with sodium) were applied on top of the TiO_2 and compared to the development powder alone. Dusted CHCA was also compared to TiO_2 as a development matrix combination.

Results: All compounds were successfully detected when TiO2 was used as the matrix in positive mode, although the overall ion signals were lower than the previously studied CFP. TiO2 provided quality MS images of endogenous and exogenous fingerprint compounds. The subsequent addition of traditional matrices on top of the TiO2 powder was ineffective for universal detection of fingerprint compounds. TiO2 was also a more efficient matrix for endogenous compound analysis than dusted CHCA.

Conclusions: Forensic TiO_2 development powder works as an efficient single-step development and matrix technique for MALDI-MSI analysis of fingerprints in positive mode and does not require a high-resolution mass spectrometer for analysis. Additional matrix is necessary for negative mode analysis.

Introduction

Identification of individuals through fingerprint pattern comparison has been a valuable forensic tool for over a century. However, traditionally if no pattern match exists in a database, the value of the fingerprint drastically decreases. Recent research efforts are focused on developing chemical analysis methods to increase the evidentiary value of fingerprints.

Gas chromatography – mass spectrometry (GC-MS) and liquid chromatography – tandem mass spectrometry (LC-MS/MS) are chromatography-based techniques that have been applied to the chemical analysis of latent fingerprints. Chromatography methods have made significant advances in identifying chemicals that are endogenous to fingerprints, including amino acids,[1] fatty acids (FAs),[2] wax esters (WEs),[3] and triacylglycerols (TGs) among others.[4] However, these approaches require an extraction, potential derivatization, and may need multiple fingerprints. Additionally, they are unable to separate background chemicals from the surface the fingerprint was deposited on and destroy the fingerprint evidence through the extraction process.

MS imaging (MSI) approaches are utilized to collect both a chemical and spatial profile of a fingerprint without performing an extraction. In research studies, chemical profiling of latent fingerprint residue by MSI has focused on identifying the lifestyle,[5] gender,[6,7] ethnicity and/or age[8] of an unknown individual based on both endogenous and exogenous compounds. Compiling individual profiles in real forensic cases would drastically increase the evidentiary value of a latent fingerprint, particularly for fingerprints that lack a known match in a database.

Matrix-assisted laser desorption/ionization (MALDI)-MSI is one of the most common surface analysis techniques for latent fingerprints. This technique requires the application of a matrix on top of the sample surface to absorb laser energy and assist with desorption/ionization of the analytes. Alpha-cyano-4-hydroxycinnamic acid (CHCA)[9–11] and 2,5-dihydroxybenzoic acid (DHB)[5,12] are organic matrices utilized by many researchers studying latent fingerprints. Silver is also commonly used as a sputtered metal matrix for the analysis of latent fingerprints in both positive and negative polarities.[5,12,13]

Latent fingerprints require forensic development for visualization at a crime scene. Before MALDI-MSI could be adopted into the forensic workflow, researchers need to show how various forensic development techniques affect the chemicals that can be detected with MALDI-MSI, and how any changes to the compounds detected may impact the chemical profiling potential. Recent research efforts have shown compounds can still be detected following many types of development, such as powder dusting, cyanoacrylate fuming, and porous surface techniques.[11–14] These articles emphasized the need for a traditional MALDI matrix for analysis. We have recently demonstrated carbon-based forensic powder (CFP) as an effective one-step development and matrix application that did not require an additional MALDI matrix for analysis.[15] Utilizing the existing development powder as a matrix streamlines the forensic

process by designing an analysis approach around current field practices rather than developing lab techniques that require changes to field methods.

Although CFP is a common development powder for light colored surfaces, it is not useful on dark surfaces. Titanium oxide development powder (TiO_2) is a whitish gray powder employed by forensic personnel for use on dark surfaces. Titanium oxide nanoparticles have previously been used as matrices for MALDI analysis.[16] This work investigates the feasibility of using TiO_2 following development as an existing MALDI matrix by a direct comparison to the matrix efficiency of CFP, and the commonly used MALDI matrix CHCA. The effect of adding additional matrix on top of TiO_2 development is also investigated as previous research has noted additional MALDI matrices are necessary following forensic development.

Experimental

Sample Preparation for MALDI-MSI Analysis

Fingerprint collection and analysis was approved by the Iowa State University Internal Review Board. Pre-cleaned glass slides were cut in half. Groomed fingerprints were prepared by touching the finger to the forehead and depositing a fingerprint across the cut on the glass slide for split fingerprint comparison. One half of the fingerprint was developed with CFP (Hi-Fi Volcano Latent Print Powder No. 101L; Sirchie, Youngsville, NC) while the other was developed with forensic TiO_2 (Latent print powder L-1200, chemistry gray; Sirchie). Each print was dusted with a DNA free brush from Sirchie (DNA 122L), with one brush dedicated to each powder. Every experiment shown in this work was performed at least three times.

In a separate experiment, fingerprints were dusted with TiO_2 and one of four additional matrices were applied on top. CHCA was prepared at 5 mg/mL in 70:30 (v:v) acetonitrile:0.1% aqueous trifluoroacetic acid. DHB was prepared at 40 mg/mL in 70:30 (v:v) methanol:0.1%

aqueous trifluoroacetic acid. CHCA and DHB, both purchased from Sigma-Aldrich (>98%, St. Louis, MO) were sprayed on top of the TiO_2 developed fingerprints using a TM Sprayer from HTX Technologies (Chapel Hill, NC). Both matrices were sprayed at a flow rate of 0.1 mL/min for 8 passes with 3 mm spacing in a crisscross pattern. The nozzle temperature was 75 °C and the nitrogen pressure was 10 PSI with a velocity of 1200 mm/min. Silver was sputtered for 5 seconds at 40 mA using a Cressington 108auto Sputter Coater (Ted Pella, Redding, CA). For a combination of sodium gold as a matrix, 10 mM sodium acetate (Alfa Aesar, Haverhill, MA) in methanol was sprayed using a TM Sprayer. A flow rate of 0.03 mL/min, nozzle temperature of 30 °C, velocity of 1200 mm/min, and nitrogen pressure of 10 PSI was utilized. A total of 8 passes with 3 mm spacing in a crisscross pattern was used. Following the sodium spraying, gold was sputtered for 20 seconds at 40 mA.

The optimal matrix was then compared to the TiO_2 powder alone using split fingerprints (as described above). If an additional matrix was shown to increase the signal to noise (S/N) ratio, one half of a fingerprint was dusted with CFP while the other was dusted with TiO_2 and the optimal matrix was applied for comparison.

Mock exogenous fingerprints were prepared by applying sunscreen, sunburn relief spray, and/or bug spray per manufacturer's instructions. Exogenous fingerprints were also prepared by handling the powder forms of procaine and pseudoephedrine to mimic illicit drug handling. A mandarin orange was handled in a consumption scenario prior to depositing fingerprints. Finally, spilled wine was touched before depositing a fingerprint. All consumer products were purchased from a local retailer. Fingerprints were deposited and prepared in the same split manner as described above. The exogenous fingerprints were compared in the same way as the endogenous, with the exception that only silver was applied for additional matrix comparison.

The comparison of both endogenous and exogenous compounds in positive mode was repeated between the dusted TiO_2 powder and CHCA manually ground with a mortar and pestle. The size of the ground CHCA was not measured. The dusted CHCA was also sprayed with a solvent (70:30 (v:v) acetonitrile:0.1% aqueous trifluoroacetic acid) in a separate experiment to mimic the dry-wet method suggested by the Francese group.[17,18] A flow rate of 0.03 mL/min, nozzle temperature of 30 °C, velocity of 1200 mm/min, and nitrogen pressure of 10 PSI was utilized. A crisscross pattern with 3 mm spacing was used for a total of 8 passes.

Mass Spectrometry Imaging

A MALDI-LTQ-Orbitrap Discovery (Thermo Finnigan, San Jose, CA) modified to incorporate an external frequency tripled 355 nm Nd:YAG laser (UVFA; Elforlight, Ltd., Daventry, UK) was utilized to analyze all fingerprint samples. High-resolution mass spectra and images were acquired in the Orbitrap mass analyzer, which has a mass resolution of 30,000 at *m/z* 400. Data was acquired using a 100-micron raster step, laser spot size of approximately 15 microns, and ten laser shots per pixel over the mass range 100-1000. Data was collected in both positive and negative polarities. Approximately 2700 pixels were acquired for each condition of the split fingerprint.

Data Analysis

ImageQuest and Xcaliber software (Thermo Finnigan) were utilized to manually analyze the mass spectra. The signal intensity and noise of each peak were averaged across the entire analyzed fingerprint region and extracted. A S/N ratio was calculated for each compound studied using the formula: $\Sigma Ii/(\Sigma Ni^2)^{1/2}$. Ii and Ni represent the intensity and noise, respectively, of each adduct i (i = H^+, Na^+, and K^+). S/N ratios were then plotted on graphs. S/N ratios drastically different than those for other values on the same graph were multiplied by a factor to show the

S/N ratios on the same graph. Any multiplication factors are indicated on the graphs. Normalization for any donor variation from day-to-day was not performed, therefore S/N ratios cannot be compared on different graphs as the data from each graph was collected on different days and may vary in overall signal.

Results and Discussion

General Compatibility of TiO_2 with MALDI-MSI

CFP proved to be comparable or better than common organic matrices based on S/N ratios and MS images of fingerprint compounds when used as a one-step development and matrix combination in our previous work.[15] For this reason, the efficiency of TiO_2 as a development and matrix combination was directly compared to CFP. In **Figure 1** the positive mode mass spectra of fingerprints dusted with CFP and TiO_2 development powders are shown. While CFP was shown to work effectively as a matrix, the low mass range was contaminated with carbon clusters requiring the use of a high mass resolution mass spectrometer (HRMS) for analysis. TiO_2 does not cause the significant contamination peaks in the low mass range, suggesting it would be a viable matrix for an instrument lacking a HRMS such as a MALDI-time-of-flight (TOF) mass spectrometer. The two FAs and cholesterol highlighted in both spectra would likely be indistinguishable from carbon cluster peaks if utilizing a MALDI-TOF, especially considering the low abundance of the FAs and cholesterol (**Figure 1B**). For the higher mass range over *m/z* 500, the WE, diacylglycerol (DG), and TG regions of the spectra are visible for both CFP and TiO_2 as the matrix. The MS image of TG 46:0 shows the applicability of both powders as matrices for MALDI analysis. TG x:y indicates the total carbon chain length of x and the number of double bonds of y, which is used throughout the paper. The quaternary ammonium compound behentrimonium, an ingredient in many consumer products such as

shampoos and lotions, is very readily desorbed with TiO_2 and can be seen at *m/z* 368.42 in **Figure 1**. While quaternary ammonium compounds are present in many consumer products and may not be informative on their own, a combination of these with other exogenous compounds may provide more details about an individual's chemical lifestyle.

TiO_2 powder, however, is not a useful matrix in negative mode. **Figure S1** shows the negative mode spectra of fingerprints developed with CFP and TiO_2. While the CFP mass spectrum is dominated by carbon clusters, FA peaks can still be seen with a HRMS. In contrast, the fingerprint MALDI-mass spectra with TiO_2 matrix contains no FA peaks and was not useful for the desorption/ionization of fingerprint compounds in negative mode. The corresponding MS images support the spectra comparison, showing no signal for FA 16:0 in the TiO_2 developed fingerprint.

It was previously shown that MALDI-MSI analysis is almost non-destructive and that fingerprints can be preserved for forensic evidence after the MALDI-MSI analysis with CFP.[15] This is because MALDI-MS is extremely sensitive and sufficient chemical information can be obtained with under-sampling conditions. To demonstrate that this is also the case for TiO_2, a split fingerprint before and after MALDI-MSI analysis is shown in **Figure 2**. The before and after images show no loss of ridge detail, indicating MALDI-MSI leaves the fingerprint intact. The MS image of a sodiated hexose at *m/z* 203.05 from the analyzed region shows the clear ridge detail and quality MS images, in spite of the gentle MALDI-MS analysis. Both powders are commonly utilized to develop fingerprints in the forensic field as their effective adhesion to fingerprint residue is shown in **Figure 2**. As expected, the contrast is clearer with TiO_2 on the dark surface than with CFP. We also tested commercially available TiO_2 nanoparticles as

development and matrix powders, but their performance was poorer than forensic TiO_2 powders, most likely because the lack of additives that improve adhesion to fingerprints.

Positive Mode Comparison of TiO_2 and CFP

While both CFP and TiO_2 were able to desorb/ionize compounds in positive mode, there are differences in the efficiency of both as matrices. The S/N ratio, rather than absolute ion intensity or relative abundance, is the most appropriate method to compare the efficiency of two matrices because of the difference in optimal experimental conditions. Each independent experiment was performed and compared in parallel. The overall variation might have come from not only analytical variation but also variation in fingerprint chemicals.

The S/N ratios of endogenous compounds utilizing dusted TiO_2 and CFP as matrices in the positive mode analysis of fingerprints are shown in **Figure 3A**. Each compound analyzed could be detected with both matrices, but there were differences in the S/N ratios. CFP proved to be the better matrix for the analysis of TGs. The two matrices were much more comparable with the low mass endogenous compounds, although FAs showed higher S/N ratios when TiO_2 was utilized as the matrix. The MS image of TG 48:1 clearly shows higher signal on the half dusted with CFP. Cholesterol is a low mass endogenous compound that was more comparable between the two matrices, which is easily seen in the MS image as both halves of the fingerprint show ridge detail at comparable intensities despite the overall lower S/N ratio of cholesterol compared to other compounds.

To further investigate the compatibility of TiO_2 with MALDI-MSI, mock fingerprints contaminated with select exogeneous compounds were made. In **Figure 3B**, the efficiency of TiO_2 and CFP are compared as matrices for exogenous compounds. The exogenous compounds tested include outdoor related compounds, compounds to mimic illicit drugs, and food related

compounds from contact with a mandarin orange. A quaternary ammonium compound is also shown, although this compound was not intentionally added and likely originated from personal hygiene products such as a soap, lotion, or shampoo. The S/N ratios were overall comparable for the majority of exogenous compounds studied. There are a few notable exceptions. CFP gave higher S/N ratios for sunscreen compounds including avobenzone, octocrylene, and oxybenzone, this was also apparent in the MS image of avobenzone at *m/z* 311.16. TiO_2 provided higher S/N ratios for procaine, an amine containing compound, as well as behentrimonium, a quaternary ammonium compound. The higher efficiency of TiO_2 as a matrix for procaine is demonstrated in the MS image at *m/z* 237.16.

TiO_2 proved to be useful for development and as a matrix in positive mode, as shown in **Figures 1-3**, but previous research in the field has suggested that adding a matrix on top of existing development is necessary and improves the signal.[11,13,14] **Figure S2A** compares the performance of four matrices commonly used in fingerprint analysis on top of TiO_2 development powder for endogenous compound analysis. Among the four matrices, sodium gold showed the highest S/N ratio for TGs and sputtered silver showed highest signals for FAs (**Figure S2A**). When they are further compared, however, TiO_2 powder alone resulted in higher S/N ratios for TGs (**Figure S2B**), whereas additional sputtered silver proved more efficient for FAs than the TiO_2 powder alone (**Figure S2C**). Unfortunately, the additional silver on top of the TiO_2 powder decreased the S/N ratio of TGs.

In the case of exogenous compounds, previous work by this group has shown that silver works particularly well as a matrix for the analysis of exogenous compounds.[5] When compared with TiO_2 alone, the addition of silver improved S/N ratios for a few select compounds such as oxybenzone and pseudoephedrine (**Figure S3**); however, there was no significant improvement

for other compounds. Overall, additional silver does improve the S/N ratio of some endogenous and exogenous compounds but is not universally applicable and decreased the S/N ratio of other compounds.

Negative Mode Comparison with Additional Silver

As discussed above, TiO_2 is not useful in negative mode (**Figure S1**) for the analysis of endogenous or exogenous compounds. This is not surprising considering metal oxide nanoparticles are well known to be efficient matrices in positive mode but not in negative mode.[16] This is likely due to the fact that the electronegative oxygen-rich surface may interfere the production of negative ions. The use of additional silver matrix was explored to improve the desorption/ionization of selected endogenous and exogenous compounds in negative mode, as silver has proven to be a useful matrix for both endogenous and exogenous compounds in negative mode analysis.[5,19]

In **Figure 4A**, the S/N ratios of FAs from fingerprint halves developed with TiO_2 and sputtered with silver were comparable to those from the CFP half of the fingerprints. S/N ratios of exogenous compounds are higher when CFP is used as the matrix, but each compound is detectable with the TiO_2 silver combination (**Figure 4B**). Negative mode analysis would not be possible without the addition of silver matrix. The MS images of both an endogenous FA and exogenous procaine show ridge detail for the TiO_2 silver combination as well as the CFP, emphasizing the utility of both.

Positive Mode Comparison of TiO_2 and CHCA

While CFP was proven to be an efficient one-step development and matrix application, CHCA showed more success with exogenous compound analysis in our previous work.[15] Additionally, CHCA is a light colored powder and has been used as a dusted matrix by the

Francese group.[17,18] To ensure a thorough comparison of TiO_2 to other work studying latent fingerprints, the efficiency of TiO_2 as a matrix was also compared to dusted CHCA.

Figure 5A shows the optical image of a TiO_2 and CHCA dusted fingerprint before and after MALDI analysis. The forensic TiO_2 powder used in this study is manufactured specifically for developing and visualizing latent fingerprints, particularly on dark surfaces, and this is apparent in the optical image. The TiO_2 provides more fingerprint ridge detail, although the CHCA did adhere to the fingerprint.

In the comparison of endogenous fingerprint compound analysis via MALDI, TiO_2 was much more efficient than CHCA (**Figure 5B**). The majority of the compounds studied were hardly detectable with CHCA when used as a dusted matrix, with the exception of cholesterol. The MS images of both a TG and cholesterol agree with the S/N ratio comparison. The analysis of exogenous compounds led to an opposite outcome; CHCA was much better for most of the exogenous compounds studied (**Figure 5C**). With the exception of two sunscreen compounds (avobenzone, octocrylene), CHCA provided higher S/N ratios for all compounds including quaternary ammonium compounds that were not purposefully added. Two examples of the MS images shown agree with the S/N ratio comparison; CHCA gives the higher quality images for exogenous compounds. The success of CHCA with exogenous compounds is not surprising as this same trend was observed in a comparison to CFP.[15]

Previous work with dusted CHCA utilized a dry-wet matrix, dusting followed by the spraying of a solvent for crystallization.[17,18] Our work is emphasizing a single-step development and matrix application, but we also applied this solvent spray step to the CHCA in an effort to improve the use as a dusted matrix. The additional solvent did improve the S/N ratios of TGs and

squalene; however, the S/N ratios and quality of the MS images were still much lower than those from fingerprints developed with TiO_2 (**Figure S4**).

We also tested whether additional silver sputter on top of TiO_2 would improve exogenous compounds when compared to the dusted CHCA. In **Figure S5** a similar result to the previous comparisons is seen. The additional silver did improve the S/N ratios of a few compounds (i.e. picaridin, pseudoephedrine, and hexose compounds), but the improvement is not universal and a decrease in S/N ratios is noted for some compounds following the application of silver, especially quaternary ammonium compounds.

Conclusions

Previous research into MALDI-MSI of latent fingerprints has stated that additional MALDI matrices are necessary for the detection of fingerprint compounds following forensic development. This work, however, shows that TiO2 development powder does in fact work as an existing MALDI matrix, likely due to the efficient adherence to fingerprint residue. TiO2 can be utilized for single-step development and matrix application to streamline the MALDI-MSI analysis of fingerprints in the forensic workflow. TiO2 was also shown to be a more efficient dusted matrix for the analysis of endogenous compounds, when compared to dusted CHCA, a matrix commonly used for the analysis of fingerprints by MALDI.

Applying an additional MALDI matrix on top of the development powder does not uniformly improve the detection of fingerprint compounds. A universal approach to the analysis of developed fingerprints by MALDI-MSI would be to utilize the forensic development powder itself as the matrix, when possible. Forensic development powders are specifically designed to adhere to fingerprint residue, providing sufficient matrix coverage for MALDI-MSI analysis of fingerprints.

References

1. De Puit M, Ismail M, Xu X. LCMS analysis of fingerprints, the amino acid profile of 20 donors. *J Forensic Sci*. 2014;59(2):364-370. doi:10.1111/1556-4029.12327

2. Croxton RS, Baron MG, Butler D, Kent T, Sears VG. Variation in amino acid and lipid composition of latent fingerprints. *Forensic Sci Int*. 2010;199(1-3):93-102. doi:10.1016/j.forsciint.2010.03.019

3. Girod A, Weyermann C. Lipid composition of fingermark residue and donor classification using GC/MS. *Forensic Sci Int*. 2014;238:68-82. doi:10.1016/j.forsciint.2014.02.020

4. Girod A, Ramotowski R, Weyermann C. Composition of fingermark residue: A qualitative and quantitative review. *Forensic Sci Int*. 2012;223(1-3):10-24. doi:10.1016/j.forsciint.2012.05.018

5. Hinners P, O'Neill KC, Lee YJ. Revealing individual lifestyles through mass spectrometry imaging of chemical compounds in fingerprints. *Sci Rep*. 2018;8:5149. doi:10.1038/s41598-018-23544-7

6. Ferguson LS, Wulfert F, Wolstenholme R, et al. Direct detection of peptides and small proteins in fingermarks and determination of sex by MALDI mass spectrometry profiling. *Analyst*. 2012;137(20):4686-4692. doi:10.1039/c2an36074h

7. Emerson B, Gidden J, Lay JO, Durham B. Laser desorption/ionization time-of-flight mass spectrometry of triacylglycerols and other components in fingermark samples. *J Forensic Sci*. 2011;56(2):381-389. doi:10.1111/j.1556-4029.2010.01655.x

8. Zhou Z, Zare RN. Personal Information from Latent Fingerprints Using Desorption Electrospray Ionization Mass Spectrometry and Machine Learning. *Anal Chem*. 2017:acs.analchem.6b04498. doi:10.1021/acs.analchem.6b04498

9. Kaplan-Sandquist K, LeBeau MA, Miller ML. Chemical analysis of pharmaceuticals and explosives in fingermarks using matrix-assisted laser desorption ionization/time-of-flight mass spectrometry. *Forensic Sci Int*. 2014;235:68-77. doi:10.1016/j.forsciint.2013.11.016

10. Bradshaw R, Wolstenholme R, Blackledge RD, Clench MR, Ferguson LS, Francese S. A novel matrix-assisted laser desorption/ionisation mass spectrometry imaging based methodology for the identification of sexual assault suspects. *Rapid Commun Mass Spectrom*. 2011;25(3):415-422. doi:10.1002/rcm.4858

11. Bradshaw R, Bleay S, Wolstenholme R, Clench MR, Francese S. Towards the integration of matrix assisted laser desorption ionisation mass spectrometry imaging into the current fingermark examination workflow. *Forensic Sci Int*. 2013;232:111-124. doi:10.1016/j.forsciint.2013.07.013

12. O'Neill KC, Hinners P, Lee YJ. Chemical imaging of cyanoacrylate-fumed fingerprints by matrix-assisted laser desorption/ionization mass spectrometry imaging. *J Forensic Sci*. 2018;doi: 10.11. doi:10.1111/1556-4029.13773

13. Lauzon N, Dufresne M, Beaudoin A, Chaurand P. Forensic analysis of latent fingermarks by silver-assisted LDI imaging MS on nonconductive surfaces. *J Mass Spectrom*. 2017;52(6):397-404. doi:10.1002/jms.3938

14. Kaplan-Sandquist KA, LeBeau MA, Miller ML. Evaluation of four fingerprint development methods for touch chemistry using matrix-assisted laser desorption ionization/time-of-flight mass spectrometry. *J Forensic Sci*. 2015;60(3):611-618. doi:10.1111/1556-4029.12718

15. Hinners P, Lee YJ. Carbon-Based Fingerprint Powder as a One-Step Development and Matrix Application for High-Resolution Mass Spectrometry Imaging of Latent Fingerprints. *J Forensic Sci*. 2019;64(4):1048-1056. doi:10.1111/1556-4029.13981

16. Yagnik GB, Hansen RL, Korte AR, Reichert MD, Vela J, Lee YJ. Large scale nanoparticle screening for small molecule analysis in laser desorption ionization mass spectrometry. *Anal Chem*. 2016;88(18):8926-8930. doi:10.1021/acs.analchem.6b02732

17. Ferguson L, Bradshaw R, Wolstenholme R, Clench M, Francese S. Two-step matrix application for the enhancement and imaging of latent fingermarks. *Anal Chem*. 2011;83(14):5585-5591. doi:10.1021/ac200619f

18. Ferguson LS, Creasey S, Wolstenholme R, Clench MR, Francese S. Efficiency of the dry-wet method for the MALDI-MSI analysis of latent fingermarks. *J Mass Spectrom*. 2013;48(6):677-684. doi:10.1002/jms.3216

19. O'Neill KC, Lee YJ. Effect of aging and surface interactions on the diffusion of endogenous compounds in latent fingerprints studied by mass spectrometry imaging. *J Forensic Sci*. 2018;63(3):708-713. doi:10.1111/1556-4029.13591

Figures

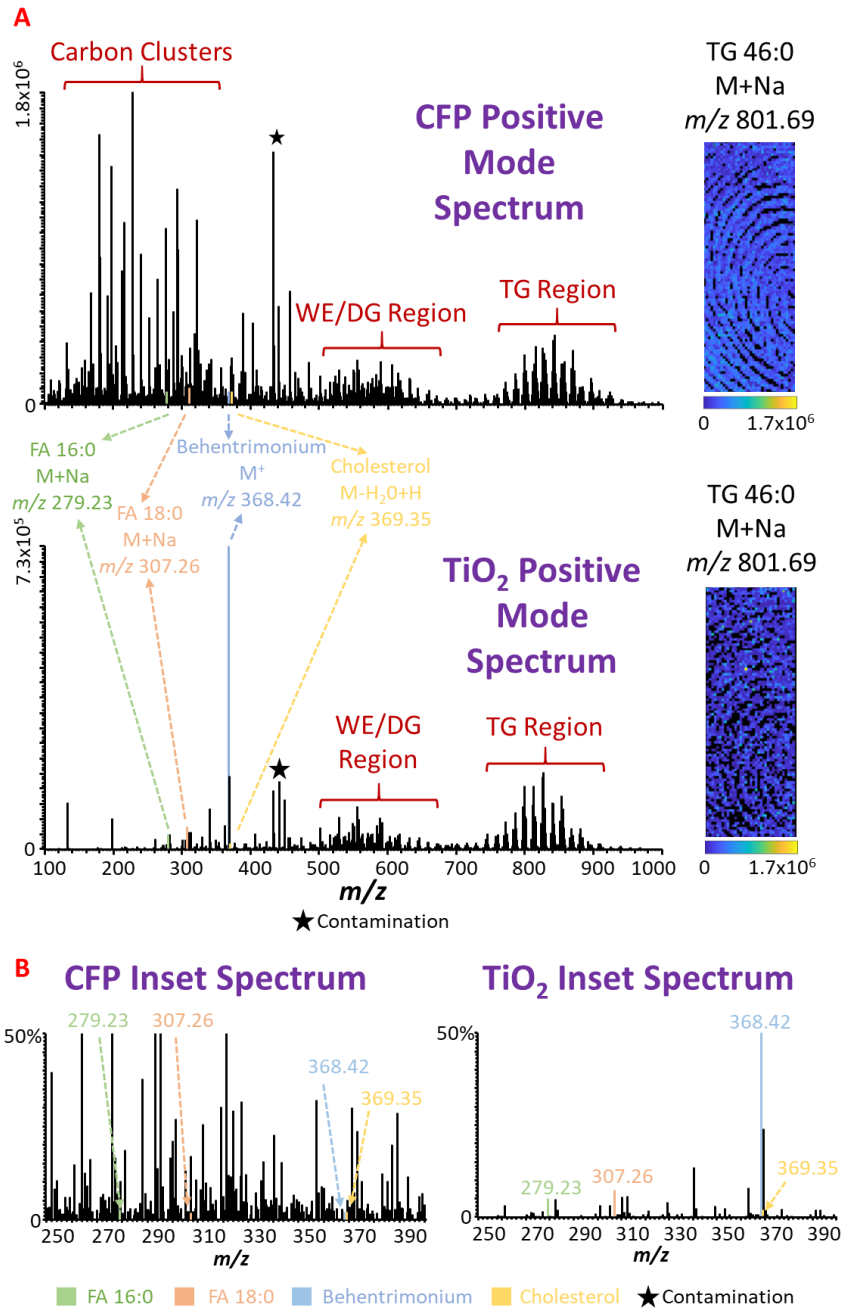

Figure 1. MALDI mass spectra of CFP and TiO_2 dusted fingerprints in positive mode **(A)**. The MS images of TG 46:0 clearly demonstrate the usefulness of both powders as MALDI matrices. Inset spectra of low mass region **(B)**. *Note: total carbon chain length (xx) and the number of double bonds (yy) in the TG are represented by xx:yy format.*

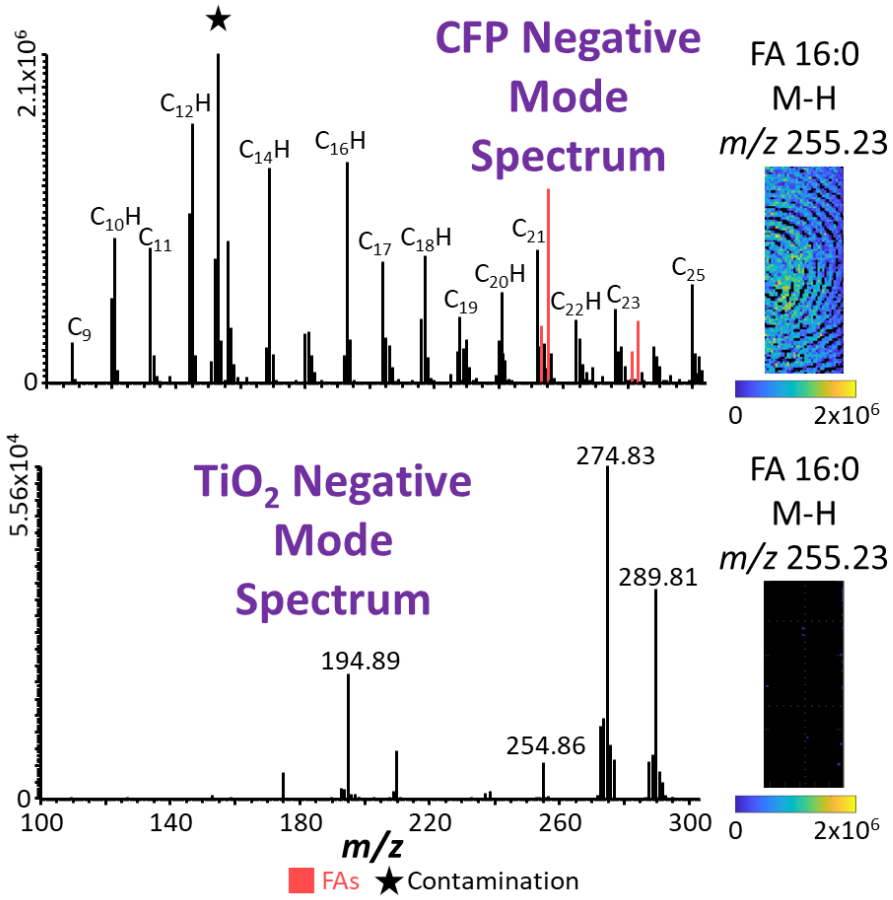

Figure 2. Negative mode mass spectra of fingerprints dusted with CFP and TiO_2 development powder. *Total carbon chain length (xx) and the number of double bonds (yy) in the FA are shown in the xx:yy format.*

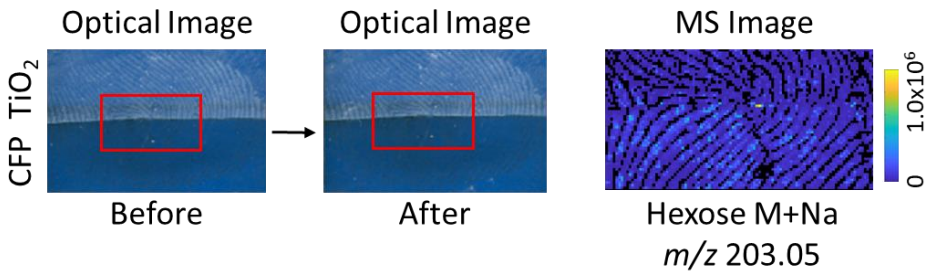

Figure 3. Optical image of a fingerprint before and after MALDI-MSI analysis. The region of the fingerprint analyzed (red box) is still visible following analysis. A MS image of a hexose at *m/z* 203.05 from the analyzed region is also shown.

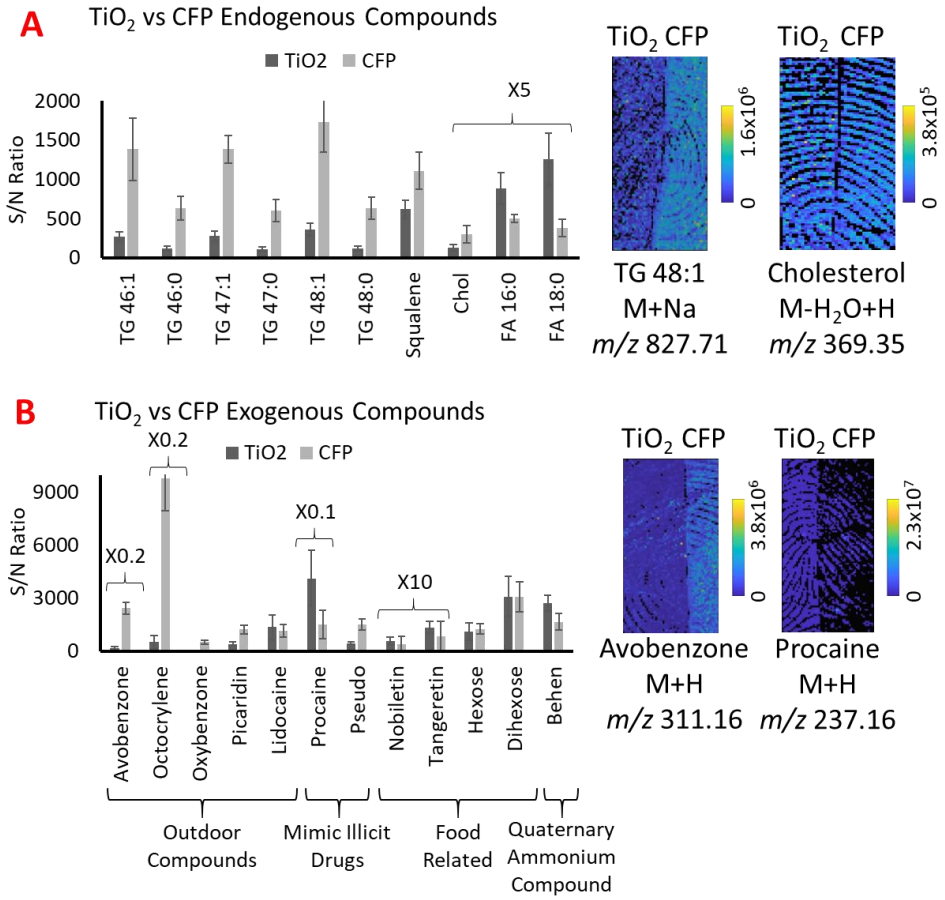

Figure 4. Endogenous compound analysis comparing the matrix efficiency of CFP and TiO_2 in positive mode **(A)**. Exogenous compound analysis comparing the efficiency of TiO_2 and CFP as matrices in positive mode **(B)**. MS images are also compared between the two matrices. *Total carbon chain length (xx) and the number of double bonds (yy) in TGs and FAs are shown in the xx:yy format. Multiplication factors for S/N ratios are shown in the exogenous graph and were used to display all compounds on the same graph. Chol: cholesterol, pseudo: pseudoephedrine, behen: behentrimonium.*

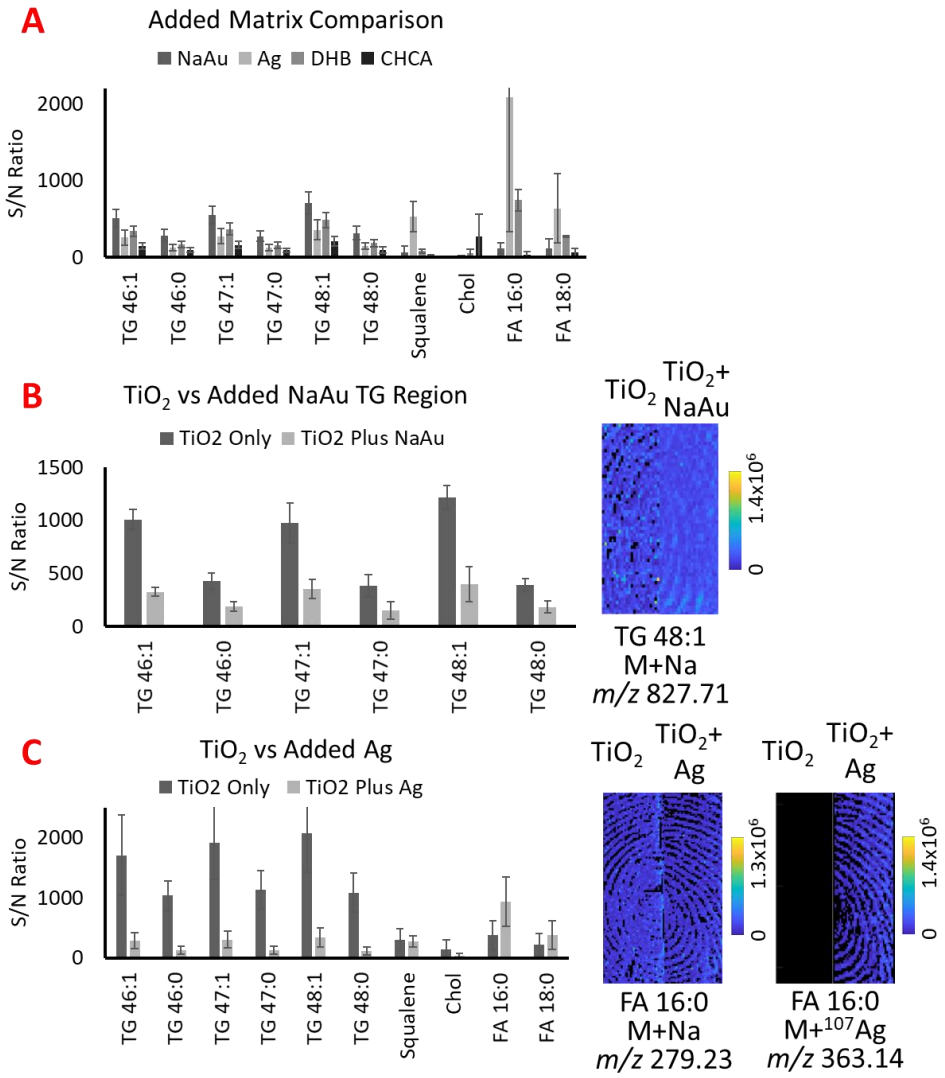

Figure 5. Positive mode comparison of four matrices on top of TiO_2 powder for the analysis of endogenous compounds **(A)**. Comparison of TiO_2 alone and TiO_2 with sodium gold for the analysis of TGs in positive mode **(B)**. TiO_2 alone compared to added silver for endogenous compounds in positive mode **(C)**. MS images are also compared. *Total carbon chain length (xx) and the number of double bonds (yy) in TGs and FAs are shown in the xx:yy format. Chol: cholesterol.*

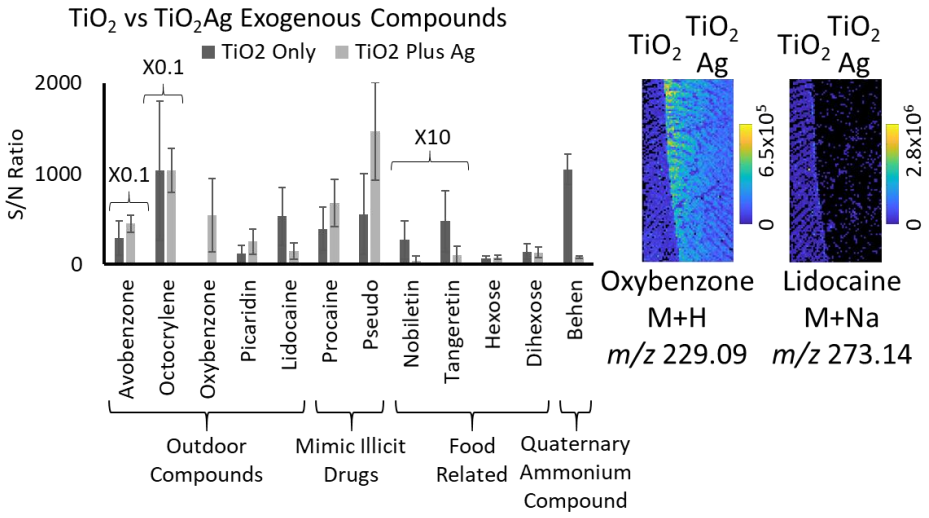

Figure 6. Exogenous compound analysis comparing the efficiency of TiO_2 alone and additional silver matrix in positive mode. MS images are also compared. *Multiplication factors for S/N ratios are shown in the graph and were used to display all compounds on the same graph. Pseudo: pseudoephedrine, behen: behentrimonium.*

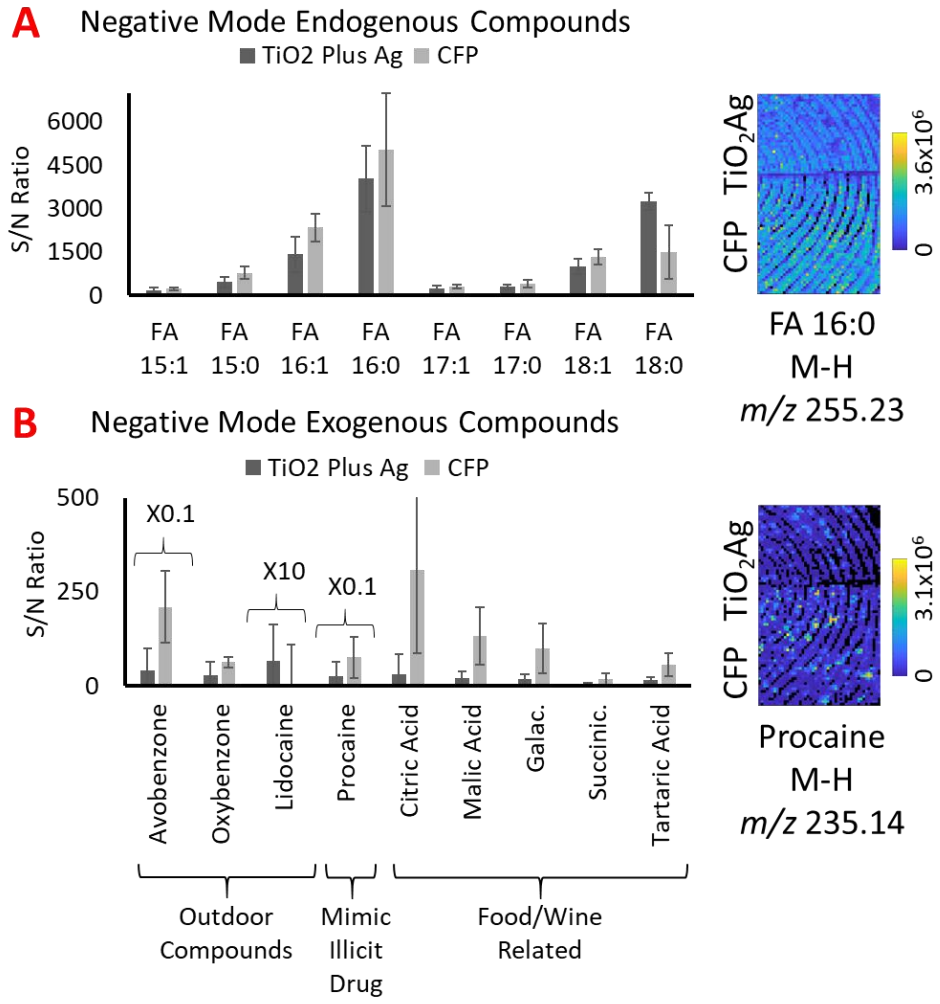

Figure 7. Negative mode endogenous **(A)** and exogenous **(B)** compound analysis comparing the efficiency of TiO_2 with additional silver and CFP for fingerprint analysis. MS images of an endogenous and exogenous compound are also compared. *Total carbon chain length (xx) and the number of double bonds (yy) in FAs are shown in the xx:yy format. Multiplication factors for S/N ratios are shown in the exogenous graph and were used to display all compounds on the same graph. Galac: galacturonic acid, succinic: succinic acid.*

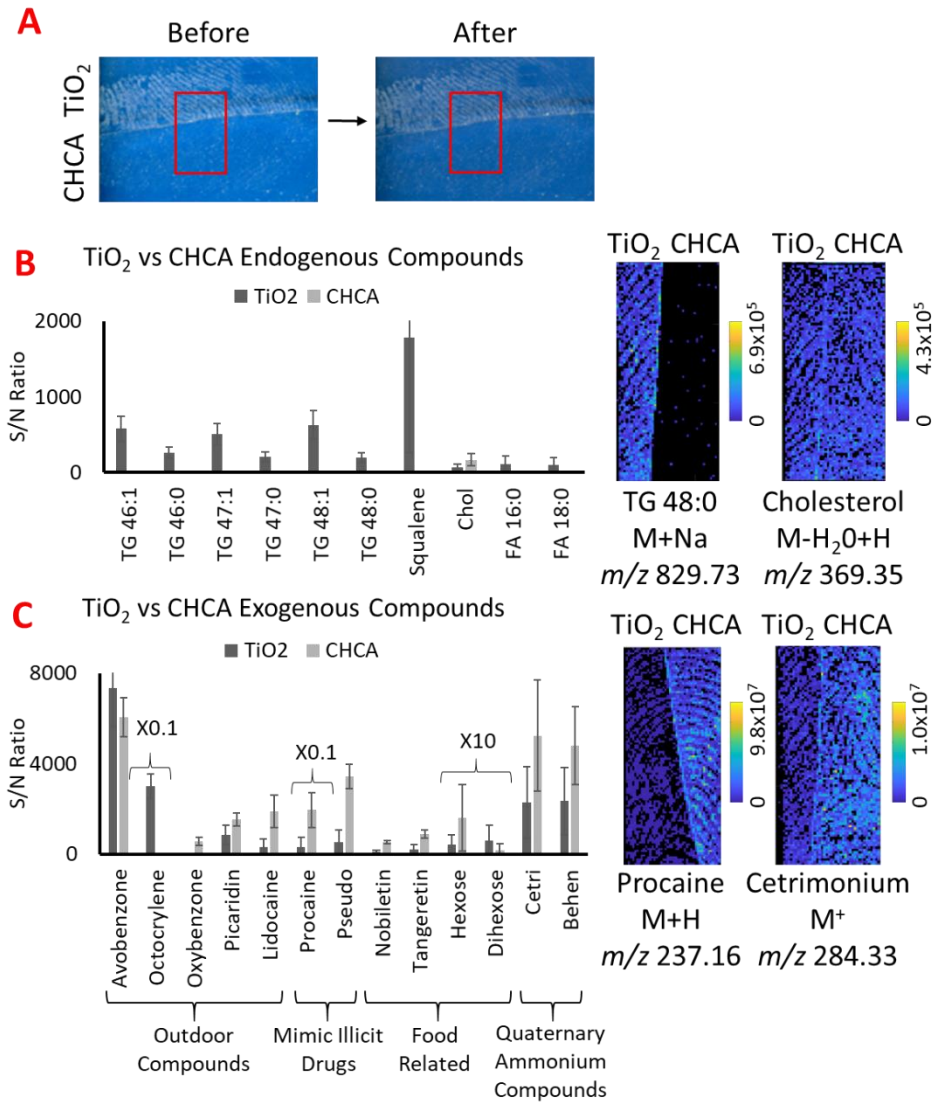

Figure 8. Optical images of a split fingerprint developed with TiO_2 and CHCA powder before and after MALDI analysis **(A)**. Positive mode comparison of the efficiency of TiO_2 and CHCA as dusted matrices for the analysis of endogenous **(B)** and exogenous compounds **(C)**. MS images are also compared for both endogenous and exogenous compounds. *Total carbon chain length (xx) and the number of double bonds (yy) in TGs and FAs are shown in the xx:yy format. Multiplication factors for S/N ratios are shown in the exogenous graph and were used to display all compounds on the same graph. Chol: cholesterol, pseudo: pseudoephedrine, cetri: cetrimonium, behen: behentrimonium.*

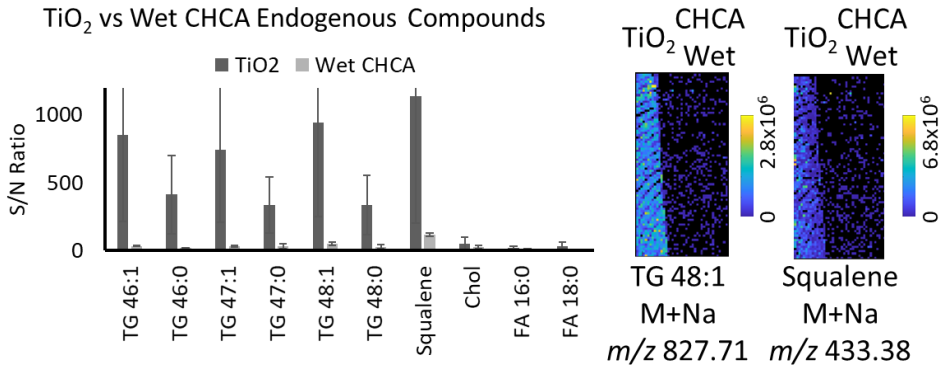

Figure 9. Comparison of the efficiency of TiO_2 powder and dusted CHCA with an additional solvent spray (wet) for the analysis of endogenous fingerprint compounds. MS images are also compared. *Total carbon chain length (xx) and the number of double bonds (yy) in TGs and FAs are shown in the xx:yy format. Chol: cholesterol.*

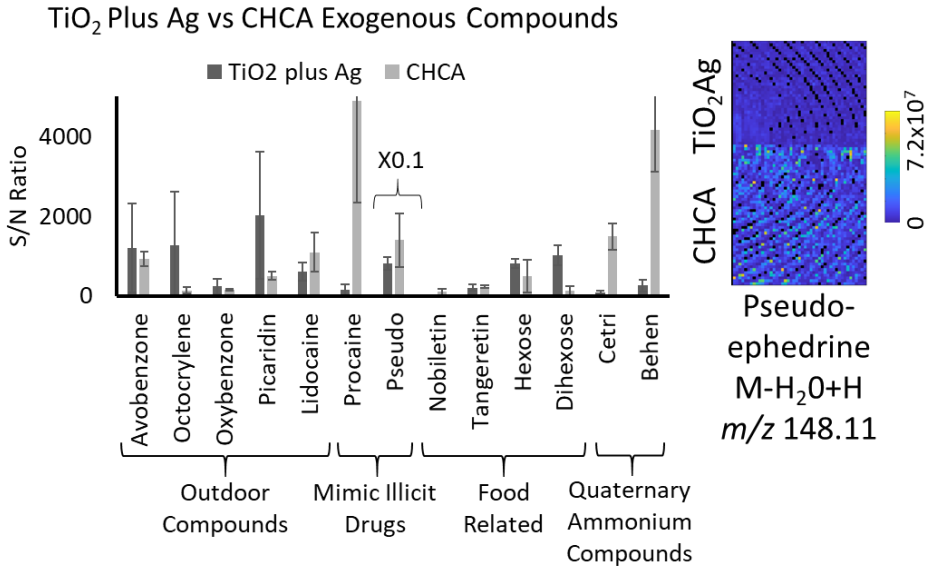

Figure 10. Exogenous compound analysis comparing the efficiency of TiO_2 plus additional silver to dusted CHCA. MS images are also compared. *Multiplication factors for S/N ratios are shown in the graph and were used to display all compounds on the same graph. Pseudo: pseudoephedrine, cetri: cetrimonium, behen: behentrimonium.*

CHAPTER 4. REVEALING INDIVIDUAL LIFESTYLES THROUGH MASS SPECTROMETRY IMAGING OF CHEMICAL COMPOUNDS IN FINGERPRINTS

Paige Hinners, Kelly C. O'Neill, and Young Jin Lee[1]

1. Department of Chemistry, Iowa State University, Ames, Iowa, 50011, USA

Modified from a manuscript published in *Scientific Reports*

Sci. Rep., 8, Article Number: 5149 (2018)

Abstract

Fingerprints, specifically the ridge details within the print, have long been used in forensic investigations for individual identification. Beyond the ridge detail, fingerprints contain useful chemical information. The study of fingerprint chemical information has become of interest, especially with mass spectrometry imaging technologies. Mass spectrometry imaging visualizes the spatial relationship of each compound detected, allowing ridge detail and chemical information in a single analysis. In this work, a range of exogenous fingerprint compounds that may reveal a personal lifestyle were studied using matrix-assisted laser desorption/ionization - mass spectrometry imaging (MALDI-MSI). Studied chemical compounds include various brands of bug sprays and sunscreens, as well as food oils, alcohols, and citrus fruits. Brand differentiation and source determination were possible based on the active ingredients or exclusive compounds left in fingerprints. Tandem mass spectrometry was performed for the key compounds, so that these compounds could be confidently identified in a single multiplex mass spectrometry imaging data acquisition.

Introduction

Fingerprints consist of ridges and valleys that form a pattern unique to the individual. The sweat and chemical residues present on a finger can leave ridge detail, or a latent fingerprint, on

objects and surfaces encountered by the fingers. Latent fingerprints have provided evidentiary value in forensic investigations for over a century, mainly as a means of identification through pattern comparison. As technology and science have advanced, so has the collection and interpretation of evidence within latent fingerprints. Chemical compounds in the residue contain detailed information about the individual depositing the fingerprint. Chromatography and mass spectrometry coupled methods, such as liquid chromatography-mass spectrometry (LC-MS) and gas chromatography-mass spectrometry (GC-MS), provide chemical fingerprint information, but typically require multiple fingerprints with no spatially relevant information[1–3].

Surface mass spectrometry techniques with imaging capabilities supply chemical and spatial information in a single fingerprint analysis. Various ionization methodologies were used for mass spectrometry imaging (MSI) of fingerprints including secondary ion mass spectrometry (SIMS)[4–6], desorption electrospray ionization (DESI)[7,8], desorption ionization on porous silicon (DIOS)[9], desorption electro-flow focusing ionization (DEFFI)[10], and matrix-assisted laser desorption/ionization (MALDI)[11–15]. A challenge to compound identification in MSI is the lack of chromatographic separation and corresponding retention time information. We have previously developed a "multiplex MSI" technique that allows for simultaneous data acquisition of high-resolution mass spectrometry and tandem mass spectrometry (MS/MS) to enable chemical composition analysis and structural elucidation of each compound[16]. The multiplex MSI technique was successfully demonstrated in fingerprint analysis, allowing fingerprint chemicals to be confidently identified in a single analysis[17].

A broad range of endogenous and exogenous fingerprint chemicals have been targeted using MALDI-MSI. Endogenous compounds, those naturally excreted from the human body, include compounds like amino acids, fatty acids, peptides, proteins, and triacylglycerols

(TGs)[12,18–21]. Researchers have utilized endogenous compounds to potentially differentiate subsets of people or identify the age of the fingerprint[4,8,12,18,19]. Exogenous compounds are those present on the fingerprint from various forms of contamination, or any chemical present that is not naturally excreted from the human body. The most studied exogenous compounds in latent fingerprints are illicit drugs and explosives. They are topics of interest in criminal investigations, making them desirable sets of compounds to study[7,9–11,22]. While the importance of exogenous compounds has been recognized with drugs and explosives, the full potential of the vast range of other exogenous compounds has yet to be explored.

We are in constant contact with diverse chemicals in our daily life. Dorrestein and colleagues recently demonstrated that the lifestyle of an individual can be revealed based on chemical compounds obtained from the hands or cell phones[23,24]. Here, we hypothesize that the lifestyle of an individual can be characterized by many types of exogenous chemicals left in fingerprints. In this work, consumer products, foods, and alcohols were investigated as sources of exogenous compounds in latent fingerprints. The variations in the chemicals present were compared for brand and type determination. The presence of a single compound may not be sufficient to provide detailed information about an individual, but the compilation of multiple compounds present in a latent fingerprint may give insight into one's lifestyle.

Results and Discussion

Matrix Selection

The first step of this study was to find optimum matrices for the compounds of interest. Two organic matrices (alpha-cyano-4-hydroxycinnamic acid (CHCA) and 2,5-dihydroxybenzoic acid (DHB)) and two metal nanoparticles (gold and silver) were explored for optimum ionization across a broad range of compounds. CHCA is often used for endogenous and exogenous

fingerprint analysis via MALDI-MSI[11,21] and DHB has shown promise with triacylglycerols (TGs)[12]. However, organic matrices typically have significant matrix contamination in the low mass range, suppressing many fingerprint chemicals. Most nanoparticles have minimal to no matrix background and are utilized to avoid matrix contamination peaks. Additionally, as they do not crystallize, they can be homogeneously applied to the fingerprints or sample tissues, in this case via uniform sputter coating.

CHCA and DHB were first utilized for the sunscreen compounds but did not efficiently ionize all six active ingredients. The gold and silver nanoparticles were sputter coated and did ionize all six sunscreen target compounds with varying ionization efficiencies. Silver offers the additional advantage of adduct formation, i.e., $[M+Ag]^+$, useful in the analysis of other exogenous compounds, some of which were seen only as the silver adduct. Silver adduct formation is particularly useful for hydrophobic compounds that do not otherwise ionize. In the analysis of food oils, DHB was used as the matrix, as it can best ionize TG compounds[12,25].

Brand Comparison in Bug Spray and Sunscreen

Bug spray and sunscreen are two consumer products indicative of an outdoor lifestyle. Active ingredients are listed on the label for both products, which allows brand comparison based on the differences in active ingredients among brands. BullFrog (active ingredient: insect repellant 3535 (IR3535)), Cutter (active ingredient: N,N-diethyl-m-toluamide (DEET)), and OFF! (active ingredient: Picaridin) were the bug sprays compared in this study. MALDI mass spectra of each brand obtained from deposited fingerprints are shown in **Figure 1A**. The brand of origin could be easily correlated based on the color-coded active ingredients. All three active compounds are tertiary amines and ionized as proton ($[M+H]^+$), alkali ($[M+Na]^+$, ($[M+K]^+$), and/or silver adducts ($[M+^{107}Ag]^+$, $[M+^{109}Ag]^+$) in positive mode. BullFrog is composed of a

mixture of bug spray and sunscreen compounds. In BullFrog, oxybenzone, a UV filter in many sunscreens, is the next most abundant compound after IR3535. Fingerprint chemical images of each active ingredient were extracted from separate fingerprints to display the ridge detail in the contaminated prints (**Figure 1B**). When active ingredients of bug spray are present in a latent print, they can be related to the brand of origin, then compared to items in the suspect's possession, or may be used to narrow down the persons of interest.

Other miscellaneous ingredients that are found in **Figure 1A** include a hexose, triethyl citrate, and cetyl trimethylammonium ion. None of which are active ingredients and are not useful in distinguishing the brands of bug spray. Cetyl trimethylammonium ion is most likely from a common surfactant used in many consumer products. Sugars, specifically hexose (e.g., glucose), are regularly found as exogenous compounds of many sources in fingerprints (see later section for citrus fruits and alcohols). In this work, triethyl citrate, an ester of citric acid, has also been identified in other consumer products and foods. Triethyl citrate is a common plasticizer used in consumer products. The same inactive ingredients are also found in sunscreen (**Figure 2A**).

Each brand of sunscreen contains multiple active components as summarized in **Table 1** and the mass spectra are shown in **Figure 2A** with color-coded active ingredients. Two sunscreen brands, BullFrog and Babyganics, could be easily distinguished by the unique active ingredients: oxybenzone and IR3535 (an insect repellent) for BullFrog and octinoxate for Babyganics. Octinoxate is also present in BullFrog but in very low abundance. At a glance, Neutrogena and Coppertone are not easily distinguished as they both have avobenzone and octocrylene as the major active ingredients. However, they can be distinguished based on the relative intensities of each compound. In Neutrogena, the two active ingredients have similar

intensities with avobenzone being slightly higher, but in Coppertone octocrylene has a much higher abundance. It was reproducible across replicates, as their normalized intensities are compared in **Figure 2B**. The *m/z* 327 and *m/z* 355 peaks in Babyganics are likely related to a short chain diacylglycerol (DG) species but could not be confidently identified. Avobenzone, octocrylene, oxybenzone, and octinoxate are the most useful sunscreen compounds for brand determination. Chemical images of each relevant sunscreen compound from individual fingerprints are shown in **Figure 2C**. As with bug spray, the sunscreen brand can be compared to an individual's possessions to assist in lifestyle compilation.

To further investigate the ability to distinguish brands, we applied principal component analysis (PCA) to the bug spray and sunscreen data. Initially we applied PCA to the entire spectrum of the bug spray and sunscreen replicate fingerprint data. Normalized intensities in the *m/z* range of 150 to 500 with more than one percent ion signals were submitted to MetaboAnalyst[26]. As shown in **Figure 3A** and **Figure 3B**, there is some separation between the brands in both bug spray and sunscreen, but the separation is not complete. Specifically, in **Figure 3B** overlap is seen in sunscreen between Coppertone and Neutrogena. This was expected as both Coppertone and Neutrogena contain the same five active ingredients with some differences in abundance.

To avoid the effect of sample variation due to non-active ingredients, another PCA analysis was performed with active ingredients only, as shown in **Figure 3C** and **Figure 3D**. As expected, the separation is much better than the full mass spectra suggesting the importance of a targeted approach. When only active ingredients are compared for their normalized signal intensities as shown in **Figure 3C** for bug spray and **Figure 3D** for sunscreen, the separation is very clear between the brands. This emphasizes the importance of establishing a mass list of

known compounds when studying exogenous compounds in latent fingerprints for lifestyle markers. In some sense, it is similar to typical metabolomics workflow. Untargeted statistical analysis is commonly performed, such as PCA or hierarchical clustering analysis, when compounds of interest are not well established[27]. Quantitative profiling of selected target compounds, however, gives better insight about the biological processes once characteristic compounds are identified. For the rest of this paper, our effort will be focused on finding characteristic marker compounds.

Food Oils

Another set of compounds likely to be present in a latent fingerprint are food oils, from cooking or eating. TGs are the main constituent of cooking oils, mostly produced from plant seeds. Human fingerprints also contain TGs, secreted from glands, but those from plants have distinct patterns of fatty acyl chains. **Figure 4** compares TG profiles of five cooking oils (olive, canola, sesame, corn, and grapeseed), a vegetable oil spray, and a human fingerprint. As expected, each oil shows patterns distinguishable from human TGs and other cooking oils. The most abundant TG species in olive and canola oil is TG 54:3 as a sodiated adduct at *m/z* 907. TG 54:4 at *m/z* 905, TG 54:5 at *m/z* 903, and TG 54:6 at *m/z* 901 are the most abundant species in sesame, corn, and grapeseed oil, respectively, all as sodium adducts. The four abundant TGs in food oil are present only in minimal abundance in human fingerprints. Olive oil has very narrow unsaturation patterns, dominated by TG 54:3 and TG 52:2. In contrast, other oils have broad unsaturation patterns, mostly TG 52:1-4 and TG 54:2-6, with only subtle differences, but clearly distinguishable by the most abundant TG species. In canola oil the abundances of TG 54:6/54:5/54:4/54:3 are 30/70/80/100 compared to 50/95/100/65, 85/100/65/25, and

100/65/40/15 in sesame, corn, and grapeseed oil respectively. These TG profiles are similar to those reported by others[28–30].

Vegetable oil spray contained soybean lecithin in addition to soybean oil, which led to the presence of phosphatidylcholines (PCs) along with the TGs. Vegetable oil spray is easily identified in fingerprints due to multiple unique TGs and PCs. Other oils, such as coconut oil, can also be easily distinguished as shown in **Figure 5**. The mass spectrum of coconut oil is dominated by DGs and TGs in the *m/z* 500-800 region[29]. TGs of human origin appear in the broad mass range of *m/z* 750-1000, TG 43:x to 60:x, as shown in **Figure 4**, and are quite different from plant oils. TG 52:x and 54:x series overlap with plant TGs, but they are much less abundant, whereas the most abundant TG 48:x series in fingerprints is absent in plant oils. As also shown in **Figure 4**, TGs in human and plant oil can be easily distinguished in a food oil contaminated fingerprint, and the identity of the oil species could be easily determined as canola oil based on the most abundant TG and the broader unsaturation pattern. Previous work by Ng et al. showed that vegetable oils from different manufacturers displayed similar TG profiles, despite differences in oil processing, demonstrating reproducible TG profiles for source determination[30]. Food oil can tell more of an individual's story, such as which cooking oil was used when they cooked or ate prior to leaving a fingerprint behind.

Alcohol Compounds

Whether it be from a consumption situation or the presence in a bar, identifying compounds related to alcoholic beverages in a fingerprint can provide a piece of a person's lifestyle. The analysis of wine proved to be the most informative in negative mode, due to several organic acids known to be present in wine, including gallic, tartaric, succinic, malic, and galacturonic acids **Figure 6A**. Tartaric acid and malic acid are the most abundant acids in

wine[31], and the presence of these acids, especially tartaric acid, is a strong indication of wine. In positive mode, proline, hexose, and anhydrofructose were the most abundant wine related peaks, but these compounds are not exclusive to wine. Although these compounds are not individually exclusive, the combination of these compounds may suggest the potential presence of wine. Fingerprint images of malic acid, tartaric acid, proline, and hexose are included in **Figure 6B**. If wine related compounds are confirmed in a latent print, they would indicate a wine drinker as the fingerprint source or suggest the person was recently in an establishment that serves wine.

Other alcohol beverages, such as beer and whiskey, were also investigated for their potential as exogenous compounds in latent fingerprints. Both beer and whiskey were dominated by sugars, lacking unique compounds for identification (**Figure 7**). When PCA analysis is performed between beer and whiskey (**Figure 7B**) or among three alcohols including wine (**Figure 7C**), separation could be made between alcohol beverages, suggesting they could be distinguished in a similar way to sunscreen (**Figure 3**). However, major compounds identified in beer or whiskey could have come from any number of sources, making it impossible to relate back to beer and whiskey specifically. For example, triethyl citrate, glucose (hexose), and sucrose ($hexose_2$) are also found in citrus fruits (see next section) as well as bug spray and sunscreen fingerprints (**Figure 1A** and **Figure 2A**).

Citrus Fruits

Citrus fruits are commonly eaten using bare hands, likely leading to compound transfer onto the fingers. The chemical compounds in mandarins, lemons, and limes were explored. While multiple compounds were identified in the mass spectra (**Figure 8A**), the presence of citric acid in combination with abundant sugars are a good indication of a citrus fruit. Citric acid is present in all three fruits, but the abundance is consistently higher (>5 times) in the lemon and

the lime, which instead have lower abundance of sugars than in the mandarin. The mandarin could be differentiated based on the higher intensity of sugars, and the presence of naringenin, hesperetin, and malic acid in negative mode. In **Figure 8B** chemical images of three citrus related compounds from two different fingerprints are displayed. The type of citrus fruit leading to compounds in a latent print could be used for comparison with those in an individual's habitual space.

Mock Experiment and Multiplex Fingerprint Imaging

To further explore the usefulness of lifestyle markers, our previously developed multiplex MSI method was applied to the analysis of fingerprints. This approach can simultaneously acquire fingerprint MS images in high-resolution as well as thousands of MS/MS spectra of potential marker compounds for confident identification. It can be accomplished in a single data acquisition by dividing each imaging pixel into multiple pixels with different MS events. A simultaneous analysis is crucial when only a single print is recovered from a crime scene. Often, useful and unique exogenous compounds are of low signal intensity. We made a mass list of unique lifestyle marker compounds for bug sprays, sunscreens, food oils, alcohols, and citrus fruits. This precursor mass list was included in the data acquisition software to initiate their automatic fragmentation when the precursor mass was detected. Abundant contamination peaks, matrix peaks, or other peaks of non-interest are added in the exclusion list in the multiplex MS method. The combination of a precursor mass list and exclusion list lead to improved detection, fragmentation, and identification of low abundance useful exogenous compounds. MS/MS for low abundance compounds may not otherwise be acquired.

Table 2 summarizes a list of the key compounds studied in this paper and their major product ions in MS/MS. When multiple adducts are detected for a compound (e.g., $[M+H]^+$,

$[M+Na]^+$, $[M+K]^+$, $[M+^{107}Ag]^+$, $[M+^{109}Ag]^+$), an adduct form with the most efficient MS/MS was included in the table. Compounds in a latent fingerprint can be compared to the table and identification can be made based on accurate mass and MS/MS.

As a mock experiment to demonstrate how multiplex MS imaging can be used to identify lifestyle markers from latent fingerprints, two overlapping fingerprints were prepared with different sources of exogeneous compounds. One print was purposefully contaminated with wine while the other was contaminated from a mandarin fruit. In **Figure 9A** a negative mode mass spectrum and the related mass spectral images of the two overlapped fingerprints are displayed. Two compounds, citric acid and tartaric acid, were present in different prints and the corresponding exact masses were used to individually extract the two prints. Citric acid originated from the mandarin fruit, while the tartaric acid was from the wine contaminated fingerprint. Malic acid had previously been identified in both mandarin fruit and wine and appeared in both but with a higher abundance in the mandarin contaminated print. Confident identification cannot be made with accurate mass only. The multiplex method allowed MS/MS of citric acid, tartaric acid, and malic acid from the precursor mass list, which matches with the MS/MS library (**Table 2**). Citric acid is a good indication of citrus fruit but not a definitive clue for mandarin; however, the existence of naringenin and hesperetin in the MS spectrum gives confidence it is from mandarin. A combined chemical image of two compounds, citric acid and tartaric acid, was extracted and displays the distinct prints each compound is related to (**Figure 9B**). The fingerprint images and multiple MS/MS spectra were obtained in a single data acquisition, demonstrating the efficiency and usefulness of the multiplex MSI technique. The combination of ridge detail and confirmed fragmentation pattern are strong evidence for detailed chemical information about the individual depositing the fingerprint.

Conclusions

In addition to the ridge pattern, the exogenous chemical compounds present in latent fingerprints provide hidden evidentiary value. Products applied, food and beverages consumed, and various environmental contacts will lead to a variety of chemical compounds in a latent fingerprint that can provide lifestyle information of an individual. MALDI-MSI proved to be efficient at ionizing a broad range of exogenous compounds in conjunction with silver sputter coating as a matrix. The simultaneous collection of a high-resolution image along with MS/MS through our multiplex capabilities allowed spatial determination and confident compound identification in a single fingerprint analysis. It is important to note that the work presented here demonstrates proof-of-concept for exogenous compound source determination in latent prints that can be used to provide lifestyle information of the individuals. More work needs to be done before applying to real forensic cases, such as a large population study accompanied with statistical analysis or aged (non-ideal) sample studies. While the exogenous compounds studied here are not exhaustive, the further development of an exogenous compound database combined with multiplex MSI will facilitate lifestyle determination based on fingerprint chemical compounds.

Materials and Methods

The methods and analyses carried out in this work were approved by and in accordance with the Iowa State University Internal Review Board guidelines, specifically the collection of fingerprints for analysis. Experiments were conducted using the researchers own fingerprints, so informed consent documents were not required.

Sample Preparation and Matrix Application

All consumer products were available over the counter and purchased from a local retailer. The bug spray and sunscreen were applied per product instructions, and a fingerprint was then deposited on a glass slide pre-cleaned with methanol. Citrus fruits were handled as if being consumed or cut into slices prior to handling and fingerprint deposition. All alcohol and food oil samples were touched to mimic a spill or the handling of food-ware before making a fingerprint on the glass slide. Hesperetin was purchased from Sigma (St. Louis, MO, USA) for the best purity available and prepared at a concentration of 100 μM in methanol, and 5 μL was spotted onto a glass slide. A triethyl citrate standard was purchased from TCI America (Portland, OR, USA) and prepared using the above-mentioned procedure. All prints and standards were allowed to dry under ambient conditions before matrix was applied.

Organic matrices, DHB and CHCA (Sigma), were sublimated following previously published guidelines[32]. Gold and silver targets (Ted Pella; Redding, CA, USA) were sputter coated (108 Auto Sputter Coater, Ted Pella) at 40 mA for 10 and 5 seconds, respectively.

Instrumentation, Data Acquisition, and Data Analysis

A linear ion trap-Orbitrap mass spectrometer with a MALDI ion source (MALDI LTQ-Orbitrap Discovery, Thermo Scientific; San Jose, CA, USA) was coupled with a 355 nm Nd:YAG laser (UVFQ, Elforlight Ltd.; Daventry, UK). Imaging and profiling of fingerprint samples was done with a 100 μm raster step, 10 laser shots per raster step, and a 30 μm laser spot size. Scans were collected for *m/z* 50-1000 (mass resolution of 30,000 at *m/z* 400). For multiplex MSI, a spiral raster step was employed as previously described[16,17]. A precursor mass list and an exclusion mass list were imported into the Excalibur data acquisition program (Thermo Scientific) for the efficient precursor ion selection in data-dependent MS/MS scans. Collision

energies were broadly assigned depending on the precursor mass range for optimal fragmentation (75 for masses greater than 300 Da, and 125 for masses less than 300 Da). An isolation width of 2.0 Da was used. Positive and negative ion mode were employed for profiling, imaging, and multiplex MSI.

QualBrowser (Thermo Scientific) software was used to average and export all mass spectra. Chemical fingerprint images were generated using ImageQuest (Thermo Scientific) software with a mass tolerance of ±0.05 Da. The intensity scale of each image was arbitrarily adjusted based on the individual compound intensity to produce quality images. Each compound was confirmed using a standard and/or database comparison for fragmentation patterns. To compare the intensity of active ingredients among distinct brands, the mass spectra were exported to an Excel spreadsheet using QualBrowser. The intensities of all the adducts were summed for each ingredient and normalized to the most abundant compound in each data set. The three replicates were averaged, and the standard deviation was calculated. The averages and standard deviations were plotted for comparison and included in **Figure 2B** for sunscreen.

Principal Component Analysis

Data for PCA was extracted using the QualBrowser software. The data was averaged over the *m/z* range 150-500, as most relevant compounds are found in this region. Each peak was normalized to the most abundant peak in the mass region. Peaks with a normalized intensity of less than one percent were not extracted. Three replicates of each brand being studied were included in the PCA. The mass list was then uploaded to MetaboAnalyst for statistical analysis[26]. Scores plots for both bug spray and sunscreen mass spectra were included in **Figure 3**. For a targeted approach, peak intensity tables of the active ingredients were uploaded rather than the entire mass list.

References

1. Cadd, S. J. *et al.* Extraction of fatty compounds from fingerprints for GCMS analysis. *Anal. Methods* **7,** 1123–1132 (2015).

2. Croxton, R. S., Baron, M. G., Butler, D., Kent, T. & Sears, V. G. Development of a GC-MS method for the simultaneous analysis of latent fingerprint components. *J. Forensic Sci.* **51,** 1329–1333 (2006).

3. De Puit, M., Ismail, M. & Xu, X. LCMS Analysis of Fingerprints, the Amino Acid Profile of 20 Donors. *J. Forensic Sci.* **59,** 364–370 (2014).

4. Muramoto, S. & Sisco, E. Strategies for Potential Age Dating of Fingerprints Through the Diffusion of Sebum Molecules on a Nonporous Surface Analyzed Using Time-of-Flight Secondary Ion Mass Spectrometry. *Anal. Chem.* **87,** 8035–8038 (2015).

5. Bailey, M. J. *et al.* Enhanced imaging of developed fingerprints using mass spectrometry imaging. *Analyst* **138,** 6246–6250 (2013).

6. Sisco, E., Demoranville, L. T. & Gillen, G. Evaluation of C60 secondary ion mass spectrometry for the chemical analysis and imaging of fingerprints. *Forensic Sci. Int.* **231,** 263–269 (2013).

7. Bailey, M. J. *et al.* Rapid detection of cocaine, benzoylecgonine and methylecgonine in fingerprints using surface mass spectrometry. *Analyst* **140,** 6254–6259 (2015).

8. Zhou, Z. & Zare, R. N. Personal Information from Latent Fingerprints Using Desorption Electrospray Ionization Mass Spectrometry and Machine Learning. *Anal. Chem.* **89**, 1369-1372 (2017).

9. Guinan, T., Della Vedova, C., Kobus, H. & Voelcker, N. H. Mass spectrometry imaging of fingerprint sweat on nanostructured silicon. *Chem. Commun.* **51,** 6088–6091 (2015).

10. Forbes, T. P. & Sisco, E. Chemical imaging of artificial fingerprints by desorption electro-flow focusing ionization mass spectrometry. *Analyst* **139,** 2982–2985 (2014).

11. Kaplan-Sandquist, K., LeBeau, M. A. & Miller, M. L. Chemical analysis of pharmaceuticals and explosives in fingermarks using matrix-assisted laser desorption ionization/time-of-flight mass spectrometry. *Forensic Sci. Int.* **235,** 68–77 (2014).

12. O'Neill, K. C. & Lee, Y. J. Effect of Aging and Surface Interactions on the Diffusion of Endogenous Compounds in Latent Fingerprints Studied by Mass Spectrometry Imaging,. *J. Forensic Sci.* **63**, 708-713 (2017).

13. Beinsen, A. & Abel, B. Matrix Assisted and Matrix Free Mass Spectrometric Imaging of Latent Fingermarks. *Curr. Top. Anal. Chem.* **8,** 77-81 (2011).

14. Bailey, M. J. *et al.* Chemical Characterization of Latent Fingerprints by Matrix-Assisted Laser Desorption Ionization, Time-of-Flight Secondary Ion Mass Spectrometry, Mega Electron Volt Secondary Mass Spectrometry, Gas Chromatography/Mass Spectrometry, X-ray Photoelectron Spec. *Anal. Chem.* **84,** 8514–8523 (2012).

15. Francese, S. in *Advances in MALDI and Laser-Induced Soft Ionization Mass Spectrometry* (ed. Cramer, R.) 93–128 (Springer International Publishing, 2016). doi:10.1007/978-3-319-04819-2

16. Perdian, D. C. & Lee, Y. J. Imaging MS Methodology for More Chemical Information in Less Data Acquisition Time Utilizing a Hybrid Linear Ion Trap- Orbitrap Mass Spectrometer. *Anal. Chem.* **82,** 9393–9400 (2010).

17. Yagnik, G. B., Korte, A. R. & Lee, Y. J. Multiplex mass spectrometry imaging for latent fingerprints. *J. Mass Spectrom.* **48,** 100–104 (2013).

18. Ferguson, L. S. *et al.* Direct detection of peptides and small proteins in fingermarks and determination of sex by MALDI mass spectrometry profiling. *Analyst* **137,** 4686–4692 (2012).

19. Emerson, B., Gidden, J., Lay, J. O. & Durham, B. Laser desorption/ionization time-of-flight mass spectrometry of triacylglycerols and other components in fingermark samples. *J. Forensic Sci.* **56,** 381–389 (2011).

20. Lauzon, N., Dufresne, M., Chauhan, V. & Chaurand, P. Development of laser desorption imaging mass spectrometry methods to investigate the molecular composition of latent fingermarks. *J. Am. Soc. Mass Spectrom.* **26,** 878–886 (2015).

21. Wolstenholme, R., Bradshaw, R., Clench, M. R. & Francese, S. Study of latent fingermarks by matrix-assisted laser desorption/ionisation mass spectrometry imaging of endogenous lipids. *Rapid Commun. Mass Spectrom.* **23,** 3031–3039 (2009).

22. Groeneveld, G., de Puit, M., Bleay, S., Bradshaw, R. & Francese, S. Detection and mapping of illicit drugs and their metabolites in fingermarks by MALDI MS and compatibility with forensic techniques. *Sci. Rep.* **5,** 11716 (2015).

23. Bouslimani, A. *et al.* Lifestyle chemistries from phones for individual profiling. *Proc. Natl. Acad. Sci. U. S. A.* **113,** E7645–E7654 (2016).

24. Petras, D. *et al.* Mass Spectrometry-Based Visualization of Molecules Associated with Human Habitats. *Anal. Chem.* **88**, 10775-10784 (2016).

25. Asbury, G. R., Al-Saad, K., Siems, W. F., Hannan, R. M. & Hill, H. H. Analysis of triacylglycerols and whole oils by matrix-assisted laser desorption/ionization time of flight mass spectrometry. *J. Am. Soc. Mass Spectrom.* **10,** 983–991 (1999).

26. Xia, J. & Wishart, D. S. Using metaboanalyst 3.0 for comprehensive metabolomics data analysis. *Curr. Protoc. Bioinforma.* **2016,** 14.10.1-14.10.91 (2016).

27. Dettmer, K., Aronov, P. A. & Hammock, B. D. Mass spectrometry-based metabolomics. *Mass Spectrom. Rev.* **26,** 51–78 (2007).

28. Calvano, C. D., De Ceglie, C., D'Accolti, L. & Zambonin, C. G. MALDI-TOF mass spectrometry detection of extra-virgin olive oil adulteration with hazelnut oil by analysis of phospholipids using an ionic liquid as matrix and extraction solvent. *Food Chem.* **134,** 1192–1198 (2012).

29. Schiller, J., Sub, R., Petkovic, M. & Arnold, K. Triacylglycerol analysis of vegetable oils by matrix-assisted laser desorption and ionization time-of-flight (MALDI-TOF) mass spectrometry and 31P NMR Spectroscopy. *J. Food Lipids* **9,** 185–200 (2002).

30. Ng, T. T., So, P. K., Zheng, B. & Yao, Z. P. Rapid screening of mixed edible oils and gutter oils by matrix-assisted laser desorption/ionization mass spectrometry. *Anal. Chim. Acta* **884,** 70–76 (2015).

31. Rajković, M., Novaković, I. D. & Petrović, A. Determination of titratable acidity in white wine. *J. Agric. Sci.* **52,** 169–184 (2007).

32. Hankin, J. A., Barkley, R. M. & Murphy, R. C. Sublimation as a Method of Matrix Application for Mass Spectrometric Imaging. *J. Am. Soc. Mass Spectrom.* **18,** 1646–1652 (2007).

Figures and Tables

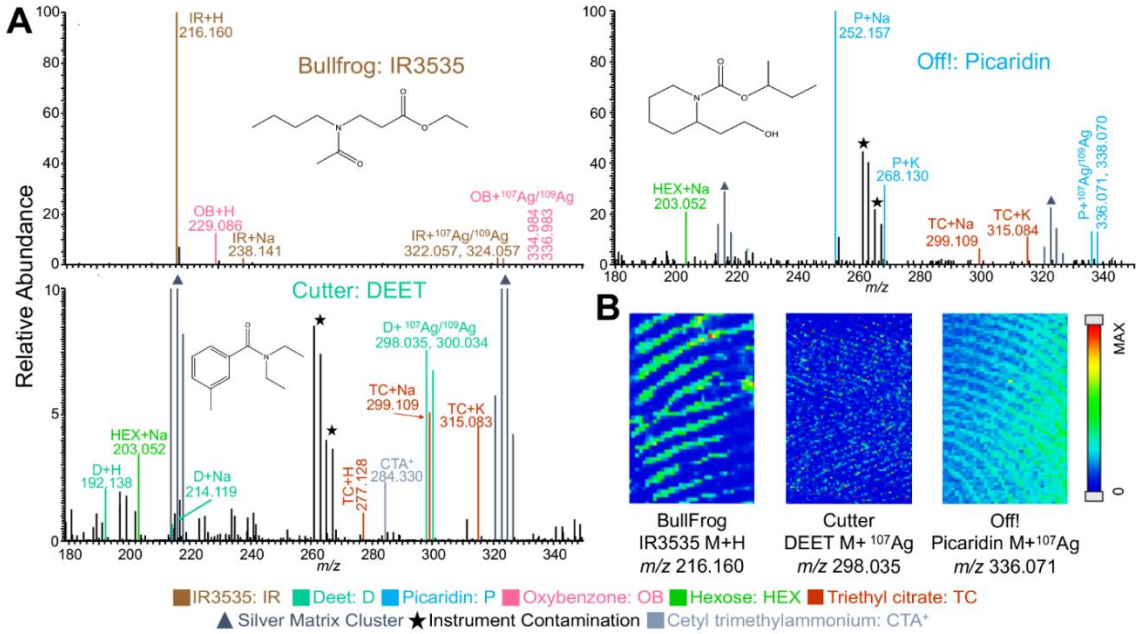

Figure 1. (A) Representative positive mode mass spectra of fingerprints containing three bug spray brands (BullFrog, Cutter, and OFF!) by MALDI-MSI with silver sputter. **(B)** Chemical images of the three active ingredients.

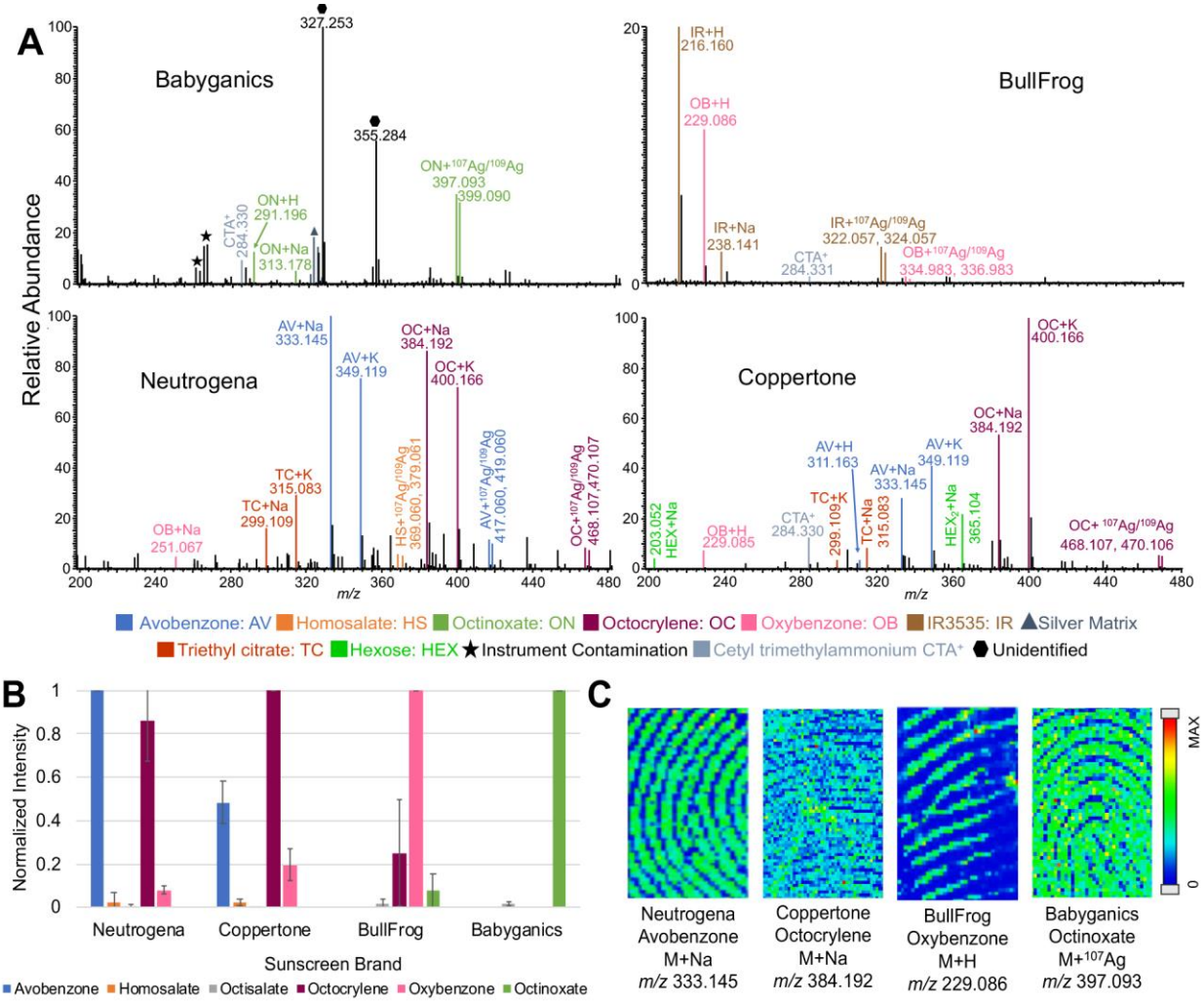

Figure 2. (**A**) Representative positive mode mass spectra of four sunscreen brands (Babyganics, BullFrog, Neutrogena, and Coppertone) by MALDI-MSI with silver sputter. (**B**) Comparison of each active ingredient across the four brands. The adduct intensities are summed for each active ingredient and normalized to the most abundant compound. Error bars show the standard deviation from three replicates. (**C**) Chemical images of the four sunscreen active ingredients used in brand determination.

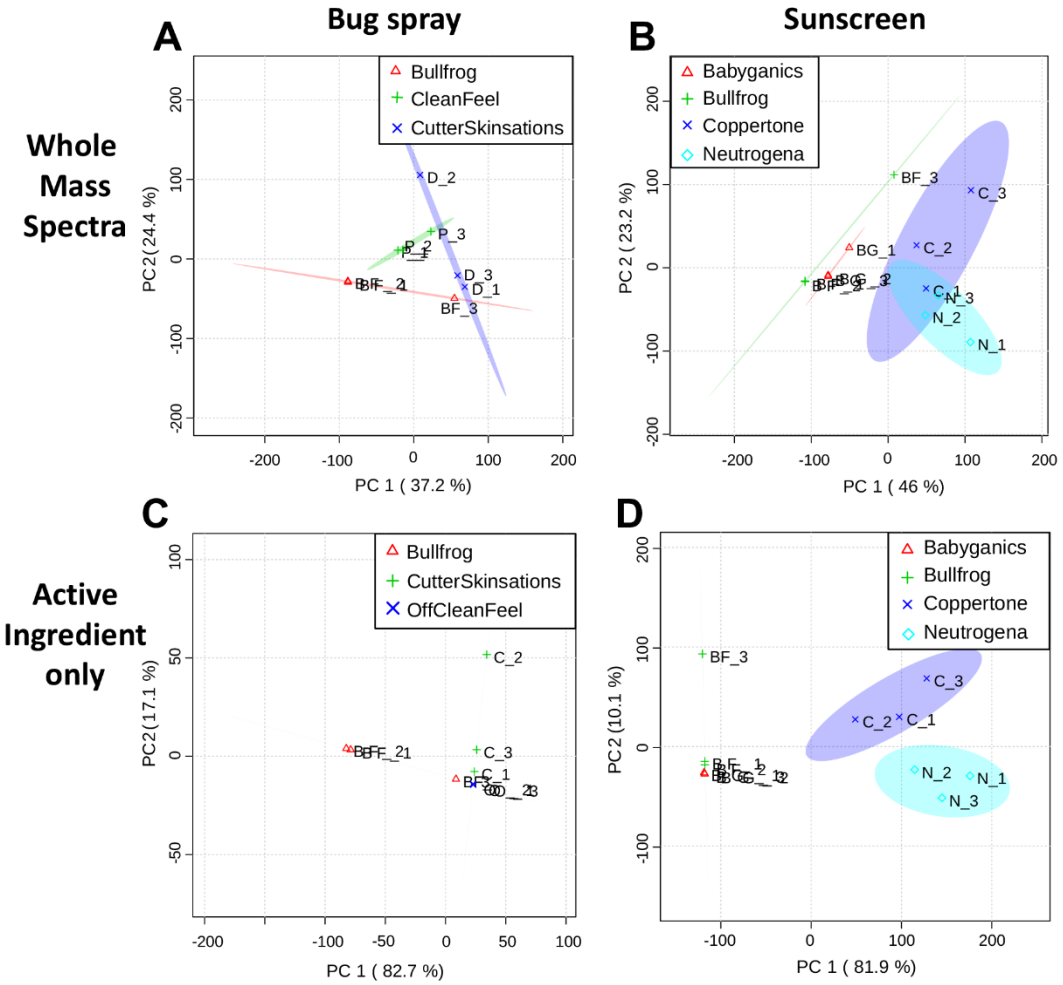

Figure 3. PCA scatter plots of **(A, C)** bug spray and **(B, D)** sunscreen containing fingerprints using either entire mass spectrum **(A, B)** or only active ingredients **(C, D)**.

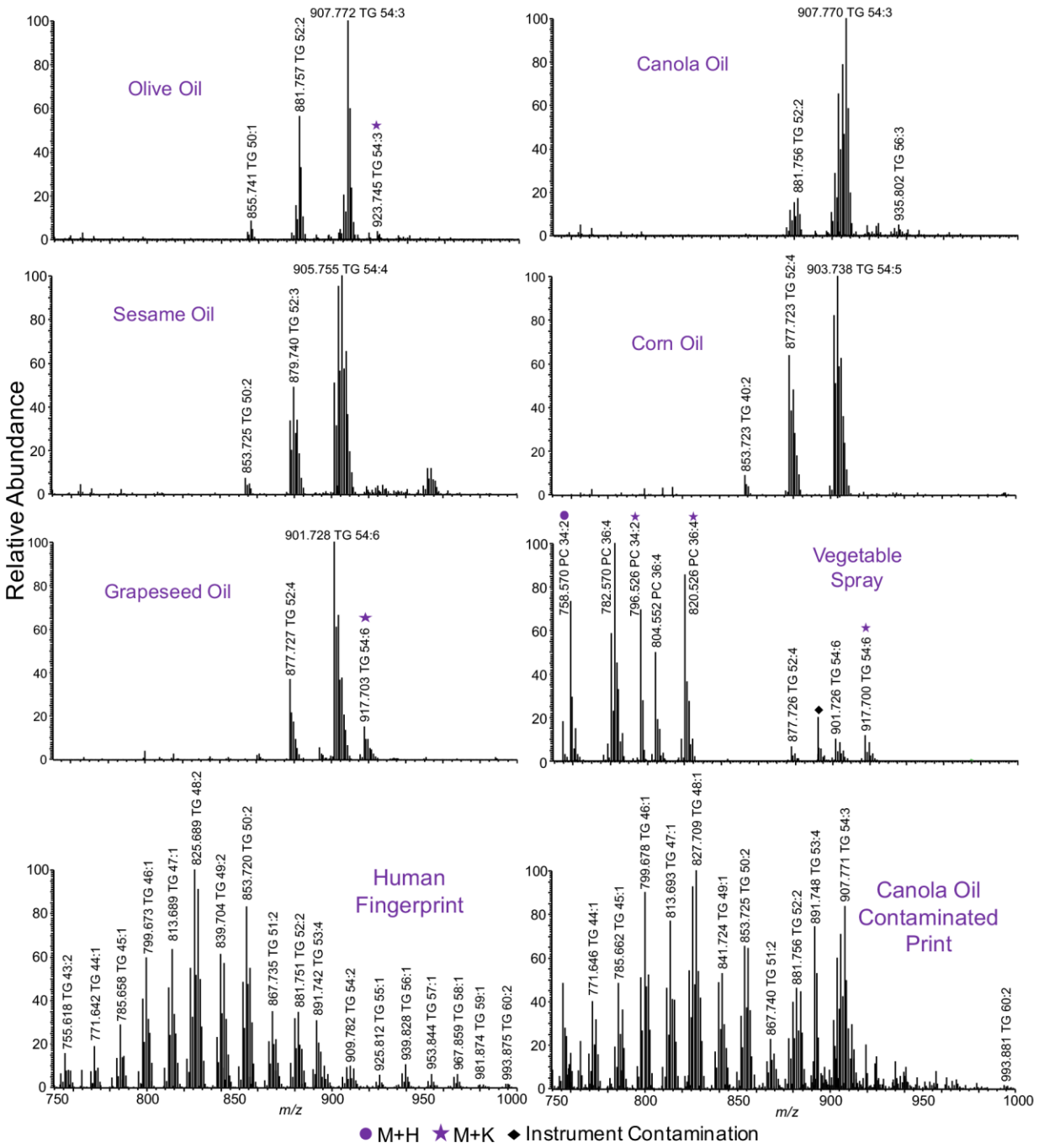

Figure 4. Representative positive mass spectra of five plant-based food oils, a vegetable oil spray, and human fingerprints with and without contamination by MALDI-MSI with DHB as the matrix. All non-labeled TGs are observed as sodium adducts and others are as proton or potassium adducts as labeled.

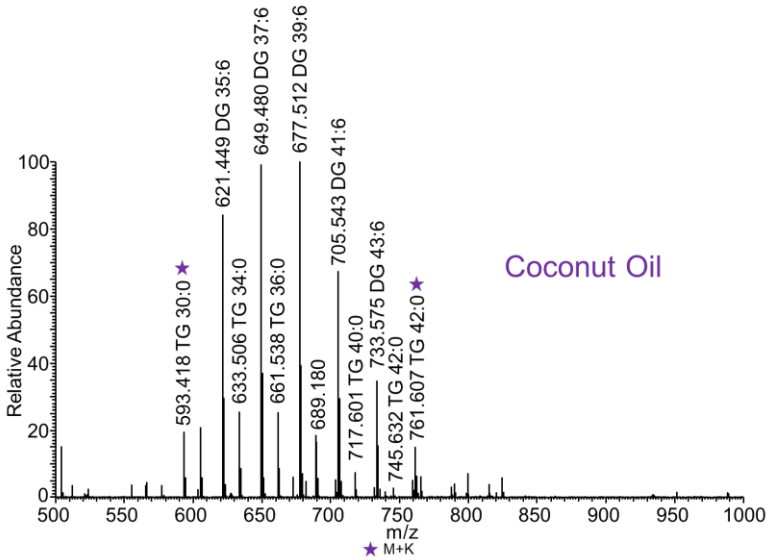

Figure 5. The TGs and DGs indicative of coconut oil are in the *m/z* range of 500-800, a lower mass range than most plant-based food oils. Note that all DGs present contain five oxygens, therefore they are considered a natural DG rather than MALDI generated.

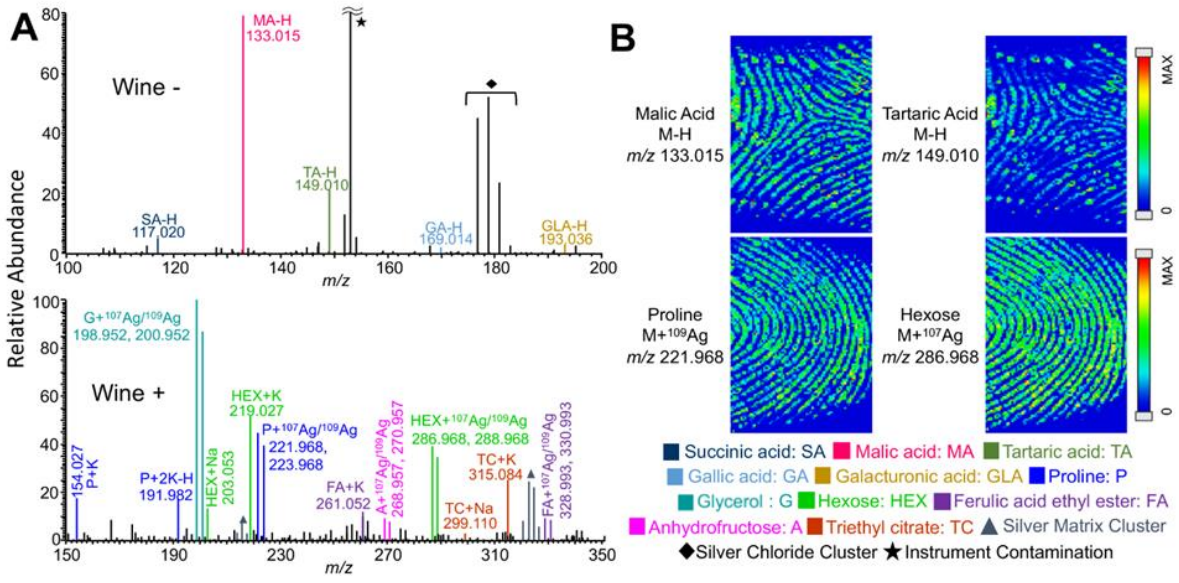

Figure 6. (A) Representative negative and positive mode mass spectra of wine by MALDI-MSI with silver sputter. **(B)** Chemical images of wine related compounds from contaminated fingerprints.

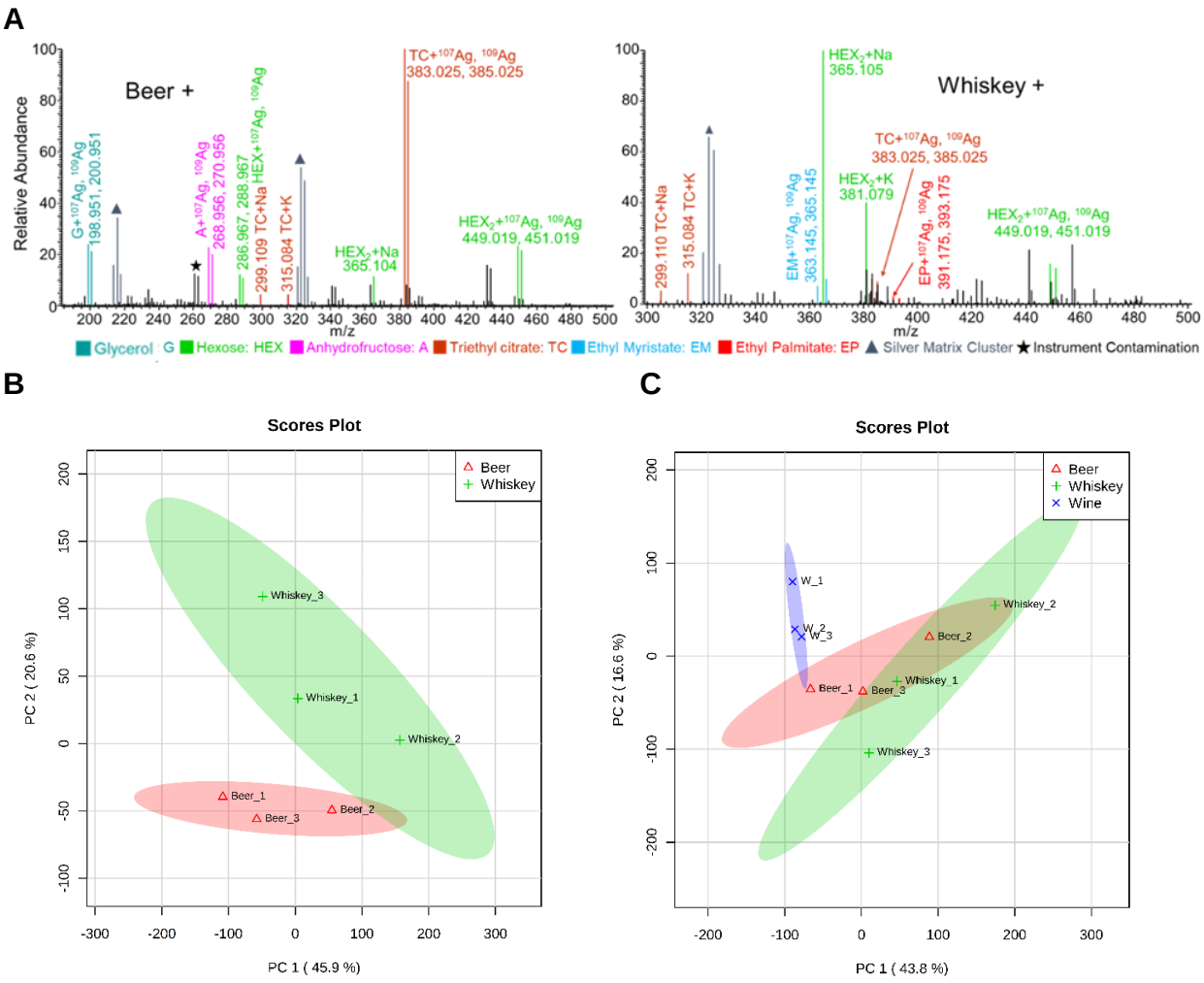

Figure 7. (A) The positive mode mass spectra of beer and whiskey using silver matrix for MALDI-MSI. **(B)** PCA analysis of beer and whiskey only. **(C)** PCA analysis of beer, whiskey, and wine. Beer and whiskey lacked unique compounds that could be used for definitive source identification.

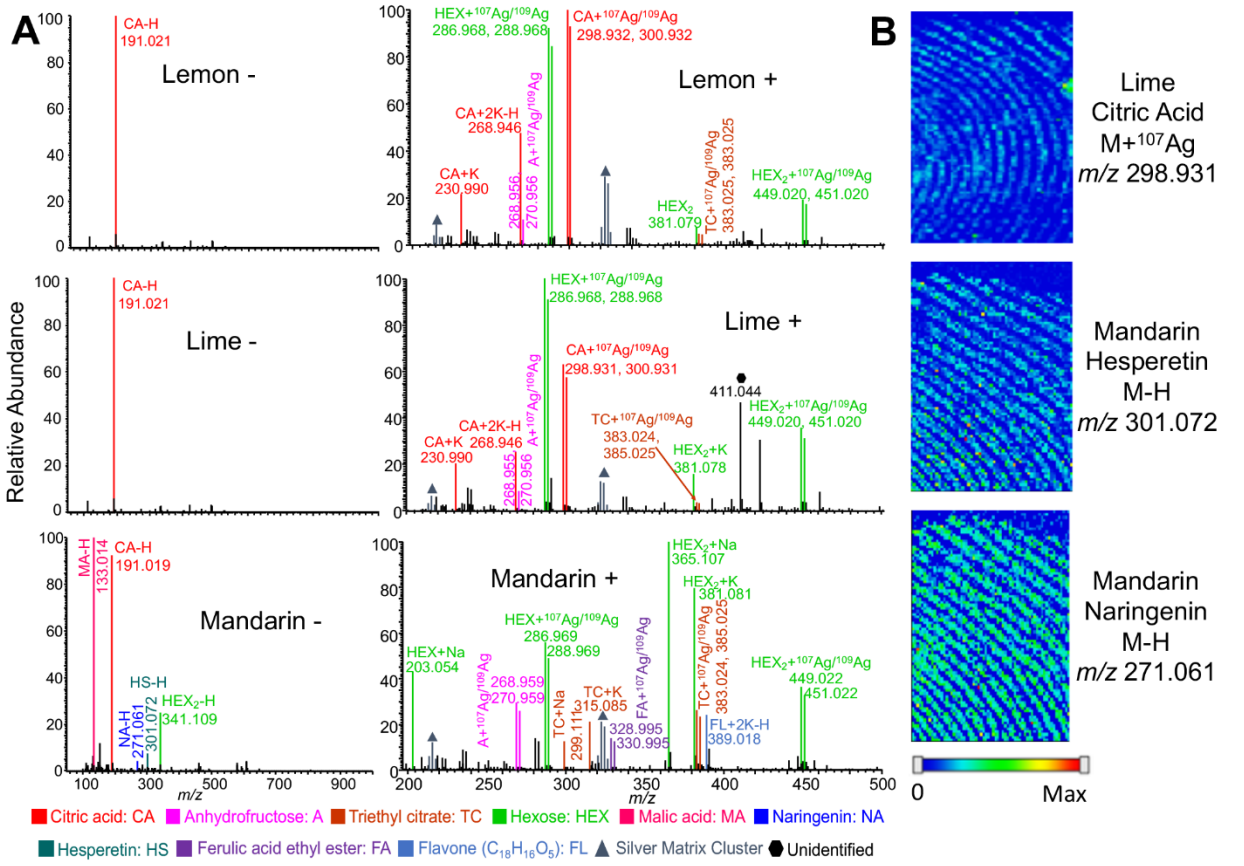

Figure 8. (A) Representative mass spectra of lemon, lime, and mandarin in negative and positive modes by MALDI-MSI with silver sputter. **(B)** Three chemical images related to citrus fruits.

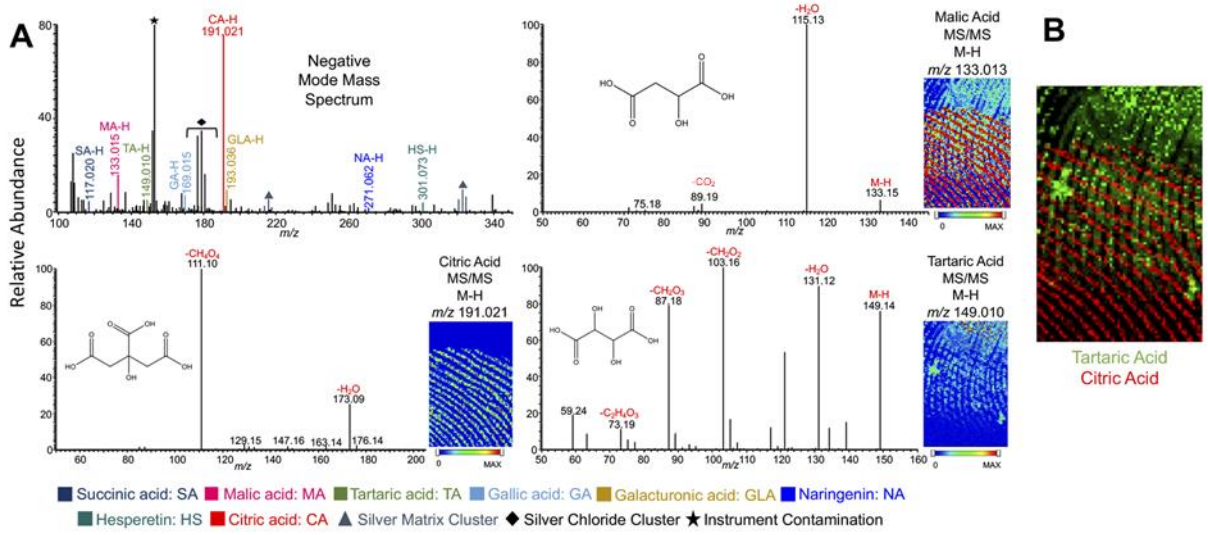

Figure 9. (A) Negative mode mass spectrum and MS/MS spectra of three exogenous compounds from a mock experiment obtained in a single multiplex acquisition by MALDI-MSI with silver sputter. **(B)** Chemical images of two compounds differentiating the overlapped fingerprints.

Table 1. The active ingredient list of each sunscreen brand. Y=Yes, N=No.

Compound/Brand	Neutrogena	Coppertone	BullFrog	Babyganics
Avobenzone	Y	Y	N	N
Homosalate	Y	Y	N	N
Octisalate	Y	Y	Y	Y
Octocrylene	Y	Y	Y	N
Oxybenzone	Y	Y	Y	N
Octinoxate	N	N	Y	Y

Table 2. A list of exact *m/z* values for exogenous compounds utilized for brand or type determination, as well as the corresponding fragment ions for confident compound identification.

Compound	Source	Mode	MALDI-MS	MALDI-MS/MS
			Adduct	Product Ions
Avobenzone $C_{20}H_{22}O_3$	Sunscreen	+	311.164 $[M+H]^+$	293, 161, 135
Homosalate $C_{16}H_{22}O_3$	Sunscreen	+	369.061 $[M+^{107}Ag]^+$	354, 341, 249
Octinoxate $C_{18}H_{26}O_3$	Sunscreen	+	291.195 $[M+H]^+$	276, 179, 121
Octisalate $C_{15}H_{22}O_3$	Sunscreen	+	273.146 $[M+Na]^+$	255, 137
Octocrylene $C_{24}H_{27}NO_2$	Sunscreen	+	384.193 $[M+Na]^+$	324, 272, 228
Oxybenzone $C_{14}H_{12}O_3$	Sunscreen	+	229.086 $[M+H]^+$	151, 105
DEET $C_{12}H_{17}NO$	Bug spray	+	192.138 $[M+H]^+$	174, 119
IR3535 $C_{11}H_{21}NO_3$	Bug spray	+	216.159 $[M+H]^+$	170
Picaridin $C_{12}H_{23}NO_3$	Bug spray	+	230.175 $[M+H]^+$	212, 174
Galacturonic acid $C_6H_{10}O_7$	Wine	-	193.03 $[M-H]^-$	131, 113, 89
Gallic acid $C_7H_6O_5$	Wine	-	169.014 $[M-H]^-$	151, 141, 125
Succinic acid $C_4H_6O_4$	Wine	-	117.019 $[M-H]^-$	99, 73
Tartaric acid $C_4H_6O_6$	Wine	-	149.009 $[M-H]^-$	131, 103, 87, 73
Malic acid $C_4H_6O_5$	Wine, citrus	-	133.014 $[M-H]^-$	115, 89
Citric acid $C_6H_8O_7$	Citrus	-	191.020 $[M-H]^-$	173, 111
Hesperetin $C_{16}H_{14}O_6$	Citrus	+	408.984 $[M+^{107}Ag]^+$	301, 259
Naringenin $C_{15}H_{12}O_5$	Citrus	-	271.061 $[M-H]^-$	177, 151, 119
Nobiletin $C_{21}H_{22}O_8$	Citrus	+	403.139 $[M+H]^+$	388, 373, 342
Tangeretin $C_{20}H_{20}O_7$	Citrus	+	373.128 $[M+H]^+$	358, 343, 312

CHAPTER 5. DETERMINING FINGERPRINT AGE WITH MASS SPECTROMETRY IMAGING VIA OZONOLYSIS OF TRIACYLGLYCEROLS

Paige Hinners, Madison Thomas, and Young Jin Lee[1]

1. Department of Chemistry, Iowa State University, Ames, Iowa, 50011, USA

Modified from a manuscript published in *Analytical Chemistry*

Reprinted with permission from *Anal. Chem.* 2020, 92, 4, 3125-3132.

Abstract

Despite the common use of fingerprints as a trusted means of identification, no method currently exists to reliably establish the time since deposition of latent fingerprints. A reproducible method of establishing latent fingerprint age would allow forensic personnel to determine if a latent fingerprint was relevant to a crime. This work investigates the ambient aging of triacylglycerols (TGs) and other lipids in latent fingerprint residue utilizing matrix-assisted laser desorption/ionization - mass spectrometry imaging (MALDI-MSI). Unsaturated TGs were found to undergo ambient ozonolysis resulting in a decrease of unsaturated TGs over time. In addition, two series of compounds related to the degradation of unsaturated TGs due to ambient ozonolysis emerged with time and were detectable within a single day of aging. Tracking the degradation of unsaturated TGs over time proved to be relatively reproducible in multiple individuals and is suggested as a means of establishing latent fingerprint age.

Introduction

The unique features, or minutiae, of fingerprints have made them a trusted source of individual identification. In-depth algorithms, such as those used in the automated fingerprint identification system (AFIS), are utilized to compare the unique features of an unknown fingerprint with those in existing databases.[1] Over the past decade research has focused on

increasing the evidentiary value of fingerprints, with a particular focus on the chemical information within them. Both chromatography and surface-based techniques have detected an array of endogenous (natural) and exogenous (environmental) compounds in fingerprints. Variations in the compounds within fingerprints have been used to profile the individual's lifestyle[2], gender[3], and ethnicity[4] in research studies.

The ability to establish a suspect profile based on fingerprint chemical analysis would greatly increase the evidentiary value of fingerprints, particularly of those that lack a match in a known fingerprint database such as AFIS. Despite the reliance of the forensic field on fingerprints and the research efforts for more evidence, there is no established method for fingerprint age determination. Developing a reproducible fingerprint age determination method is crucial to reliably establish time since deposition in forensic cases.

Multiple studies, both physical and chemical based, have attempted to interpret fingerprint aging but no study has been able to solve this problem. De Alcaraz-Fossoul et al. focused on reduction in ridge width and decrease in contrast between ridges and valleys, among others, as indicators of degradation.[5–7] In spite of its potential, the use of a single donor and subjectivity of manual ridge measurements remained as significant problems. Muramoto and Sisco suggested the diffusion of a saturated fatty acid (FA) as a way of estimating fingerprint age with time-of-flight secondary ion mass spectrometry (TOF-SIMS).[8] However, in the study of the diffusion of a FA and triacylglycerol (TG) on multiple surfaces with MALDI-MSI, O'Neill and Lee demonstrated that the diffusion rate is greatly affected by the interaction between surface and fingerprint chemicals, complicating the simple diffusion model.[9]

Gas chromatography - mass spectrometry (GC-MS) analysis of fingerprint extracts has been explored to study the aging of lipids. Girod et al. was able to broadly classify the age of

unknown fingerprints as either less than or greater than eight days old and highlighted the need to consider factors such as substrate and environment in the aging model.[10] Oxidation has been suggested as a possible cause of degradation of unsaturated FAs.[11] Other work reported quick degradation of squalene, appearance of short chain FAs, and increase then decrease of saturated FAs when fingerprints were aged in sealed containers.[12] In a review article, Cadd et al. addressed the complex composition of fingerprints, including amino acids, FAs, TGs, cholesterol, and squalene and how each set of compounds may age.[13] While these reports provided some chemical information occurring during the aging, there currently is no reliable aging model, especially for the critical first few days of aging. Additionally, they require an extraction that fails to preserve the forensic evidence.

Pleik et al. monitored the ozonolysis of TGs under ambient conditions using liquid chromatography - tandem mass spectrometry (LC-MS/MS).[14] The intensity of TG 48:1 was shown to decrease with time while the associated ozonide increased with time. Atmospheric pressure MALDI-MSI was utilized to confirm the presence of the ozonide on fingerprint ridges but this experiment was performed only after 26 days of aging.[14] Blanksby and coworkers have reported ozonolysis of unsaturated lipids in nonforensic applications using both ambient ozone and ozone-induced dissociation.[15,16] They propose ozonide formation at the double bond site.

In this work, MALDI-MSI is used to determine if ambient degradation of fingerprint TGs can be utilized to establish fingerprint age, particularly within the first few days of aging which is a crucial time frame in forensics. The abundance of multiple saturated and unsaturated TGs are monitored over time to test the potential for fingerprint age determination. Importantly, the forensic evidence is maintained by avoiding an extraction. Fingerprints dusted with a forensic

development powder are also analyzed to determine the applicability of the approach on more realistic cases.

Experimental Section

The collection and use of fingerprints was approved by the Iowa State University Internal Review Board.

MALDI Sample Preparation

Fingerprints were collected from three donors. For all fingerprint samples, the donor touched their forehead a single time prior to depositing the fingerprint on a glass slide precleaned with methanol. Fresh fingerprints were collected and immediately prepared and analyzed. Samples for aging were stored under ambient conditions for various time points in a room with no windows and received fluorescent room light for approximately 8 hours per day. The temperature and humidity were monitored over the course of the study. Prior to analysis all fingerprints were sprayed with 10 mM sodium acetate (Alfa Aesar, Haverhill, MA) in methanol using a TM Sprayer (HTX Technologies, Chapel Hill, NC). A flow rate of 0.03 mL/min was used for a total of eight passes with 3 mm spacing in a crisscross pattern at a velocity of 1200 mm/min with a nitrogen gas pressure of 10 psi and nozzle temperature of 30 °C. Gold was then sputtered on top of the fingerprint for 20 s at 40 mA using a Cressington 108 Sputter Coater (Ted Pella, Redding, CA).

For quantitative analysis fresh fingerprints from the three donors used in the study were collected on three separate days. Following collection, a 1 mg/mL solution of glycerol trinonanoate (Sigma-Aldrich, St. Louis, MO) was sprayed on top of the fingerprint using the previously described TM Sprayer method prior to the sodium gold combination.

Fresh and seven-day aged fingerprints were also dusted with carbon forensic dusting powder prior to MALDI analysis. For these samples no additional matrix was applied. Additional fingerprints were aged for three days, one under ambient conditions, one in a transparent sealed container, and the final fingerprint in an opaque sealed container. These fingerprints were prepared with sodium gold as a matrix and analyzed using MALDI-MSI as noted above.

A 1 mg/mL solution of 1-oleoyl-2,3-dipalmitoyl glycerol (OPP, TG 50:1), purchased form Toronto Research Chemicals (Ontario, Canada) in chloroform was spotted (4 µL) onto a cleaned glass slide and allowed to age for 12 h under ambient conditions. The sodium acetate and gold matrix combination was applied and the fresh and aged standard were analyzed using both full scan and MS/MS. The full scan analysis of fresh and aged standards was performed on a FA (oleic acid), wax ester (WE, oleyl oleate), and diacylglycerol (DG, 1,2-dioleoyl-glycerol) at concentrations of 1 mg/mL in chloroform, all purchased from Sigma-Aldrich.

Imaging Instrumentation and Data Analysis

Following matrix application, the fingerprints and standards were analyzed using a MALDI-LTQ-Orbitrap Discovery (Thermo Finnigan, San Jose, CA). The instrument was modified to use an external frequency tripled 355 nm Nd:YAG laser (UVFQ; Elforlight, Ltd., Daventry, UK). A 100-µm raster step, laser spot size of approximately 15 µm, and ten laser shots per pixel were used to analyze approximately 2700 pixels in positive mode for the mass range of 500-1000. High-resolution MS images were collected in the Orbitrap mass analyzer with a mass resolution setting of 30,000 at *m/z* 400. MS/MS was performed using the linear ion trap with a collision energy of 75 (arbitrary units) and an isolation width of 0.5-0.8 Da. The fresh and aged

FA standard were analyzed in negative mode in the mass range of 100-1000. All other standards were analyzed in positive mode in the mass range of 100-1000.

IMZML files were generated using Image Quest Software (Thermo Finnigan) and loaded into open-source MSiReader software.[17,18] Images were generated for a mass list of known lipids and theoretical ozonolysis peaks. A peak list with intensities was exported for the known mass list using the region-of-interest tool for relative quantitation analysis. The intensity of each compound was averaged per pixel.

QTOF Analysis for Mechanism Confirmation and Fatty Acid Quantitation

OPP was spotted onto a precleaned glass slide and allowed to age for 12 h. Following aging, a fresh and aged standard were removed from the glass slide using chloroform. The samples were dried down and reconstituted in 300 µL of chloroform. The fresh and aged standards were directly electrosprayed into an Agilent 6540 QTOF (Santa Clara, CA). A flow rate of 0.5 mL/min with an 80:20 mixture of acetonitrile:water was utilized to inject 5 µL of the standards. A gas temperature of 300 °C and flow of 5 L/min were utilized with a sheath gas temperature of 320 °C and flow of 11 L/min. Mass spectra were acquired in the mass range of 500 to 1200.

Five fingerprints from three donors were collected on the inside of scintillation vials and 500 µL of chloroform was added along with 1 µL of 1 mg/mL FA 19:0 to serve as an internal standard. Each vial was vortexed for 1 min to ensure all fingerprint residue was removed from the vial. The samples were dried completely and then reconstituted in 300 µL of chloroform. The fingerprint samples were direct injected into the QTOF as described above. MassHunter software (Agilent) was utilized to quantify the FAs in each participant.

Results and Discussion

Aging of Fingerprint Triacylglycerols

A combination of sprayed sodium and sputtered gold was utilized as the matrix based on previous work done by Dufresne and coworkers.[19] The addition of sodium to the sample ensures all TG related peaks are observed as the sodium adduct. **Figure 1** shows the MALDI mass spectra for the TG region of representative fresh (**A**) and aged latent fingerprints (**B** and **C**). TGs commonly found in human fingerprints appear in the *m/z* range of 740 to 890 as a series of clusters with 14 Da spacing corresponding to alkyl chains in fatty acyl groups. Each cluster is made of multiple two Da series that vary depending on the degree of unsaturation or double bonds in the fatty acyl groups. TGs with fatty acyl chain lengths ranging from 42 to 52 carbons are the focus of this study as they are the most abundant and do not overlap with potential vegetable oil contamination.[2] The TG region is typically Gaussian shaped with 46 to 48 carbon side chains being the most abundant.

Unsaturated TGs (blue) are more abundant than saturated TGs (red) in a fresh fingerprint (**Figure 1A**); however, they decrease over time and are finally overtaken by saturated TGs at day seven (**Figure 1B** and **1C**). More drastic change is noted in the mass spectra of aged fingerprints in the approximate mass range of 640 to 800. Two series of new peaks, colored in purple and green, emerge with fingerprint age (**Figure 1B** and **1C**), both of which have a gaussian shape pattern similar to unsaturated TGs in the fresh spectrum (**Figure 1A**). Thanks to the high mass resolution of the Orbitrap used in this study, the chemical formula of each of these compounds could be assigned based on accurate mass (**Table 1, 2, 3**). The purple and green series are oxygen containing hydrocarbons similar to TGs which have six oxygens (O6 series), but with fewer carbons and one or two additional oxygens (O7 and O8 series), respectively. Interestingly,

the O8 series is detected mostly as a deprotonated two sodium adduct, $[M-H+2Na]^+$, as will be further discussed later. The decrease of the unsaturated TGs and the increase of O7 and O8 series with aging are directly correlated, suggesting unsaturated TGs (O6) converted to O7 and O8 series compounds over time.

This trend is also clear in selected MS images shown in **Figure 2**. TG 48:0, a saturated TG, remains clearly visible on the fingerprint ridges with its abundance mostly consistent over time. In comparison, the ridge patterns degrade over time for unsaturated TGs. Specifically, the more unsaturated (e.g., TG 48:3 or TG 48:4), the more rapidly the ridge pattern degrades. The ridge pattern is barely seen for TG 48:4 on Day 1 while it is still visible for TG 48:1 on day 7 although at a significantly decreased abundance. The MS images are compelling support for the degradation of the unsaturated TGs with time. In contrast, MS images of purple (O7) and green (O8) peaks are completely absent on Day 0 but become clearer as the fingerprint ages.

Ambient Ozonolysis of Triacylglycerols

Pleik et al. suggested ozonolysis as the mechanism for ambient degradation of unsaturated TGs.[14] In their work, fingerprints were allowed to age under ambient conditions, and analyzed using electrospray ionization (ESI)-LC-MS/MS after extraction with chloroform. The decrease of unsaturated TGs and increase of an ozonide was reported. A more thorough mechanism of ozonolysis has previously been reported by Blanksby[15,16] as shown in **Scheme 1** for 1-oleoyl-2,3-dipalmitoyl glycerol (OPP, TG 50:1), with the chemical formula of $C_{53}H_{100}O_6$. OPP reacts with ozone on the double bond site becoming $C_{53}H_{100}O_9$, primary ozonide, which may go through rearrangement to form a secondary ozonide or decompose to an aldehyde ($C_{44}H_{82}O_7$).[15,16] In MS/MS with ozone induced dissociation, the Blanksby group proposed the secondary ozonide decomposes to an aldehyde and “Criegee ions” ($C_{44}H_{82}O_8$). They suggested

multiple Criegee ion isomers are possible and refer to them collectively as "Criegee ions": carbonyl oxide form, vinyl hydroperoxide, and carboxylic acid form as shown in **Scheme 1**. The vinyl hydroperoxide and carboxylic acid forms are suggested to be more stable than the carbonyl oxide. Note that the color code in **Scheme 1** coordinates with subsequent figures for ease of explanation.

Figure 3 shows the fresh and aged MALDI-MS spectra of the OPP standard. In the MALDI-MS spectrum of aged OPP (**Figure 3B**), we do not see primary or secondary ozonides of OPP ($C_{53}H_{100}O_9$), presumably due to the unstable nature of the ozonide in vacuum MALDI conditions. The O7 compound, $[C_{44}H_{82}O_7+Na]^+$, at *m/z* 745.60 is presumed to be the aldehyde in **Scheme 1**, while the O8 compounds of $[C_{44}H_{82}O_8+Na]^+$ and $[C_{44}H_{82}O_8-H+2Na]^+$ at *m/z* 761.59 and 783.57, respectively, are assigned as Criegee ions. While we cannot distinguish the structural isomers of Criegee ions, the deprotonated doubly sodiated Criegee ion at *m/z* 783.57 is very likely from the carboxylic acid isomer by replacing the acidic proton with a sodium ion and the other sodium ion adducted to one of the ester groups. A double alkaline ion adduct is commonly found in positive mode MALDI-MS spectra of acidic lipids, e.g., phosphatidylethanolamines $[PE+2K-H]^+$.[20] MS/MS was performed on aged OPP and fingerprints to further support an ambient ozonolysis mechanism.

In **Figure 4A-D**, the MS/MS, acquired using the linear ion trap, is shown for OPP (TG 50:1, *m/z* 855.7), O7 aldehyde (*m/z* 745.6), and Criegee ions (*m/z* 761.6 and 783.6). The major fragmentations for OPP (**Figure 4A**) are the loss of the palmitic acid (16:0) at *m/z* 599.5 and the oleic acid (18:1) at *m/z* 573.5. MS/MS of the O7 aldehyde, **Figure 4B,** shows the loss of the 16:0 chain at *m/z* 489.4 and the loss of the aldehyde chain at *m/z* 573.5, consistent with the structure in **Scheme 1**. The MS/MS of the O8 sodiated Criegee ion (*m/z* 761.6) in **Figure 4C** includes the

loss of the 16:0 chain at *m/z* 505.4 and a loss of a four-oxygen chain at *m/z* 573.5, consistent with the Criegee ion isomers in **Scheme 1**. In contrast, MS/MS of the O8 doubly sodiated Criegee ion shows only the loss of the 16:0 at *m/z* 527.4 as a diagnostic fragment (**Figure 4D**), suggesting the ester bond with sodiated carboxylate group does not easily dissociate.

MS/MS of the same masses as OPP and its ozonolysis products are compared in aged fingerprints as shown in **Figure 4E-H**. In a fingerprint, various different chain combinations that contain the same total number of carbons and double bonds would appear at the same masses. For example, in addition to OPP (TG 18:1/16:0/16:0), other TG 50:1 species such as TG 18:1/17:0/15:0 would contribute to *m/z* 855.7. In MS/MS of *m/z* 855.7 (**Figure 4E**), the loss of 16:0 and 18:1 are detected as the major fragments similar to the MS/MS of OPP (**Figure 4A**); however, also detected are the loss of 15:0 (*m/z* 613.6) and 17:0 (*m/z* 585.5), which are most likely the products in MS/MS of TG 18:1/17:0/15:0. Similarly, in MS/MS of *m/z* 745.6 (O7 aldehyde product), *m/z* 761.6 and *m/z* 783.6 (Criegee ions) shown in **Figure 4F-H**, the major products are the same as those of OPP (**Figure 4B-D**), but some other products are detected including those from TG 18:1/17:0/15.0.

A fresh and aged OPP standard were also analyzed using direct injection ESI-QTOF to support the ambient ozonolysis mechanism. As shown in **Figure 5**, both the ozonide and aldehyde were observed in the aged spectrum; however, no Criegee ions were observed. This is consistent with the report from the Blanksby group that the ozonide can partially decompose to an aldehyde product in ambient conditions but Criegee ions can only be detected in MS/MS.[15] It is also in good agreement with our hypothesis that the Criegee ions are a result of in-source MALDI dissociation of the ozonide. The presence of ozonolysis related peaks in both the MALDI and ESI spectra confirms the ozonolysis of unsaturated TGs.

Determining Fingerprint Age from Triacylglycerol Degradation

The drastic change of the TG patterns within the first few days of aging as shown in **Figure 1** and **Figure 2** suggest that tracking the degradation of unsaturated TGs could be used to determine the age of fingerprints left at a crime scene. To test this hypothesis, a week-long aging study was performed under ambient conditions for three participants. The fingerprints were stored on a lab shelf, exposed to the room light and air, imitating typical office environments. The temperature was +/- one degree of 22 °C, but the humidity varied approximately 18% over the week as shown in the representative graph in **Figure 6**.

The study was performed three times to determine the reproducibility. Normalized abundance changes are shown in **Figure 7A-C** for unsaturated TGs, the aldehydes, and the Criegee ions for three individuals. In the assumption that there is no dramatic change in saturated TGs, as seen in **Figure 2**, the total ion signals of unsaturated TGs, aldehydes, and Criegee ions are normalized to the sum of saturated TG signals to account for day-to-day variation in instrument response. The overall trend is similar to **Figure 1** and **Figure 2**, decrease of the unsaturated TGs and increase of ozonolysis peaks, but the change is most dramatic within the first three days of aging. Interestingly, the three participants do show slight differences in the rate of decrease of the unsaturated TGs as well as increase of the aldehyde and Criegee ions.

Particularly for Person 2, unsaturated TGs decrease and the ozonolysis peaks increase more slowly than the other participants. It took almost three days for unsaturated TGs of Person 2 to catch up to the amount of decrease in a single day for Person 1 or 3. The O7 and O8 series increase for the first few days, but then begin to vary drastically among the replicates (**Figure 7B-C**). This is likely due to the further degradation of ozonides or O7 aldehydes into smaller compounds and/or additional ozonolysis of TGs with multiple unsaturations. Considering the

intermediate nature of O7 and O8 compounds, the degradation of unsaturated TGs with apparent first order kinetics is expected to be much more reliable for fingerprint age determination.

It is worth mentioning that the rate of degradation is quite reproducible for each participant despite the fact that key variables of this experiment were not controlled (e.g., humidity or the concentration of ambient ozone). This suggests that it is possible to reliably determine the fingerprint age for a given individual. However, variation in the degradation rate between individuals as shown in **Figure 7A** suggests there is a limitation to universally applying this approach to unknown individuals to accurately determine the deposition time. For example, a normalized unsaturated TG value near one would indicate an approximately one-day old fingerprint for Person 1, but that fingerprint would be three to five days old for Person 2. To explain individual differences in the degradation rate of unsaturated TGs, we hypothesized that other lipids present in fingerprints affect the degradation rate, especially FAs, WEs, and DGs which also have unsaturated double bonds. **Figure 8** shows the fresh and aged mass spectra of an unsaturated FA, DG, and WE standard. The aldehyde and Criegee ions were observed following aging of each compound type, suggesting that ozonolysis of unsaturated fatty acyl chains is occurring not only in TGs but also in any compound containing unsaturated fatty acyl chains.

To further explore the effect of other lipids, quantification of these lipids was performed for the same three participants. FAs were quantified using an ESI QTOF in negative mode and five dissolved fingerprints in triplicate using FA 19:0 as an internal standard. WEs, DGs, and TGs were quantified by MALDI-MSI in positive mode using a sprayed internal standard (glycerol trinonanoate) prior to analysis of a region of a single fingerprint. Overall, Person 2 contained a higher amount of lipids, roughly five times more, than Person 1 and Person 3 as shown in **Figure 9**. The higher abundance of lipids, particularly unsaturated, was true for FAs,

WEs, DGs, and TGs. It is consistent with the fact that Person 2 showed the slowest rate of degradation of unsaturated TGs (**Figure 7A**). While the exact mechanism is still unknown and a large-scale, well-controlled study would be necessary for better understanding, it seems high lipid abundance is a key variable affecting the rate of TG degradation in each individual. In a real application, one may envision that a forensic practitioner could collect fingerprints of a suspect to determine the lipid content or even perform an aging experiment in an environment with similar ozone content. This would allow for more accurate determination of the time since deposition of fingerprints collected from a crime scene.

Forensic Considerations

Any method to determine fingerprint age would require the compatibility with forensic development and knowledge of the impact of storage after collection from a crime scene on the fingerprint compounds. Both fresh and seven-day aged fingerprints were developed with carbon forensic powder (CFP), as it was previously shown to be an effective one-step development and matrix powder and did not require the addition of sodium and gold.[22] In **Figure 10** the TG region of developed fresh and aged fingerprints are shown. The emergence of ozonolysis peaks and decrease of unsaturated TGs were also clearly detected in the CFP developed fingerprint.

Furthermore, to determine whether fingerprints would continue to age after the collection, fingerprints were placed in two sealed containers (opaque and transparent) and aged for three days alongside a fingerprint at ambient conditions. In **Figure 11** the mass spectra of the fingerprints aged in sealed containers show no ozonolysis degradation, while the fingerprint aged under ambient conditions does show the degradation. This indicates that fingerprints collected at a crime scene would not continue to degrade if properly stored. Hence, the degree of aging could then be attributed to the amount of time since deposited at the crime scene and not influenced by

the time lag between collection and analysis. Additionally, MALDI-MSI analysis has been shown to be nondestructive so the fingerprints can be maintained as forensic evidence.[22]

Conclusions

MALDI-MSI analysis of the unsaturated TG abundance in fingerprints was demonstrated as a means of establishing time since deposition of latent fingerprints. Degradation of unsaturated TGs due to ambient ozonolysis was shown to be reproducible for each individual under semicontrolled environment conditions. Differences in the rate of degradation in individuals was attributed to differences in the abundance of unsaturated lipids in the fingerprint. Importantly, even after forensic development TGs and their ozonolysis products could be detected in latent fingerprints using MALDI-MSI, making this approach more compatible with current forensic practices and streamlining the process.

Further research will be performed to study the impact of the level of ozone and other environmental factors, such as humidity, on the rate of degradation. More participants will also be included in the future study to refine the conclusions presented in this work.

References

(1) *The Fingerprint Sourcebook*; U.S. Department of Justice, Office of Justice Programs, National Institute of Justice, 2011.

(2) Hinners, P.; O'Neill, K. C.; Lee, Y. J. Revealing Individual Lifestyles through Mass Spectrometry Imaging of Chemical Compounds in Fingerprints. *Sci. Rep.* **2018**, 8:5149. https://doi.org/10.1038/s41598-018-23544-7.

(3) Zhou, Z.; Zare, R. N. Personal Information from Latent Fingerprints Using Desorption Electrospray Ionization Mass Spectrometry and Machine Learning. *Anal. Chem.* **2017**, 89, 1369-1372. https://doi.org/10.1021/acs.analchem.6b04498.

(4) Ferguson, L. S.; Wulfert, F.; Wolstenholme, R.; Fonville, J. M.; Clench, M. R.; Carolan, V. A.; Francese, S. Direct Detection of Peptides and Small Proteins in Fingermarks and Determination of Sex by MALDI Mass Spectrometry Profiling. *Analyst* **2012**, 137, 4686–4692. https://doi.org/10.1039/c2an36074h.

(5) De Alcaraz-Fossoul, J.; Mestres Patris, C.; Barrot Feixat, C.; McGarr, L.; Brandelli, D.; Stow, K.; Gené Badia, M. Dating Latent Fingermarks (Part I): Minutiae Count as One Indicator of Degradation. *J. Forensic Sci.* **2016**, 61, 322–333. https://doi.org/10.1111/1556-4029.13007.

(6) De Alcaraz-Fossoul, J.; Barrot Feixat, C.; Tasker, J.; McGarr, L.; Stow, K.; Carreras-Marin, C.; Turbany Oset, J.; Gené Badia, M. Latent Fingermark Aging Patterns (Part II): Color Contrast Between Ridges and Furrows as One Indicator of Degradation. *J. Forensic Sci.* **2016**, 61, 947–958. https://doi.org/10.1111/1556-4029.13099.

(7) De Alcaraz-Fossoul, J.; Barrot Feixat, C.; Carreras-Marin, C.; Tasker, J.; Zapico, S. C.; Gené Badia, M. Latent Fingermark Aging Patterns (Part III): Discontinuity Index as One Indicator of Degradation. *J. Forensic Sci.* **2017**, 62, 1180–1187. https://doi.org/10.1111/1556-4029.13438.

(8) Muramoto, S.; Sisco, E. Strategies for Potential Age Dating of Fingerprints Through the Diffusion of Sebum Molecules on a Nonporous Surface Analyzed Using Time-of-Flight Secondary Ion Mass Spectrometry. *Anal. Chem.* **2015**, 87, 8035–8038. https://doi.org/10.1021/acs.analchem.5b02018.

(9) O'Neill, K. C.; Lee, Y. J. Effect of Aging and Surface Interactions on the Diffusion of Endogenous Compounds in Latent Fingerprints Studied by Mass Spectrometry Imaging. *J. Forensic Sci.* **2018**, 63, 708–713. https://doi.org/10.1111/1556-4029.13591.

(10) Girod, A.; Spyratou, A.; Holmes, D.; Weyermann, C. Aging of Target Lipid Parameters in Fingermark Residue Using GC/MS: Effects of Influence Factors and Perspectives for Dating Purposes. *Sci. Justice* **2016**, 56, 165–180. https://doi.org/10.1016/j.scijus.2015.12.004.

(11) Pleik, S.; Spengler, B.; Schäfer, T.; Urbach, D.; Luhn, S.; Kirsch, D. Fatty Acid Structure and Degradation Analysis in Fingerprint Residues. *J. Am. Soc. Mass Spectrom.* **2016**, 27, 1565–1574. https://doi.org/10.1007/s13361-016-1429-6.

(12) Archer, N. E.; Charles, Y.; Elliott, J. A.; Jickells, S. Changes in the Lipid Composition of Latent Fingerprint Residue with Time after Deposition on a Surface. *Forensic Sci. Int.* **2005**, 154, 224–239. https://doi.org/10.1016/j.forsciint.2004.09.120.

(13) Cadd, S.; Islam, M.; Manson, P.; Bleay, S. Fingerprint Composition and Aging: A Literature Review. *Sci. Justice* **2015**, 55, 219–238. https://doi.org/10.1016/j.scijus.2015.02.004.

(14) Pleik, S.; Spengler, B.; Ram Bhandari, D.; Luhn, S.; Schäfer, T.; Urbach, D.; Kirsch, D. Ambient-Air Ozonolysis of Triglycerides in Aged Fingerprint Residues. *Analyst* **2018**, 143, 1197–1209. https://doi.org/10.1039/c7an01506b.

(15) Ellis, S. R.; Hughes, J. R.; Mitchell, T. W.; Panhuis, M. Blanksby, S. J. Using Ambient Ozone for Assignment of Double Bond Position in Unsaturated Lipids. *Analyst* **2012**, 137, 1100–1110. https://doi.org/10.1039/c1an15864c.

(16) Thomas, M. C.; Mitchell, T. W.; Harman, D. G.; Deeley, J. M.; Nealon, J. R.; Blanksby, S. J. Ozone-Induced Dissociation: Elucidation of Double Bond Position within Mass-Selected Lipid Ions. *Anal. Chem.* **2008**, 80, 303–311. https://doi.org/10.1021/ac7017684.

(17) Robichaud, G.; Garrard, K. P.; Barry, J. A.; Muddiman, D. C. MSiReader: An Open-Source Interface to View and Analyze High Resolving Power MS Imaging Files on Matlab Platform. *J. Am. Soc. Mass Spectrom.* **2013**, 24, 718–721. https://doi.org/10.1007/s13361-013-0607-z.

(18) Bokhart, M. T.; Nazari, M.; Garrard, K. P.; Muddiman, D. C. MSiReader v1.0: Evolving Open-Source Mass Spectrometry Imaging Software for Targeted and Untargeted Analyses. *J. Am. Soc. Mass Spectrom.* **2018**, 29, 8–16. https://doi.org/10.1007/s13361-017-1809-6.

(19) Dufresne, M.; Masson, J.-F.; Chaurand, P. Sodium-Doped Gold-Assisted Laser Desorption Ionization for Enhanced Imaging Mass Spectrometry of Triacylglycerols from Thin Tissue Sections. *Anal. Chem.* **2016**, 88, 6018–6025. https://doi.org/10.1021/acs.analchem.6b01141.

(20) Feenstra, A. D.; O'Neill, K. C.; Yagnik, G. B.; Lee, Y. J. Organic–Inorganic Binary Mixture Matrix for Comprehensive Laser-Desorption Ionization Mass Spectrometric Analysis and Imaging of Medium-Size Molecules Including Phospholipids, Glycerolipids, and Oligosaccharides. *RSC Adv.* **2016**, 6, 99260–99268. https://doi.org/10.1039/C6RA20469D.

(21) Duenas, M.; Larson, E.; Lee, Y. J. Towards Mass Spectrometry Imaging in the Metabolomics Scale: Increasing Metabolic Coverage Through Multiple On-Tissue Chemical Modifications. **2019**, 10, 860. https://doi.org/10.3389/fpls.2019.00860.

(22) Hinners, P.; Lee, Y. J. Carbon-Based Fingerprint Powder as a One-Step Development and Matrix Application for High-Resolution Mass Spectrometry Imaging of Latent Fingerprints **2019**, 64, 1048-1056. https://doi.org/10.1111/1556-4029.13981.

Figures and Tables

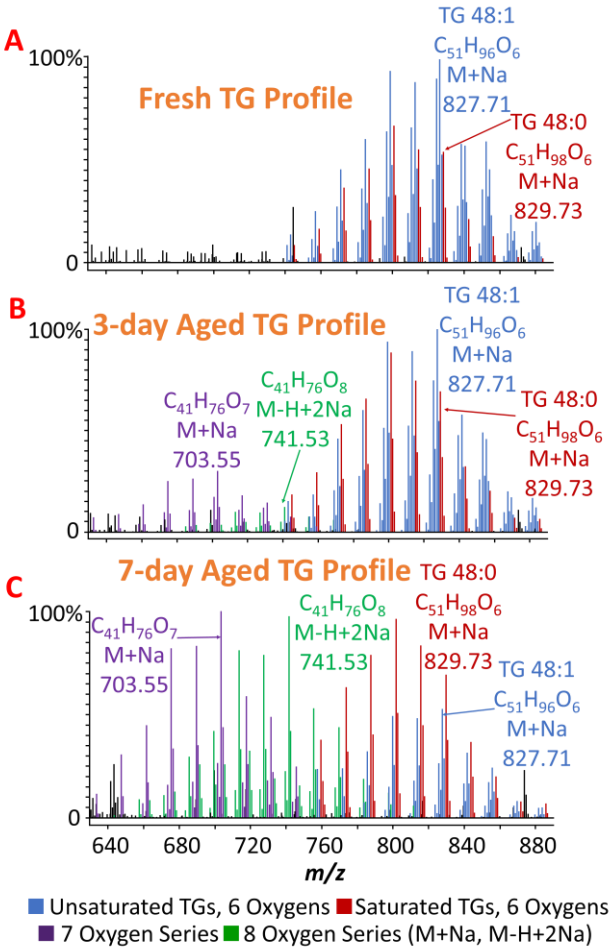

Figure 1. MALDI mass spectra of the TG region of fresh and aged latent fingerprints acquired using sodium gold as the matrix in positive mode. **(A)** Fresh fingerprint TG profile. **(B)** Three-day aged fingerprint TG profile. **(C)** Seven-day aged fingerprint TG profile. Unsaturated TGs are shown in blue and saturated in red. O7 and O8 degradation series are shown in purple and green, respectively.

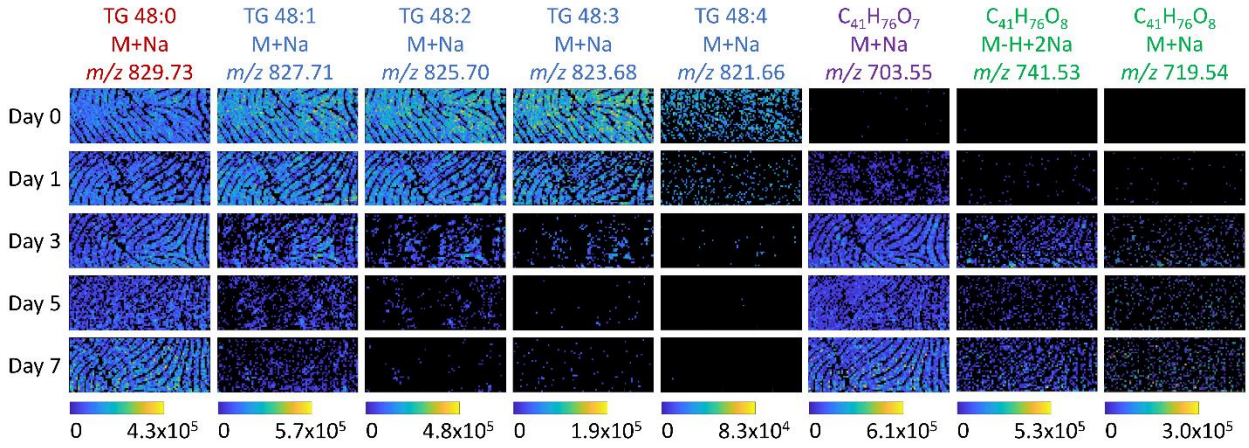

Figure 2. MALDI-MS images of TG 48:0-4 and associated O7 and O8 series in fresh and aged fingerprints. Each compound is displayed using the same scale from day zero to seven.

Scheme 1. Ambient ozonolysis mechanism as proposed by Blanksby.[15]

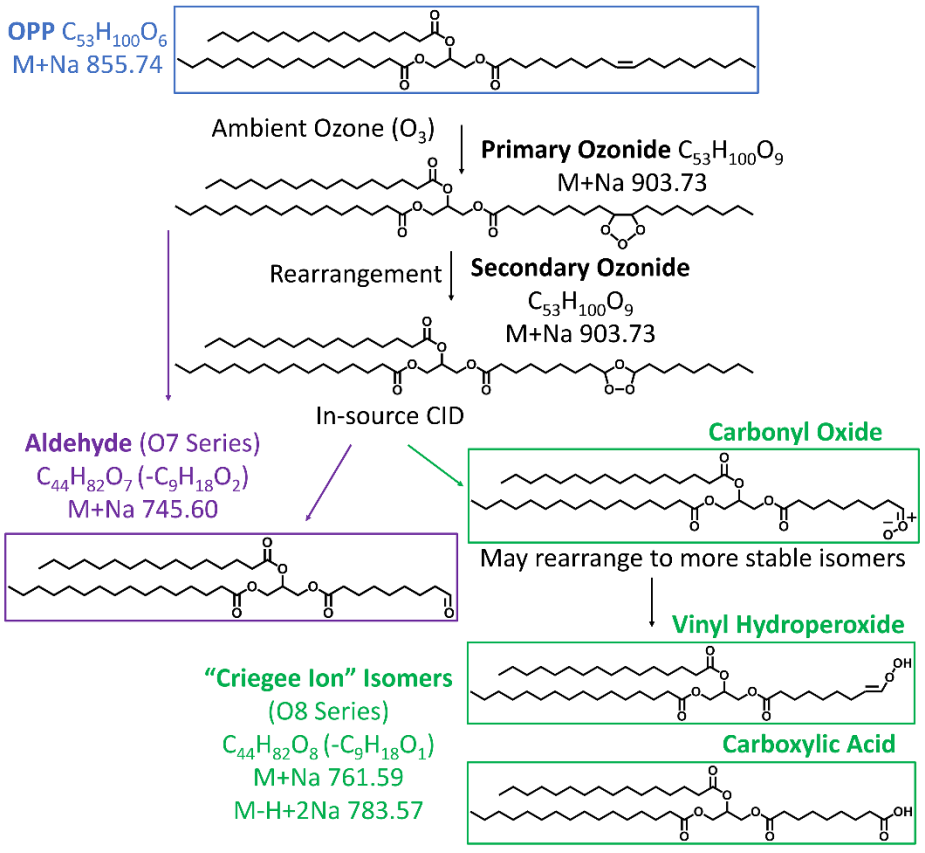

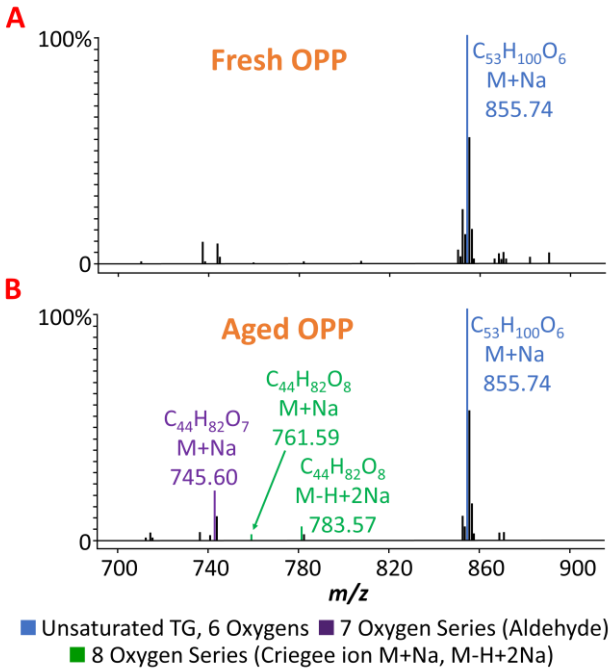

Figure 3. **(A)** MALDI mass spectrum of fresh 1-oleoyl-2,3-dipalmitoyl glycerol (OPP). **(B)** MALDI mass spectrum of 12 h aged OPP showing the emergence of new peaks.

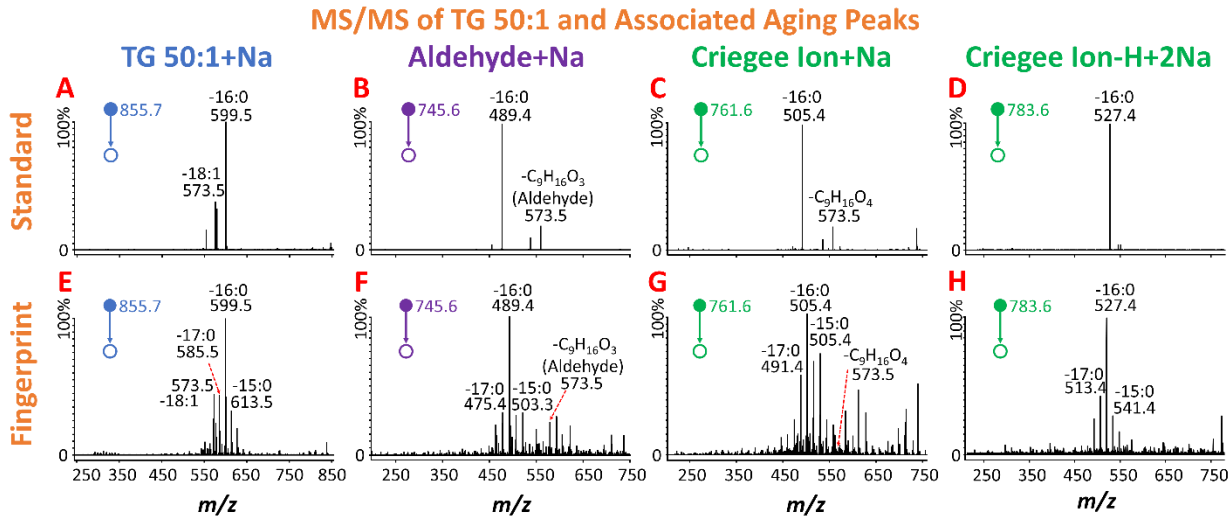

Figure 4. MS/MS of 1-oleoyl-2,3-dipalmitoyl glycerol (OPP) and associated aging peaks **(A-D)**. MS/MS of TG 50:1 and associated aging peaks from a fingerprint **(E-H)**. **(A)** MS/MS of OPP at *m/z* 855.7. **(B)** MS/MS of O7 aldehyde at *m/z* 745.6. **(C)** MS/MS of O8 Criegee ion at *m/z* 761.6. **(D)** MS/MS of O8 Criegee ion at *m/z* 783.6. **(E)** MS/MS of TG 50:1 at *m/z* 855.7 from a fingerprint. **(F)** MS/MS of O7 aldehyde at *m/z* 745.6 from an aged fingerprint. **(G)** MS/MS of sodiated O8 Criegee ion at *m/z* 761.6 from an aged fingerprint. **(H)** MS/MS of doubly sodiated O8 Criegee ion at *m/z* 783.6 from an aged fingerprint.

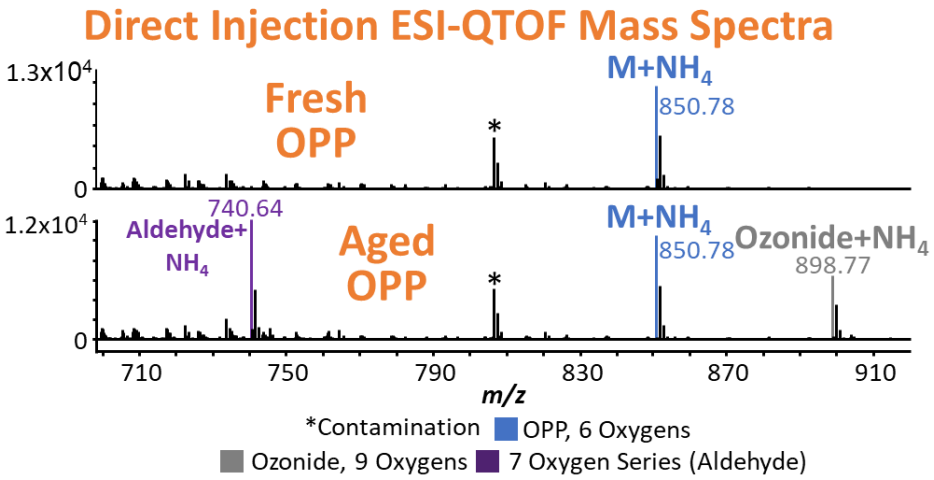

Figure 5. ESI mass spectra of fresh and aged 1-oleoyl-2,3-dipalmitoyl glycerol (OPP) obtained using direct injection ESI QTOF.

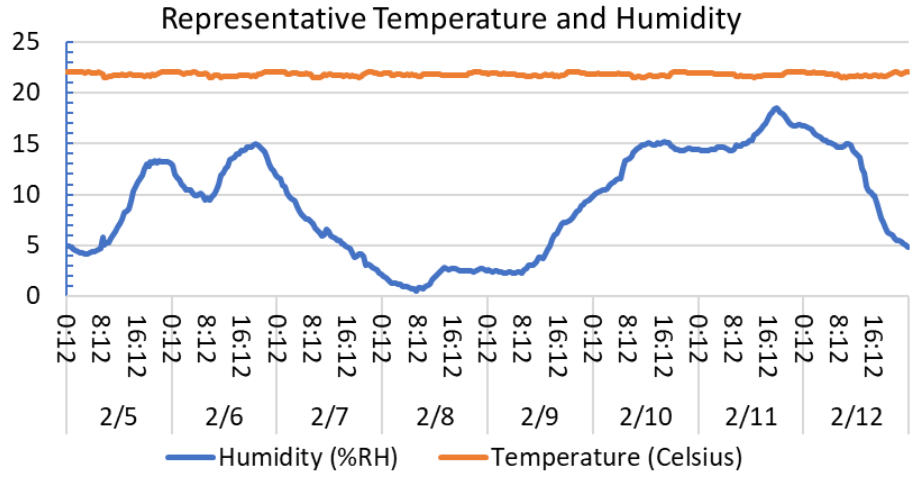

Figure 6. Representative graph tracking percent relative humidity and temperature over the course of the aging study.

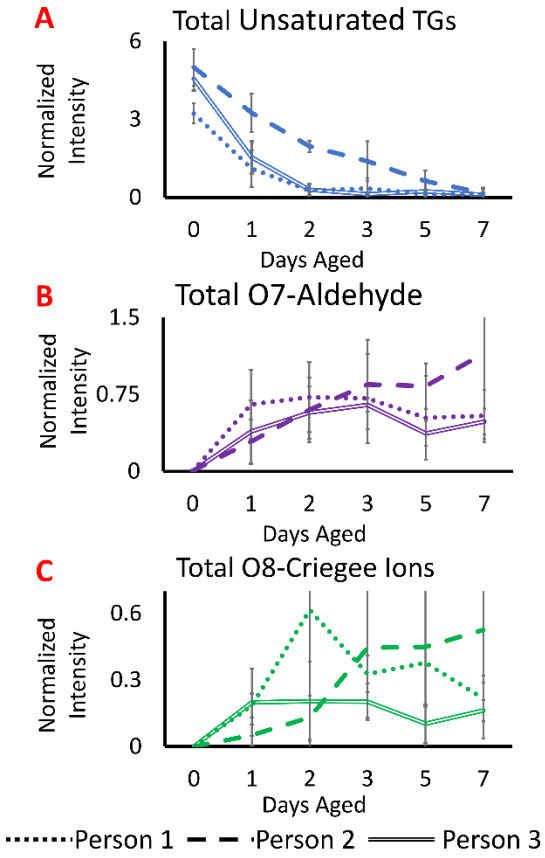

Figure 7. Summed intensity of unsaturated TGs and ozonolysis products normalized to the summed intensity of saturated TGs over a seven-day period of aging for three participants. The errors bars indicate the standard deviation of three replicates. **(A)** Unsaturated TGs, **(B)** O7 aldehydes, and **(C)** O8 Criegee ions (both adducts).

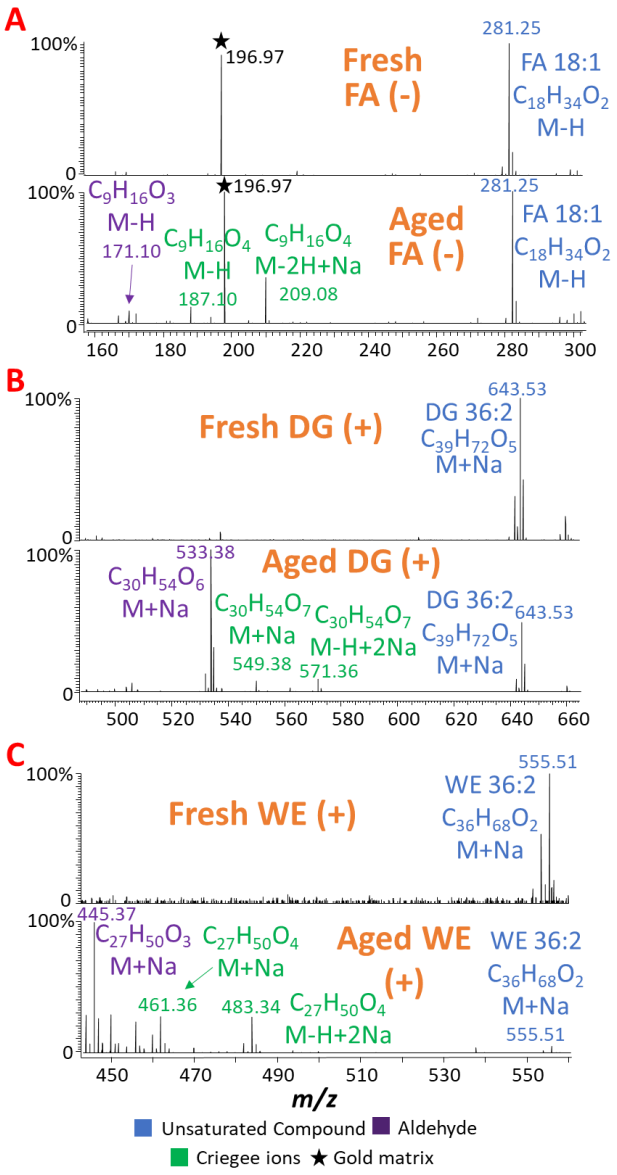

Figure 8. Fresh and aged MALDI mass spectra of **(A)** oleic acid, a fatty acid, in negative mode **(B)** 1,2-dioleoyl-glycerol, a diacylglycerol, in positive mode, and **(C)** oleyl oleate, a wax ester in positive mode.

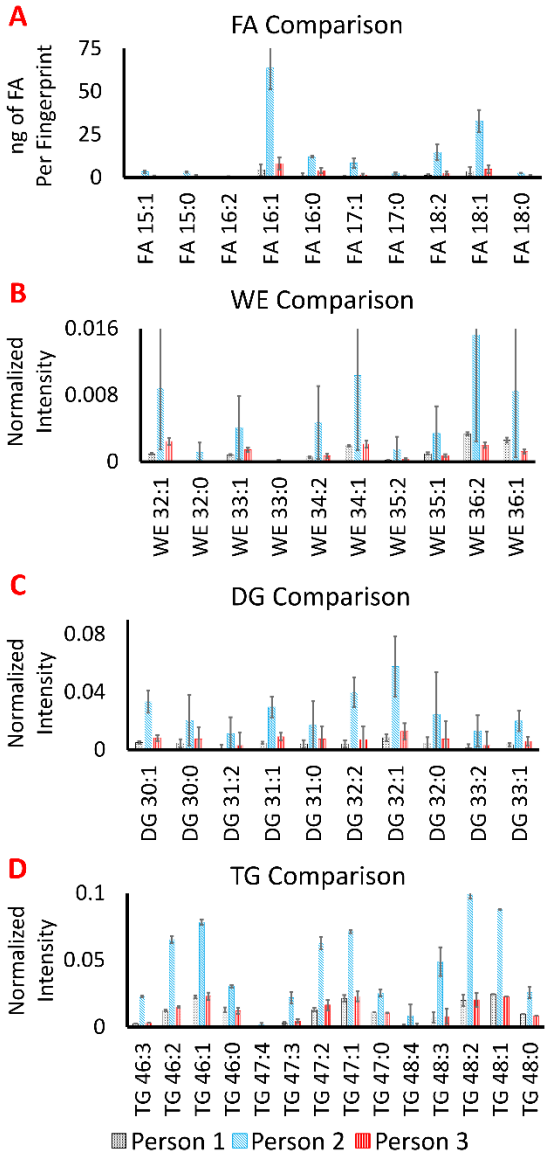

Figure 9. Quantification of FAs **(A)**, WEs **(B)**, DGs **(C)**, and TGs **(D)** in the fingerprint of three participants. FAs were quantified using a direct injection ESI-QTOF and FA 19:0 as an internal standard. WEs, DGs, and TGs were quantified using MALDI-MSI analysis and glycerol trinonanoate as an internal standard. The error bars indicate the standard deviation of three replicates.

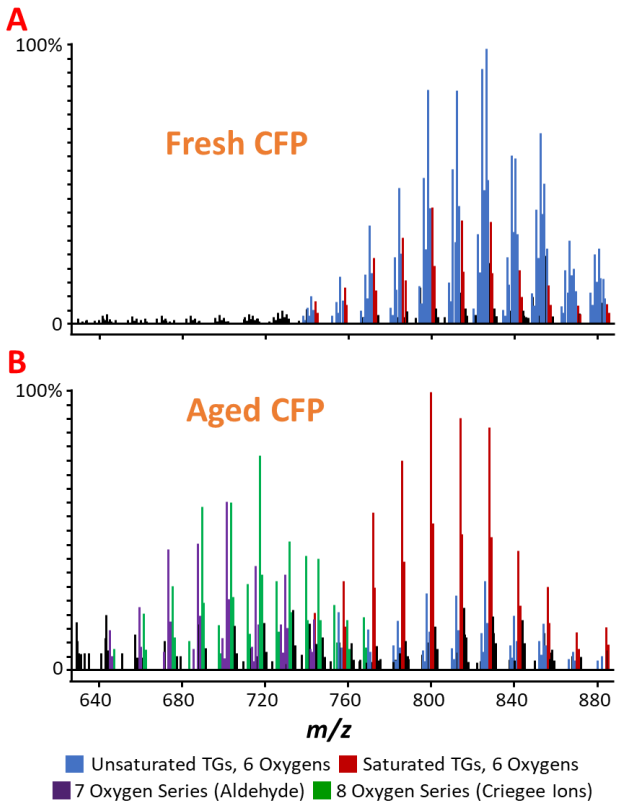

Figure 10. MALDI mass spectra of the TG region from fresh **(A)** and seven-day aged **(B)** carbon powder (CFP) developed fingerprints. Note that the CFP was utilized as an existing matrix and no sodium gold was added prior to analysis.

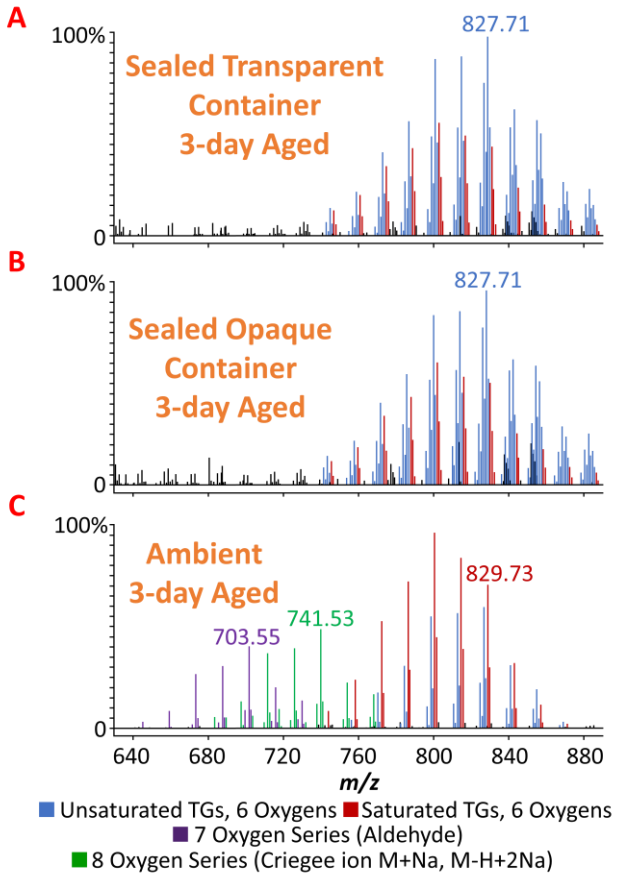

Figure 11. Mass spectra of fingerprints aged for three days in a sealed transparent container **(A)**, in a sealed opaque container **(B)**, and under ambient conditions **(C)**.

Table 1. List of all triacylglycerols (TGs) detected and used in this study along with their theoretical and experimental *m/z* values and mass errors. Red and blue indicate saturated and unsaturated TGs, respectively.

Triacylglycerols									
TG	Formula	Theoretical (M+Na)	Experimental (M+Na)	Δm (ppm)	TG	Formula	Theoretical (M+Na)	Experimental (M+Na)	Δm (ppm)
TG 42:3	$C_{45}H_{80}O_6$	739.585	739.585	-0.1	TG 48:4	$C_{51}H_{90}O_6$	821.663	821.663	-0.4
TG 42:2	$C_{45}H_{82}O_6$	741.600	741.600	0.1	TG 48:3	$C_{51}H_{92}O_6$	823.679	823.679	-0.2
TG 42:1	$C_{45}H_{84}O_6$	743.616	743.616	-0.1	TG 48:2	$C_{51}H_{94}O_6$	825.694	825.694	-0.2
TG 42:0	$C_{45}H_{86}O_6$	745.632	745.632	-0.2	TG 48:1	$C_{51}H_{96}O_6$	827.710	827.710	-0.2
TG 43:4	$C_{46}H_{80}O_6$	751.585	751.584	0.8	TG 48:0	$C_{51}H_{98}O_6$	829.726	829.725	0.6
TG 43:3	$C_{46}H_{82}O_6$	753.600	753.601	-0.2	TG 49:4	$C_{52}H_{92}O_6$	835.679	835.679	-0.3
TG 43:2	$C_{46}H_{84}O_6$	755.616	755.616	-0.2	TG 49:3	$C_{52}H_{94}O_6$	837.694	837.695	-0.3
TG 43:1	$C_{46}H_{86}O_6$	757.632	757.632	-0.6	TG 49:2	$C_{52}H_{96}O_6$	839.710	839.710	-0.2
TG 43:0	$C_{46}H_{88}O_6$	759.647	759.648	-0.2	TG 49:1	$C_{52}H_{98}O_6$	841.726	841.726	0.1

Table 1 Continued									
TG	Formula	Theoretical (M+Na)	Experimental (M+Na)	Δm (ppm)	TG	Formula	Theoretical (M+Na)	Experimental (M+Na)	Δm (ppm)
TG 44:3	$C_{47}H_{84}O_6$	767.616	767.616	-0.1	TG 49:0	$C_{52}H_{100}O_6$	843.741	843.740	1.7
TG 44:2	$C_{47}H_{86}O_6$	769.632	769.632	-0.3	TG 50:4	$C_{53}H_{94}O_6$	849.694	849.694	-0.2
TG 44:1	$C_{47}H_{88}O_6$	771.647	771.648	-0.4	TG 50:3	$C_{53}H_{96}O_6$	851.710	851.710	-0.2
TG 44:0	$C_{47}H_{90}O_6$	773.663	773.663	-0.2	TG 50:2	$C_{53}H_{98}O_6$	853.726	853.726	0.0
TG 45:4	$C_{48}H_{84}O_6$	779.616	779.616	-0.2	TG 50:1	$C_{53}H_{100}O_6$	855.741	855.741	0.5
TG 45:3	$C_{48}H_{86}O_6$	781.632	781.632	-0.2	TG 50:0	$C_{53}H_{102}O_6$	857.757	857.755	2.6
TG 45:2	$C_{48}H_{88}O_6$	783.647	783.648	-0.2	TG 51:4	$C_{54}H_{96}O_6$	863.710	863.710	0.1
TG 45:1	$C_{48}H_{90}O_6$	785.663	785.663	-0.4	TG 51:3	$C_{54}H_{98}O_6$	865.726	865.726	0.1
TG 45:0	$C_{48}H_{92}O_6$	787.679	787.679	-0.4	TG 51:2	$C_{54}H_{100}O_6$	867.741	867.741	0.2
TG 46:4	$C_{49}H_{86}O_6$	793.632	793.632	-0.5	TG 51:1	$C_{54}H_{102}O_6$	869.757	869.756	1.1
TG 46:3	$C_{49}H_{88}O_6$	795.647	795.648	-0.4	TG 51:0	$C_{54}H_{104}O_6$	871.773	871.769	3.9
TG 46:2	$C_{49}H_{90}O_6$	797.663	797.663	-0.2	TG 52:4	$C_{55}H_{98O6}$	877.726	877.726	-0.2
TG 46:1	$C_{49}H_{92}O_6$	799.679	799.679	-0.4	TG 52:3	$C_{55}H_{100}O_6$	879.741	879.741	-0.2
TG 46:0	$C_{49}H_{94}O_6$	801.694	801.694	0.1	TG 52:2	$C_{55}H_{102}O_6$	881.757	881.757	0.3
TG 47:4	$C_{50}H_{88}O_6$	807.647	807.648	-0.4	TG 52:1	$C_{55}H_{104}O_6$	883.773	883.772	1.1
TG 47:3	$C_{50}H_{90}O_6$	809.663	809.663	-0.4	TG 52:0	$C_{55}H_{106}O_6$	885.788	885.787	1.7
TG 47:2	$C_{50}H_{92}O_6$	811.679	811.679	-0.2					
TG 47:1	$C_{50}H_{94}O_6$	813.694	813.694	-0.2					
TG 47:0	$C_{50}H_{96}O_6$	815.710	815.710	0.3					

Table 2. List of all O7 series compounds detected and used in this study along with their theoretical and experimental *m/z* values and mass errors.

O7 Series			
Formula	Theoretical (M+Na)	Experimental (M+Na)	Δm (ppm)
$C_{36}H_{64}O_7$	631.454	631.452	4.3
$C_{36}H_{66}O_7$	633.470	633.468	3.8
$C_{37}H_{66}O_7$	645.470	645.468	3.5
$C_{37}H_{68}O_7$	647.486	647.483	3.8
$C_{38}H_{68}O_7$	659.486	659.484	2.9
$C_{38}H_{70}O_7$	661.501	661.499	3.4
$C_{39}H_{70}O_7$	673.501	673.499	3.8
$C_{39}H_{72}O_7$	675.517	675.515	3.4
$C_{40}H_{72}O_7$	687.517	687.515	3.2
$C_{40}H_{74}O_7$	689.533	689.530	3.5
$C_{41}H_{74}O_7$	701.533	701.530	3.4
$C_{41}H_{76}O_7$	703.548	703.546	3.2
$C_{42}H_{76}O_7$	715.548	715.546	3.3
$C_{42}H_{78}O_7$	717.564	717.562	3.3

Table 2 Continued			
Formula	Theoretical (M+Na)	Experimental (M+Na)	Δm (ppm)
$C_{43}H_{78}O_7$	729.564	729.562	3.0
$C_{43}H_{80}O_7$	731.580	731.577	3.0
$C_{44}H_{80}O_7$	743.580	743.578	2.9
$C_{44}H_{82}O_7$	745.595	745.594	2.4
$C_{45}H_{82}O_7$	757.595	757.594	2.3
$C_{45}H_{84}O_7$	759.611	759.610	1.8
$C_{46}H_{84}O_7$	771.611	771.609	2.4
$C_{46}H_{86}O_7$	773.627	773.625	1.5

Table 3. List of all O8 series compounds detected and used in this study along with their theoretical and experimental *m/z* values and mass errors.

O8 Series							
Formula	Theoretical (M-H+2Na)	Experimental (M-H+2Na)	Δm (ppm)	Formula	Theoretical (M+Na)	Experimental (M+Na)	Δm (ppm)
$C_{36}H_{66}O_8$	671.447	671.445	3.6	$C_{36}H_{66}O_8$	649.465	649.463	3.1
$C_{37}H_{66}O_8$	683.447	683.445	3.1	$C_{37}H_{66}O_8$	661.465	661.463	3.3
$C_{37}H_{68}O_8$	685.463	685.460	3.3	$C_{37}H_{68}O_8$	663.481	663.479	3.2
$C_{38}H_{68}O_8$	697.463	697.461	2.9	$C_{38}H_{68}O_8$	675.481	675.478	3.3
$C_{38}H_{70}O_8$	699.478	699.476	3.2	$C_{38}H_{70}O_8$	677.496	677.496	1.2
$C_{39}H_{70}O_8$	711.478	711.476	2.7	$C_{39}H_{70}O_8$	689.496	689.495	2.6
$C_{39}H_{72}O_8$	713.494	713.492	3.3	$C_{39}H_{72}O_8$	691.512	691.510	2.4
$C_{40}H_{72}O_8$	725.494	725.492	2.9	$C_{40}H_{72}O_8$	703.512	703.510	2.2
$C_{40}H_{74}O_8$	727.510	727.507	3.2	$C_{40}H_{74}O_8$	705.528	705.526	2.1
$C_{41}H_{74}O_8$	739.510	739.507	3.2	$C_{41}H_{74}O_8$	717.528	717.527	1.2
$C_{41}H_{76}O_8$	741.525	741.523	3.1	$C_{41}H_{76}O_8$	719.543	719.542	2.3
$C_{42}H_{76}O_8$	753.525	753.523	3.4	$C_{42}H_{76}O_8$	731.543	731.541	2.5
$C_{42}H_{78}O_8$	755.541	755.539	3.1	$C_{42}H_{78}O_8$	733.559	733.558	1.8
$C_{43}H_{78}O_8$	767.541	767.539	2.5	$C_{43}H_{78}O_8$	745.559	745.557	2.1
$C_{43}H_{80}O_8$	769.556	769.554	2.7	$C_{43}H_{80}O_8$	747.575	747.573	2.1
$C_{44}H_{80}O_8$	781.556	781.555	2.0	$C_{44}H_{80}O_8$	759.575	759.572	3.7
$C_{44}H_{82}O_8$	783.572	783.570	2.9	$C_{44}H_{82}O_8$	761.590	761.588	2.4
$C_{45}H_{82}O_8$	795.572	795.569	4.2	$C_{45}H_{82}O_8$	773.590	773.589	1.5
$C_{45}H_{84}O_8$	797.588	797.586	2.9	$C_{45}H_{84}O_8$	775.606	775.604	2.2
$C_{46}H_{86}O_8$	811.603	811.601	3.1	$C_{46}H_{86}O_8$	789.621	789.622	-0.5

CHAPTER 6. GENERAL CONCLUSION

General Summary

The work presented in this dissertation strived to further the value of latent fingerprints through chemical profiling. Chemical profiling allows information about an unknown individual to be compiled to assist in identification or what lifestyle the individual may have. This would be particularly useful if no match existed in the fingerprint database for identification purposes. Chemical analysis could also reveal information about the fingerprint itself, such as how long the fingerprint had been deposited on a surface. The work also modified existing approaches in matrix-assisted laser desorption/ionization - mass spectrometry imaging (MALDI-MSI) of latent fingerprints to make them more amenable to current forensic practices. Ultimately, developing a technology for use in the forensic world demands that current forensic practices are considered during optimization.

The common carbon forensic development powder, CFP, was shown to be an effective one-step development and matrix powder. Prior research into the compatibility had shown that fingerprints developed with CFP required additional matrix for ionization and the spectra were often contaminated with carbon cluster peaks. However, in this work it was shown that CFP developed fingerprints do not require additional matrix as CFP provided comparable or higher signal to noise ratios than the commonly used organic matrix alpha-cyano-4-hydroxycinnamic acid (CHCA). However, a high-resolution mass spectrometer (HRMS) is necessary to avoid interference from the carbon clusters. Adopting an existing forensic development technique as the MALDI matrix streamlines the process and make MALDI-MSI more accessible to the general forensic community. Developing realistic laboratory techniques and approaches that

correlate with what is used in the field is necessary in order to bridge the gap between real world forensics and research forensics.

While CFP was shown to be an efficient single-step matrix, this black powder is not used to develop on all surfaces and required the HRMS. Therefore, the usefulness of a non-carbon-based development powder, titanium oxide (TIO_2), was also explored as a development and matrix combination powder. TiO_2 worked as an existing MALDI matrix for the analysis of endogenous and exogenous compounds. Importantly, it was also shown that adding additional MALDI matrices on top of the TiO_2 did not uniformly improve the detection of fingerprint compounds as research by other groups had suggested. When possible, the fingerprints should be analyzed as received. Additional matrices should only be applied if knowledge of their effectiveness is known by the laboratory.

A lifestyle profiling approach was developed that focused on non-illicit exogenous compounds, such as consumer products and food or drink related compounds, that would assist in building an individual profile. Previous work had focused on illicit drugs and explosives, but the vast array of exogenous compounds contacted in our daily lives had not yet been investigated for latent fingerprint profiling.

Although both physical and chemical fingerprint aging studies had been performed, no study had solved the problem of determining latent fingerprint age. Therefore, MALDI-MSI was utilized to study the TGs of fingerprints allowed to age under ambient conditions. Ambient ozonolysis was shown to be a dominant mechanism of degradation of unsaturated lipids. The rate of degradation of unsaturated TGs was shown to be relatively reproducible per individual under partially uncontrolled environment conditions. Theoretically fingerprints from a suspect could be collected and aged under the known environmental conditions (i.e. concentration of ambient

ozone) and compared to the fingerprint in question to establish the age of the questioned fingerprint. Additionally, variation in abundance of unsaturated lipids including TGs, DGs, WEs, and FAs were highlighted as a potential explanation for differences in the rate of degradation from individual to individual.

Outlook

During the past ten years, researchers have focused on the chemical information within latent fingerprints, with a more recent focus on MSI approaches. The realization of the applicability of MALDI-MSI to latent fingerprints is beginning to be realized by forensic personnel, particularly in Europe due to the work by the Francese group. Although the amount of research conducted has increased, the gap between research and true forensic cases has yet to be closed. Continued research and efforts to collaborate with forensic laboratories is a must. Prior to the use in court, MALDI-MSI must be generally accepted by the forensic science community and heavily validated.

The compatibility methodologies presented in this work (Chapters 2 and 3) are a necessary step to gaining acceptance by the forensic science community. While the Francese group had utilized CHCA, a MALDI matrix, to develop latent fingerprints in a two-step process,[1,2] this powder would be expensive and is not currently used in the field by the forensic community. Utilizing an existing development powder, namely CFP or TiO_2, and demonstrating that each powder serves as a MALDI matrix makes this approach more enticing to forensic personnel. The field staff would not need additional training or changes to their practices. Fingerprints could be developed as they currently are, and MALDI-MSI could be performed using the development as a matrix. A lack of cross contamination from brushing multiple fingerprints with the same dusting brush also makes this approach more likely to be adopted. It

would not be feasible for field staff to use a single brush per fingerprint. Finally, the soft nature of MALDI and utilizing under-sampling preserves the fingerprint ridges, therefore maintaining the forensic evidence. Preservation of evidence is a common goal of forensic personnel and allows further testing by other methodologies if necessary.

Chapter 4 demonstrated that compounds related to an individual's lifestyle could be utilized to develop a suspect profile. It emphasized the importance of non-illicit substances in a chemical profiling approach. While this proof of concept study is promising, an untargeted mass spectrometry approach would be time consuming. Forensic personnel would require in-depth mass spectrometry training and the amount of time to identify unknown compounds would be difficult to quantify. A more realistic approach would be the development of precursor and MS/MS databases. An example of this would be the Global Natural Product Social Molecular Networking (GNPS) database.[3] The GNPS aids in the identification of compounds utilizing an annotated MS/MS library. Constructing one database to be used by forensic personnel that includes illicit drugs, explosives, food and drink related substances, as well as consumer products would be necessary to make lifestyle profiling from MALDI-MSI adoptable by the forensic community.

Finally, utilizing MALDI-MSI to study the ambient ozonolysis of unsaturated lipids could solve the "age old" question of establishing latent fingerprint age. The work presented in this dissertation tracked the degradation of unsaturated lipids from three participants. Further work utilizing more participants and considering environmental factors is necessary. The impact of the concentration of ozone on the rate of degradation as well as the impact of any exogenous compounds present in the residue should be evaluated. A more in-depth study will continue, specifically addressing the issues mentioned above. With a more large-scale study this approach

could be reliably utilized to establish the time since deposition of a latent fingerprint, providing the court and forensic personnel with a scientifically validated result.

The objective of this work was to apply MALDI-MSI to the analysis of latent fingerprints to increase the forensic evidence, with a specific focus on bridging the gap between forensic and research personnel. While a great deal of work is still necessary for the gap to be completely bridged, the work presented here demonstrates the feasibility of analyzing developed fingerprints and increases the potential forensic evidence within latent fingerprints through chemical profiling and age determination.

References

(1) Ferguson, L.; Bradshaw, R.; Wolstenholme, R.; Clench, M.; Francese, S. Two-Step Matrix Application for the Enhancement and Imaging of Latent Fingermarks. *Anal. Chem.* **2011**, *83* (14), 5585–5591. https://doi.org/10.1021/ac200619f.

(2) Ferguson, L. S.; Creasey, S.; Wolstenholme, R.; Clench, M. R.; Francese, S. Efficiency of the Dry-Wet Method for the MALDI-MSI Analysis of Latent Fingermarks. *J. Mass Spectrom.* **2013**, *48* (6), 677–684. https://doi.org/10.1002/jms.3216.

(3) Wang, M.; Carver, J. J.; Phelan, V. V.; Sanchez, L. M.; Garg, N.; Peng, Y.; Nguyen, D. D.; Watrous, J.; Kapono, C. A.; Luzzatto-Knaan, T.; et al. Sharing and Community Curation of Mass Spectrometry Data with Global Natural Products Social Molecular Networking. *Nat. Biotechnol.* **2016**, *34* (8), 828–837. https://doi.org/10.1038/nbt.3597.